
**EP/L014106/1**

**SUPERGEN Wind Hub**

**Deliverables:**

D3.3 Report on wind farm control algorithms to meet asset management requirements.

| | | | |
|---|---|---|---|
| Delivered by: | University of Strathclyde | | |
| Author(s): | Dr Romans Kazacocks, Matthew Cole, Professor Bill Leithead | | |
| Delivery date: | September 2019 | | |
| Distribution list: | Management Committee | | |
| | | | |


# Prologue

In this report, the investigation of the dependence of the loads on individual turbines in an offshore wind farm is reported. Three layouts of the wind farm are considered for a wide range of wind conditions, including wind direction. The relationships of loads to generated power and position of the wind turbine in the farm are explored. In addition, different farm level control algorithms to curtail the power output from the farm are compared to determine the strategy that maximises the reduction in turbine loads. The StrathFarm simulation tool has been used extensively in this work which has, also, enabled it to be thoroughly tested. Even though a large number of simulation runs are conducted, it is clear that the stochastic nature of the wind field renders the results subject to a degree of uncertainty warranting further investigation.

Following its remit to facilitate cooperation and collaboration, Supergen Wind Hub provided the cohesive element bringing together research from a number of programmes. The contributions from the following projects to the work reported here are gratefully acknowledged.

- EPSRC EP/L016680/1 DTC in Wind and Marine Energy Systems
- FP7-ENERGY-2013.10.1.6: 609795 IRPWind
- EPSRC EP/N006224/1 MAXFARM

The contributions of Lindsay Amos and Adam Stock are, also, gratefully acknowledged.

**CONTENTS**


# Validation of StrathFarm in-house modelling tool

Romans Kazacoks

April 2019

Wind Energy Systems Doctoral Training Centre, Electronic & Electrical Engineering Department, Strathclyde University, Glasgow, The United Kingdom


# 1 Abstract/Executive Summary

The report validates StrathFarm, which is an in-house wind farm modelling tool developed in the University of Strathclyde. StrathFarm was specifically developed for fast simulation of wind farms to enable estimation of performance over different mean wind speed, turbulence intensity and wind speed direction.

Additional, this report investigates the effects of wind flow direction on the loads on wind turbines within a wind farm, to determine the most critically loaded wind turbines for different wind farm layouts and their dependence on the direction of wind flow. The dependency of power efficiency on the wind flow direction is also considered in this report. Here is considered mainly fatigue loads of wind turbines. Therefore, extreme loads are beyond the scope of this investigation. Damage equivalent loads (DELs) are used to represent the fatigue loads in this study. DELs are calculated according to IEC 61400 standards [1]. The investigation is performed for two wind speeds, below (8 m/s) and above (15 m/s) rated.

The investigation has shown that StrathFarm works accurate. However, there are some moments, where StrathFarm produces suspicious output data. The suspicious behaviors or key findings during the validation/examination of StrathFarm and the effect of wind flow direction on different layouts:

- At the begging of the examination, StrathFram had issues with the changes of the flow direction. The specified angle of flow direction did not work accurate. That issues with the flow direction have been fixed. Currently, the flow direction works accurate.

- The suspicious data output was spotted for regular layout at 70 degrees wind direction flow as shown in Figure 7. The values of DELs are unexpectedly high for 1,2,5-7,9-11,12-15, 17-19 wind turbines compared to 3, 4, 8, 12, 20 machines. It was caused by the continuous wind changes for 1, 2, 5-7, 9-11, 12-15, 17-19 wind turbines. Possibly, the continuous wind changes are result of wake meandering, which produced by the upwind turbines.

- In the irregular layout at 8 m/s steady flow and 80-degree wind direction for 19th wind turbine is experienced unusual high wind speed. Possibly, the wake meandering of the upwind wind turbine, which is the 20th unit, produces the unusual high wind speed for the 19th wind turbine.

- In the installed regular layout at zero-degree flow direction, the first row of wind turbines, which includes 1-4 machines, are experienced by unusual high fatigue loads compared to the fatigue loads of same machine at the different angle of wind flow direction.

- The three layouts, which are considered in this study, demonstrate that the majority of the maximum fatigue loads occur at the range 40 and 70 degrees. Possibly, that is the consequences of the wake meandering through the propagation downwind within the layout and other influences such the extent of below and above rated operation. However, there are case, where the maximum loads appeared at 0 and 90 wind flow directions.

- The lowest power efficiency occurs at 10 degree flow direction angle for the three layouts. The regular layout is experienced same power efficiency (87%) at five and eight diameters spacing among turbine in the wind flow direction. The highest power efficiency occurs at wind flow angles, which corresponds to the angles, which produce the highest fatigue loads.

- The regular and irregular layouts are almost similar apart from one row of wind turbines. However, there are dissimilates between the distribution of DELs in regular and irregular layouts. Possibly, there are statistical uncertainties in this study. It means that the simulation time and number of seeds can be increased in order to minimize the statistical uncertainties.

Additional work is required to validate some of these results, particularly by direct comparison to the actual performance of a real wind farm with the same layout experiencing the same wind speed conditions.

## 1. Introduction

The main goal of this report to validate StrathFarm, which is an in-house wind farm modelling tool, developed at the University of Strathclyde. StrathFarm was specifically developed for fast simulation of wind farms to enable estimation of performance over different mean wind speed, turbulence intensity and wind speed direction. Here the wind turbines are chosen to be the 5MW SuperGen turbines, which are similar to 5MW NREL wind turbine model and repeat the bladed aero-elastic wind turbine model of 5MW SuperGen up to 6P frequency.

The validation focuses on the effect of wind flow direction on the loads on wind turbines within a wind farm, to determine the most critically loaded wind turbines for different wind farm layouts and their dependence direction of wind flow. The three different layouts of the wind farm are considered. The procedure of validation is based on IEC 61400 standards [1] of fatigue loads analysis. Therefore, the extreme loads analysis is beyond of the scope of this work. In addition, the impact of power curtailment, which is 20%, on the wind turbine fatigue loads is investigated.

## 2. Model

As mentioned previously, StrathFarm is fitted with 5MW SuperGen wind turbine model. Table 1 summarises the design parameters of 5MW SuperGen, which can be slightly different from 5MW NREL wind turbine.

| | |
|---|---|
| Rated power | 5 MW |
| Number of blades | 3 blades |
| Rotor position | Up-wind |
| Control | Collective pitch |
| Speed type | Variable |
| Transmission gearbox ratio | 97 |
| Rotor diameter | 126 m |
| Hub height | 90 m |
| Cut-in wind speed | 4 m/s |
| Rated wind speed | 11.4 m/s |
| Cut-out wind speed | 25 m/s |
| Rotor speed | 6.9-12.1 rpm |
| Overhang | 5 m |
| Shaft tilt | 5 degrees |
| Pre-cone | 2.5 degrees |
| Rated tip speed | 80 m/s |
| Blade mass | 17 725 kg |
| Rotor mass with hub | 109 955 kg |

**Table 1:** The key parameters of wind turbine aero-elastic model.

## 3. Analysis

The effect of wind flow direction on the fatigue load distribution within the wind farm and power efficiency of the wind farm is investigated for three wind farm layouts (regular, installed regular and irregular). Figure 1 depicts the two layout, regular and installed regular. The irregular layout is shown in Figure 14. Each of these three layouts is examined for different angles of wind flow direction, from zero to 90 degrees in 10 degrees steps (wind direction angle $\in [0:10:90]$). Figure 2 shows the direction of the wind flow from zero to 90 degrees. At zeros degree, the wind flow goes from the west to the east. At 90 degrees, the wind flow goes from the north to the south. The wind flow direction rotates clockwise. Note the rotor of wind turbines are oriented towards the wind. Therefore, there is no yaw error for the wind turbines in the StrathFarm simulation wind farm modelling tool.

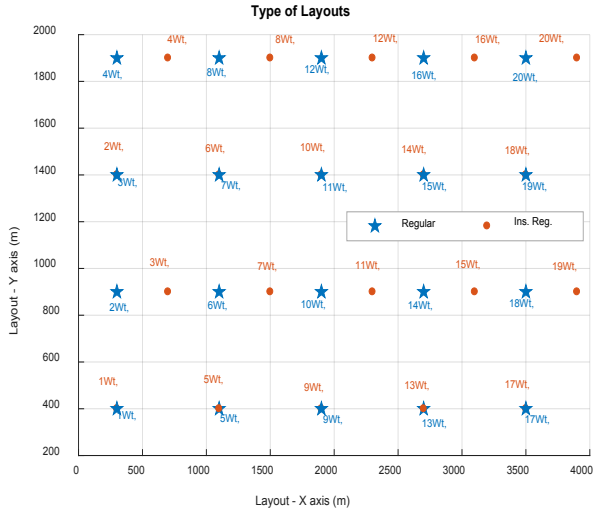


**Figure 1:** Two layouts of this study (Regular-blue star and Installed regular - red dot).

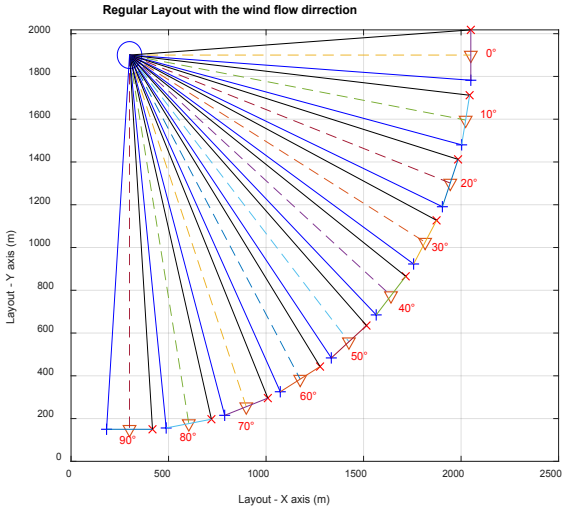


**Figure 2:** Orientation of wind flow direction for the wind turbines.

Additionally, the effect of power curtailment on loads is examined in this study. The power curtailment is applied at the wind farm level through wind farm controller. This study assumes a 20% power curtailment. Therefore, each turbine within the layout has 20 % cut of power production. The effect of power curtailment on the loads is examined for each layout and wind flow direction.

### 3.1. Initial conditions

The analysis was performed using two mean wind speed (8 and 15m/s) during normal power production conditions or design load case (DLC) 1.2 with normal turbulence model (NTM) set according to the IEC standards [1], i.e. turbulence intensity 0.12. The below rated region is represented by the 8 m/s wind speed and above rated region represented by 15 m/s. In-line with IEC standards, 6 different 'seeds' (i.e. random initiating points of the simulation) are employed per mean wind speed to reduce the uncertainty arising from the stochastic nature of the wind field.

## 3.2. References frames

This report focuses on the fatigue loads of the blade root and tower base. Hence, Figure 3 and Figure 4 depict the reference frames of blade root and tower base.

- The reference coordinate system of blade root is:
    - The X-axis follows same direction as the wind flow.
    - The Y-axis is tangential to a rotor plane, fixed to blade root and does not rotate with pitch.
    - The Z-axis follows along the span-wise or deflected neutral (pitch) axis.
- The reference coordinate system of tower base is:
    - The X-axis points along the wind flow to downstream.
    - The Z-axis is parallel to the neutral axis of tower.
    - The Y-axis is horizontal, to give a right-handed co-ordinate system independent of direction of rotation and rotor location upwind or downwind of the tower.

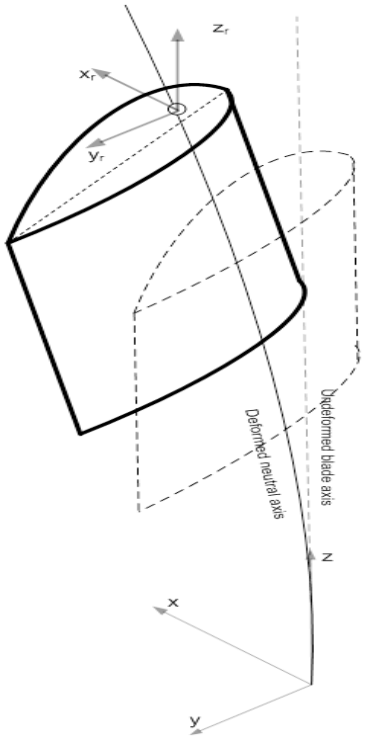


**Figure 3:** Blade root axes [2].

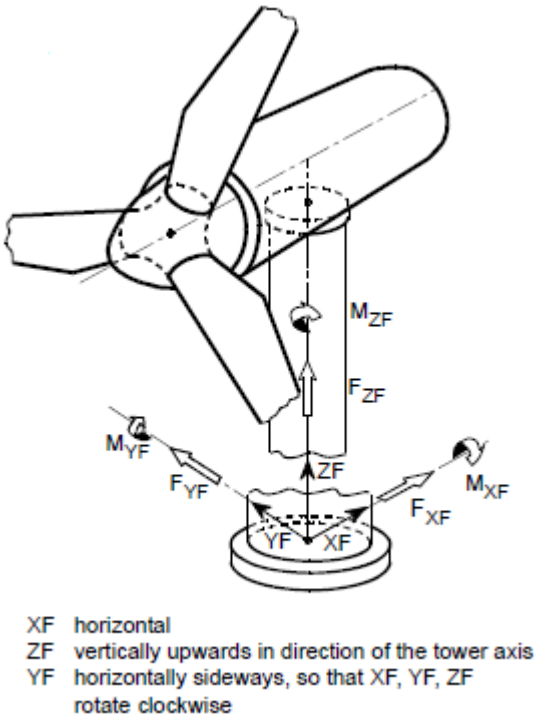


**Figure 4:** Tower base axes [3].

## 3.3. Damage equivalent loads

Damage equivalent loads (DELs) estimates are based on Palmgren-Miner linear cumulative damage theory [4], which assumes that fatigue damage increases linearly as a function of number of cycles, until it reaches the prescribed life exhausted of material [5]. Additionally, it assumes that only cycle load range contributes to fatigue damage, i.e. there is no contribution to fatigue damage from the mean value of cycles. Equation 1 shows the formula for the calculating DELs.

$$L_{DEL} = \left(\frac{\sum_{ip}\left(\sum_i^k n_i \, L_i^m\right)}{t_{sim}\, f}\right)^{\frac{1}{m}} \quad (1)$$

Where, $n_i$ is number of cycles, $L_i$is load range at bin, $m$ is Wöhler coefficient, $t_{\mathrm{sim}}$ is simulation time and $f$ is the reference frequency. The Rain flow counting (RFC) [6]–[8] is applied to count load range, mean and amount of cycles in a time series. According to the default calculation of DELs, the load range (maximum and minimum) contributes to fatigue. Therefore, the default calculation of DELs assumes that the mean load is equal to zero, which means the load cycle is completely reversed.

### 3.4. Materials

The damage equivalent loads (DELs) are used to presents the fatigue loads in this study. For the calculations of the DELs, Wöhler coefficients of 4 and 10 are used. These coefficients characterize the gradient of a material's Wöhler SN curves. Wöhler coefficients of 4 and 10 are used for steel and composite materials, respectively. The hub and tower are made from steel, but the blades are from composites.

## 4. Results

### 4.1. Accuracy check

This section shows the accuracy of changing direction of the wind flow in Strath farm as there were some issues related the changing the wind flow direction previously. The regular layout will be used to check the accuracy of the changing direction of wind flow in this document.

Figure 5 depicts the regular layout, steady flow and wind direction (zero degrees). Each wind turbine is depicted by the blue cross (X) and four line text. The first line text stands for:

1) Number of wind turbine (Wt)
2) Mean wind speed experienced by the wind turbine.
3) Calculated DELs
4) Mean value of instantaneous load.

Figure 5 depicts the regular layout at the steady flow and wind direction (zero degrees) with 15m/s mean wind speed. The wind flow goes from the west to the east. The wind speed, which experienced by wind turbines, decreases in the layout from the left to right. That happens that in the wind flow direction, every next wind turbine is located in the wake of the upwind wind turbine. The values of DELs and mean instantaneous loads increase for the machines, which are located in the wake of other wind turbines.

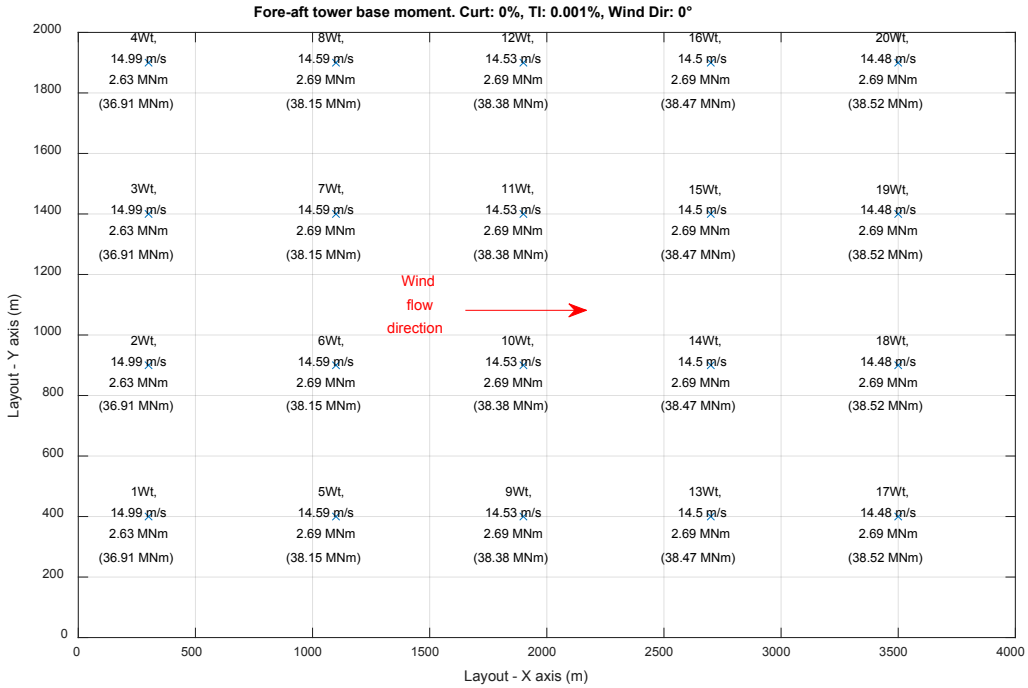


**Figure 5:** Regular layout with data of fore-aft tower base moment, no turbulence and zero degree wind flow direction of 15m/s mean speed.

Figure 6 depicts the effect of changes wind flow direction for the regular layout. Figure 6 corresponds to the regular layout, 15 m/s steady flow, fore–aft tower base moments and 90 degrees flow direction (the red arrow indicates the direction of the wind flow). So, the wind flow goes from the North to the South. The values of wind speed, DELs and instantaneous moment change in same order as the values at zero degree direction of wind flow, which are shown in Figure 5.

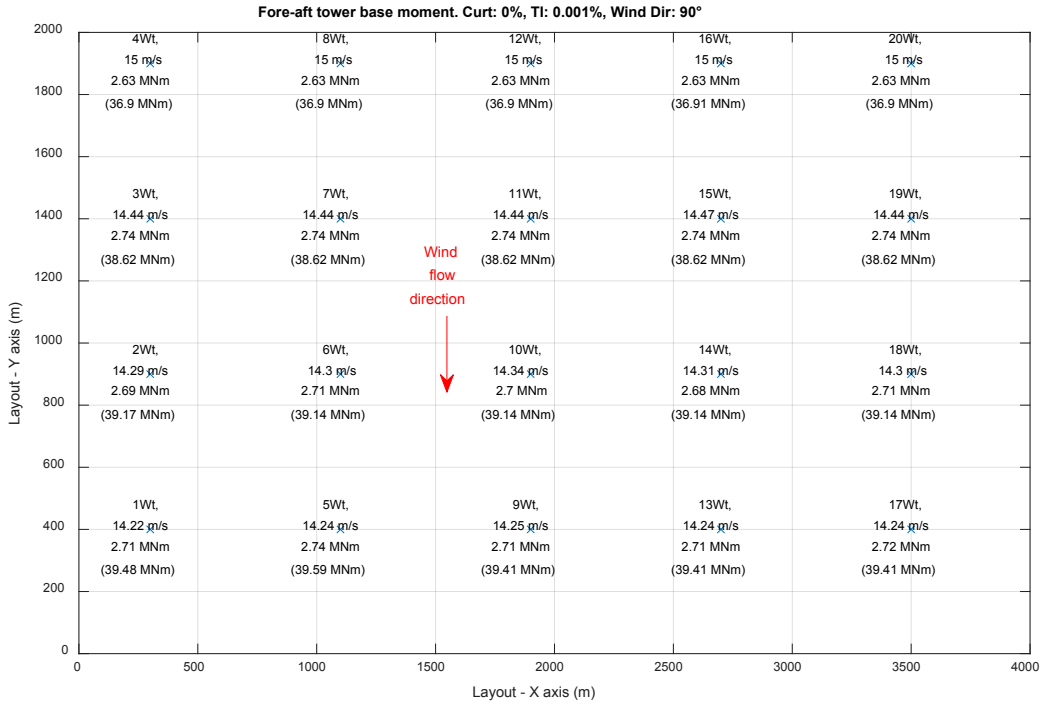

**Figure 6:** Regular layout with data of fore-aft tower base moment, no turbulence and 90 degrees flow direction of 15m/s mean speed.

Figure 5 and Figure 6 demonstrate there is no an issues regarding the changes on the wind flow direction in StrathFarm.

## 4.2. Suspicious behavior

The previous section has demonstrated that the changes of wind flow direction work accurate. In this study three different layouts, two wind speeds (below and above rated), two turbulence conditions (0 and 12% turbulence intensity), curtailment and 10 different inflow angles (0:10:90 inflow angle) were examined. Therefore, some combinations of above mentioned parameters produced suspicious data output. Therefore, this section highlights these occurred suspicious cases. This section is divided into the three sub-sections, which relate to the three examined layouts of this study.

### 3.1.1 Regular layout

The suspicious data output was spotted for regular layout at 70 degrees wind direction flow as shown in Figure 7. The values of DELs (the third line in text) are unusual high for 1,2,5-7,9-11,12-15, 17-19 wind turbines compared to 3, 4, 8, 12, 20 machines. Additionally, there are suspiciously high values of wind speed, which are shown by the second line, in the above-mentioned wind turbines.

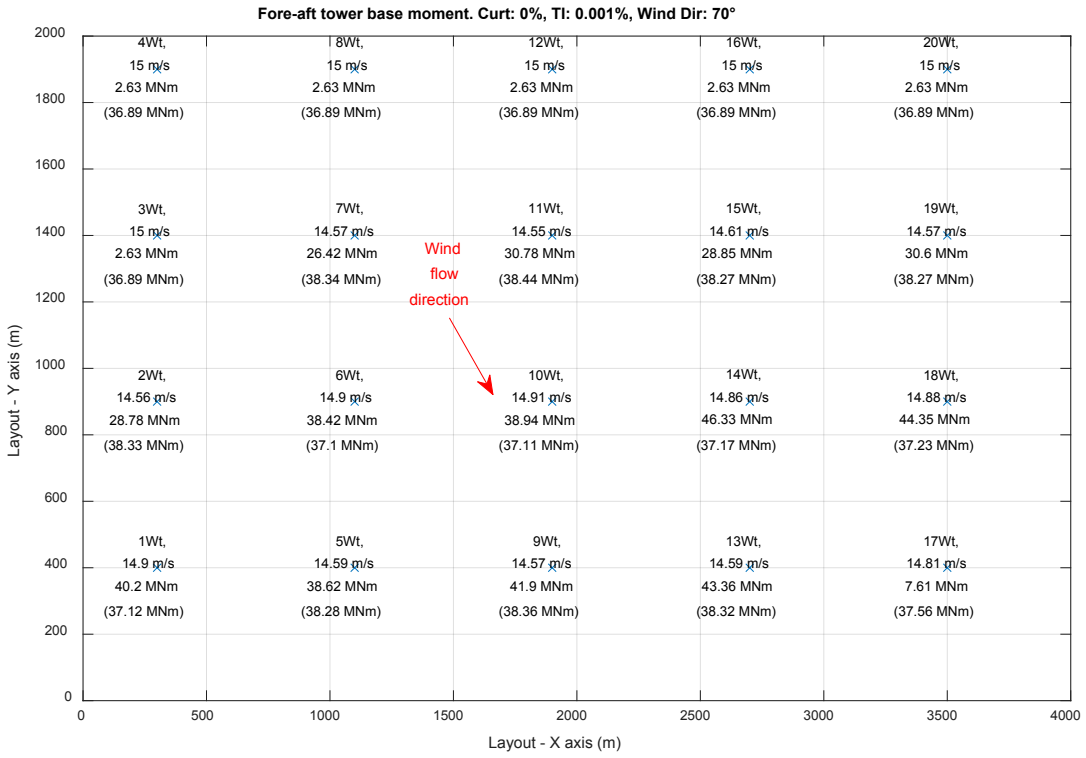


**Figure 7:** Irregular layout with data of fore-aft tower base moment, no turbulence and 90 degrees flow direction of 15m/s mean speed.

The next step is to look at the power spectral density (PSD). Figure 8 shows PSD of fore-aft tower base moment for each wind turbine of regular layout, where there is 15 m/s steady wind flow with 70 degrees wind direction. In Figure 8 there are two patterns. The lower pattern represents the 3, 4, 8, 12, 20 wind turbines. The upped (shifted) pattern corresponds to 1, 2, 5-7, 9-11, 12-15, 17-19 machines, which experienced higher values of DELs.

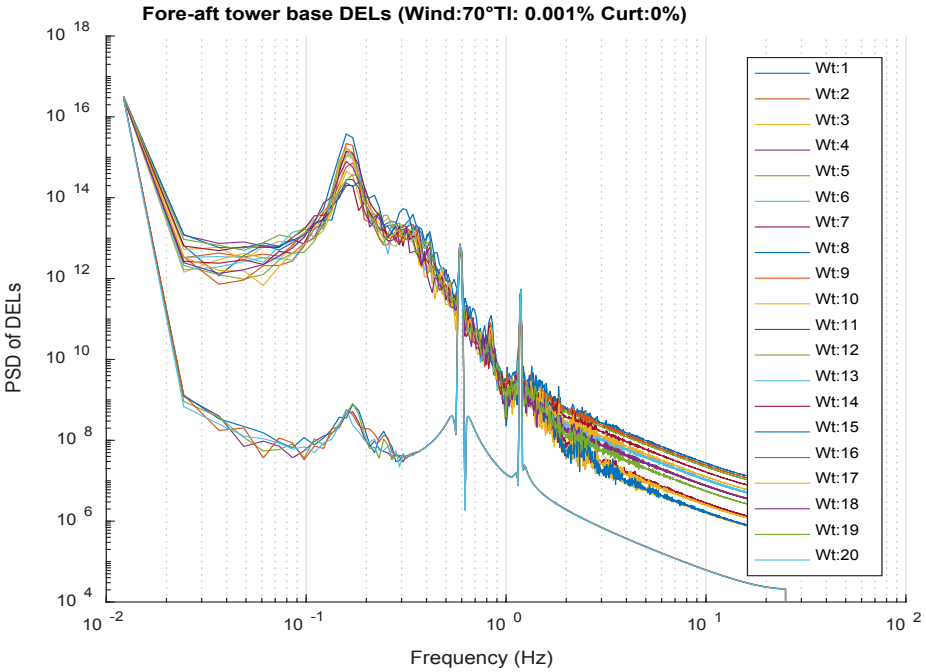


**Figure 8:** Power spectral density of fore-aft tower base moment at the regular layout. The conditions: 15m/s steady flow, 70 degrees, no curtailment

Figure 9 and Figure 10 depict the PSD of side-to-side of tower base and out-of-plane blade root moments, respectively. Both these figures include the two before-mentioned patterns, which follow same description as the provided for the patterns in the PSD of fore-aft tower base moment. The PSD of in-plane blade root moment is not presented, as there are no unusual high values of in-plane blade root moment.

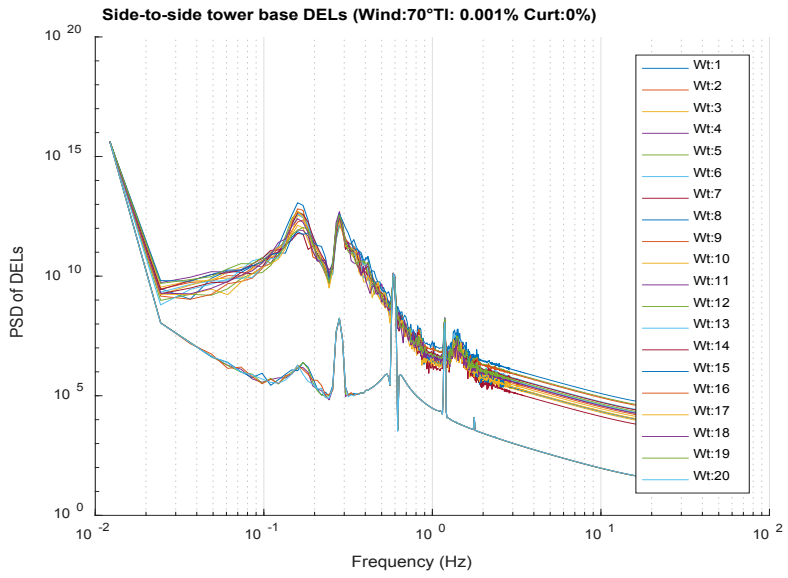

**Figure 9:** Power spectral density of side-to-side tower base moment at the regular layout. The conditions: 15m/s steady flow, 70 degrees, no curtailment

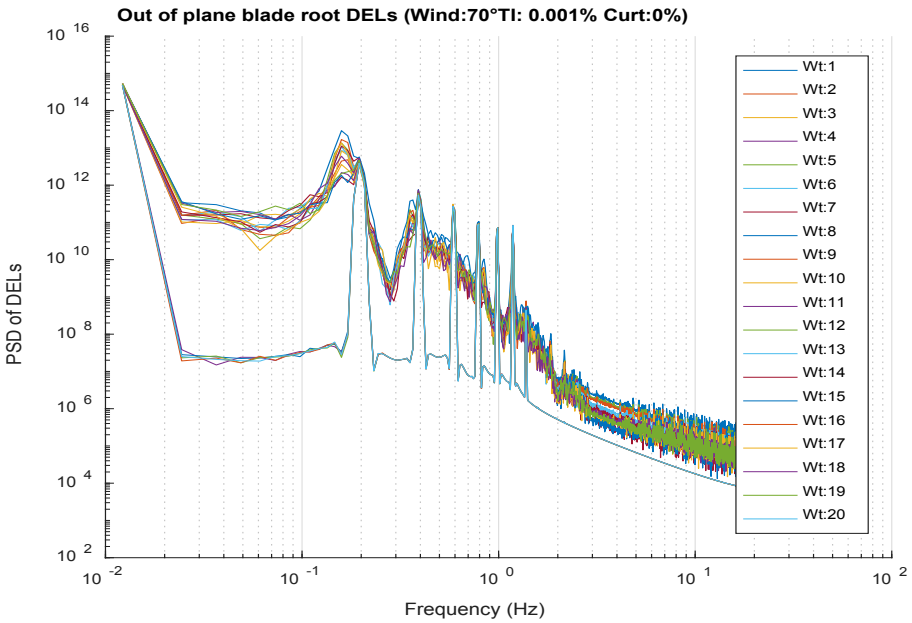


**Figure 10:** Power spectral density of out-of-plane blade root moment at the regular layout. The conditions: 15m/s steady flow, 70 degrees, no curtailment

Figure 11 depicts the wind speed deficit of the wind turbine in the regular layout with 15m/s steady flow and 70 degrees wind direction. Figure 11 demonstrates that there is continuous wind changes for 1, 2, 5-7, 9-11, 12-15, 17-19 wind turbines. The rest of wind turbines from the layout do not experienced the continuous wind speed variation. Possibly, the continuous wind changes are result of wake meandering, which produced the by the upwind turbine.

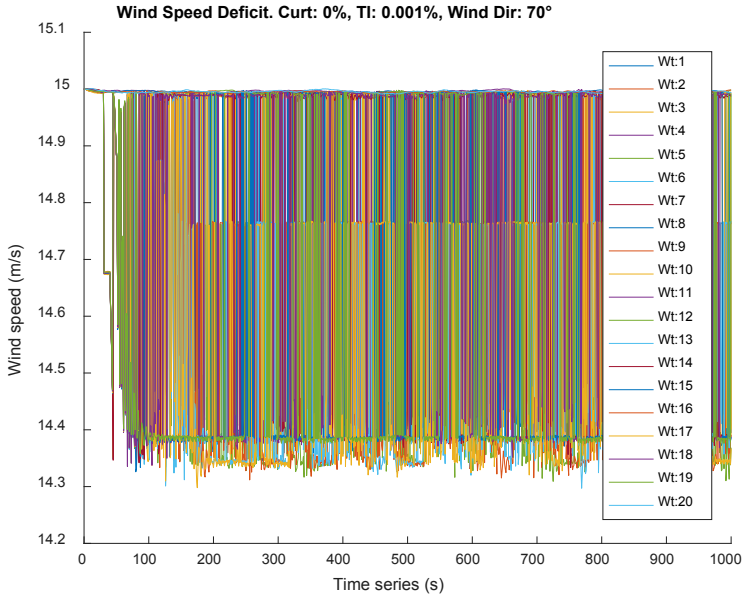


**Figure 11:** Wind speed deficit of the regular layout at 15m/s steady flow, 70 degrees wind direction

There are no unusual values of output data at same condition with turbulent (12% reference intensity) flow as shown in Figure 12 and Figure 13. Figure 12 depicts the regular layout with output data values for the fore-aft tower base moments at 15 m/s turbulent flow with wind 70 degrees direction.

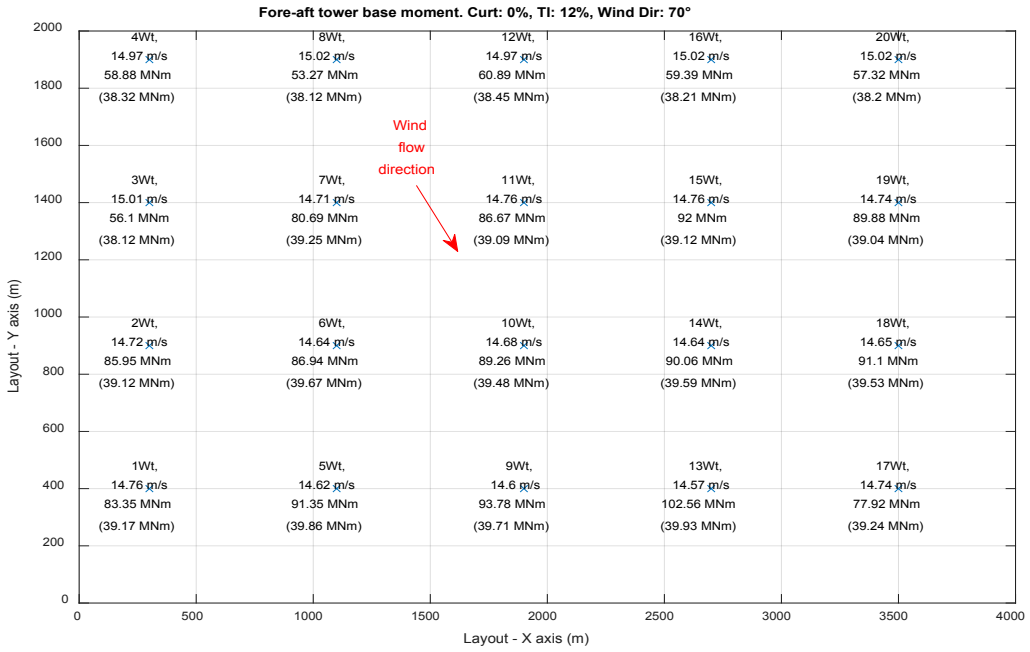


**Figure 12:** Regular layout with data of fore-aft tower base moment, 12% turbulence reference intensity and 70 degrees flow direction of 15m/s mean speed.

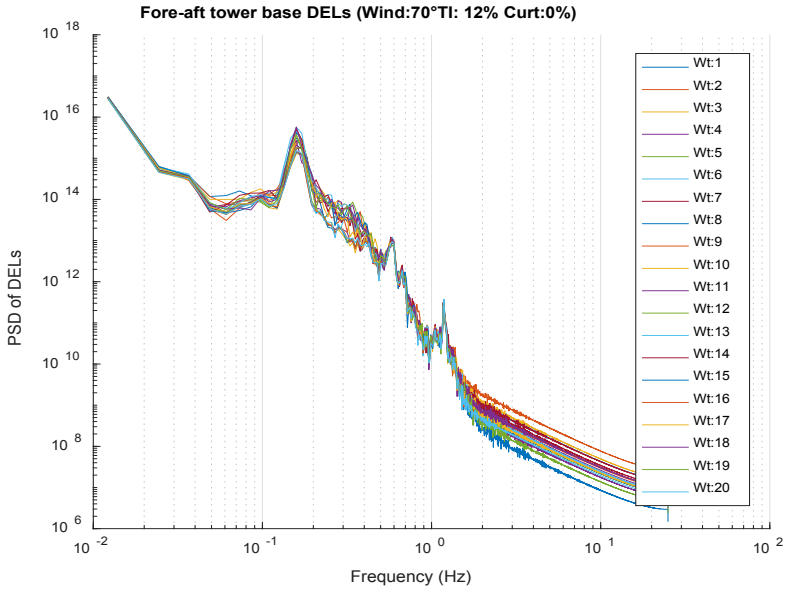


**Figure 13:** Power spectral density of fore-aft tower base moment at the regular layout. The conditions: 15m/s mean wind speed, 12% turbulence intensity, 70 degrees, no curtailment

Figure 13 demonstrates PSD of fore-aft tower base moment for each wind turbine at the regular layout with the mentioned earlier conditions. All twenty turbines have same pattern as shown in Figure 13.

### 3.1.2 Irregular layout

The suspicious output data was spotted for the irregular layout at 8 m/s steady flow and 80 degrees wind direction for 19th wind turbine as shown in Figure 14. The attention dragged by the high value of wind speed (the second line) at the 19th wind turbine.

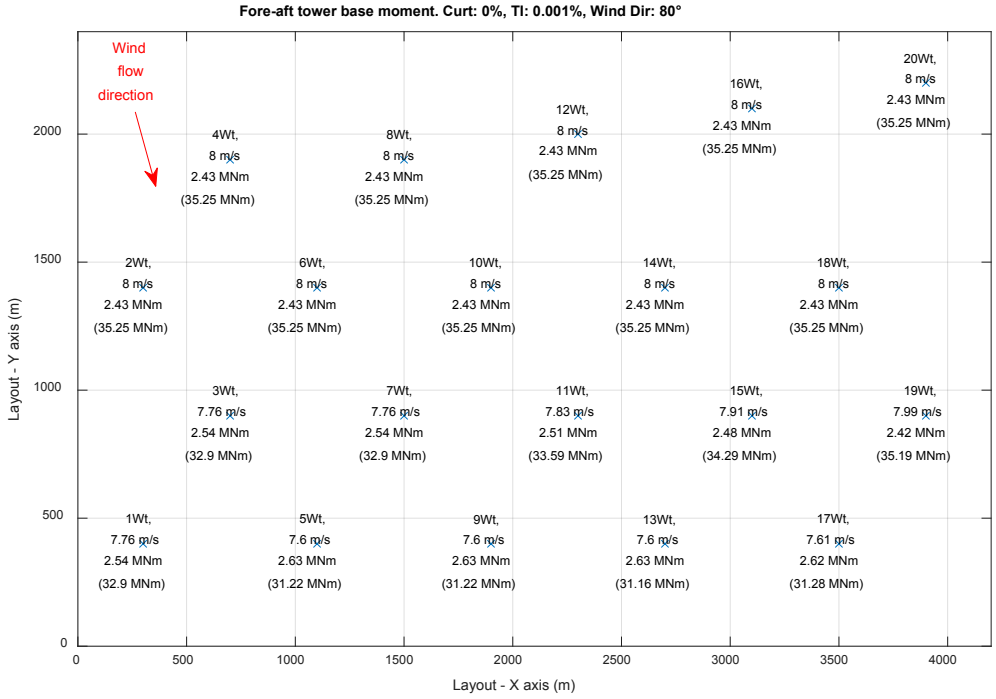


**Figure 14:** Irregular layout with data of fore-aft tower base moment, 8 m/s steady flow and 80 degrees flow direction.

Figure 15 depicts the changes of wind speed during the simulation for each wind turbine of Figure 14. Figure 15 repeats all parameters as Figure 14. Figure 15 shows that wind speed of the 19th wind turbine drops two times to value of ~7.53 m/s. The second nadir of wind speed curve of the 19th machine looks like a “spike”. Possibly, these two nadirs in the curve are results of the meandering wake of the upwind wind turbine, which is the 20th unit at Figure 14.

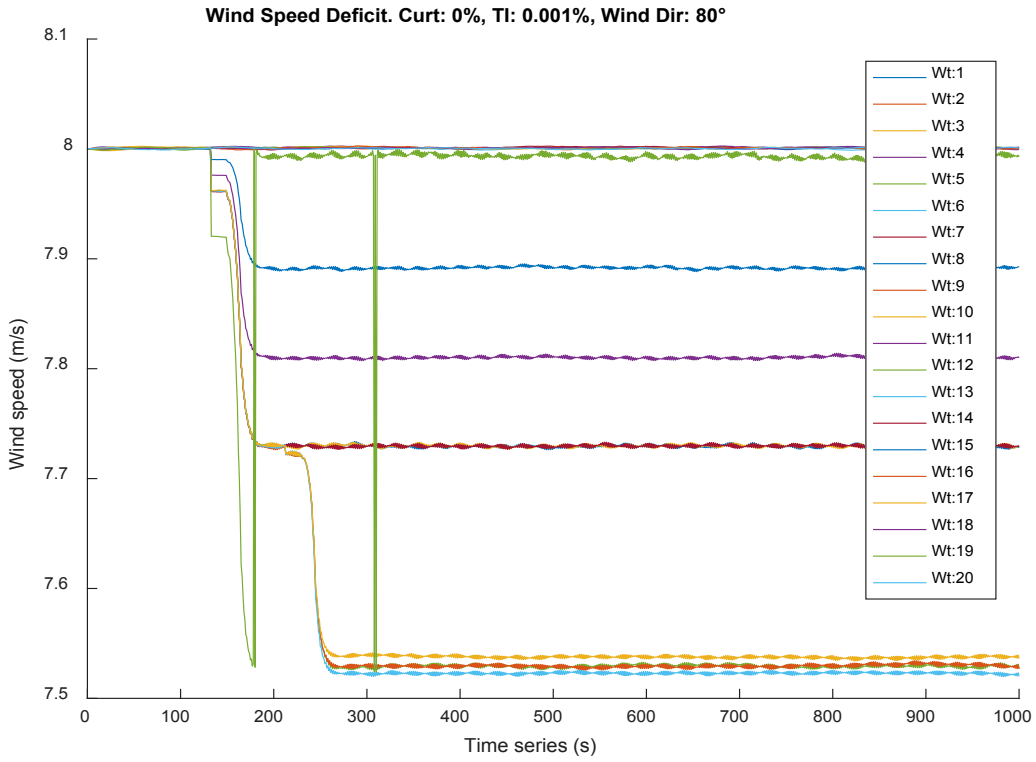


**Figure 15:** Wind speed deficit of the regular layout at 15m/s steady flow, 70 degrees wind direction.

The DEL and mean load values of the 19th wind turbine are similar to rest of wind turbines as shown in Figure 14. The PSD of fore-aft tower base and out-of-plane blade root moments are shown in Figure 16 and Figure 17 respectively. The PSD graphs of both figures do not show any negative effect from the suspicious changes of wind speed in the 19th wind turbine.

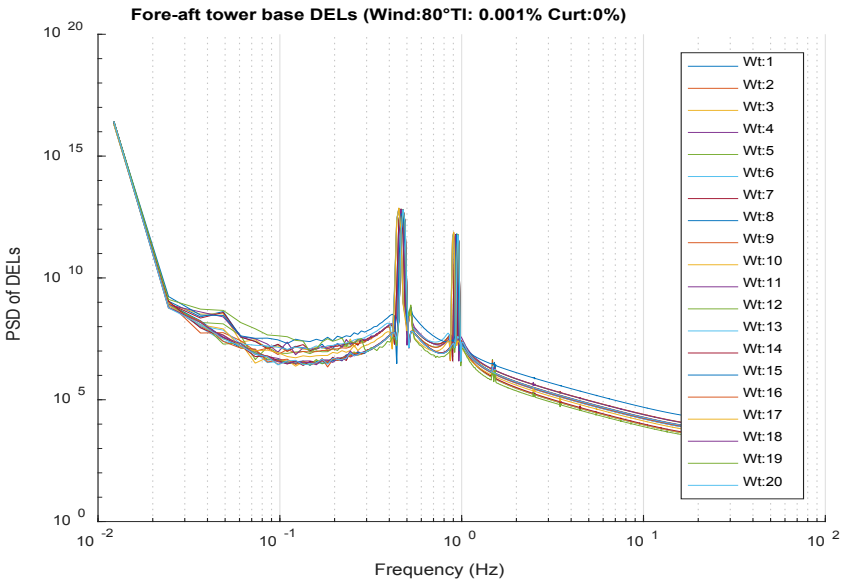


**Figure 16:** Power spectral density of fore-aft tower base moment at the irregular layout. The conditions: 8m/s steady flow, 80 degrees, no curtailment.

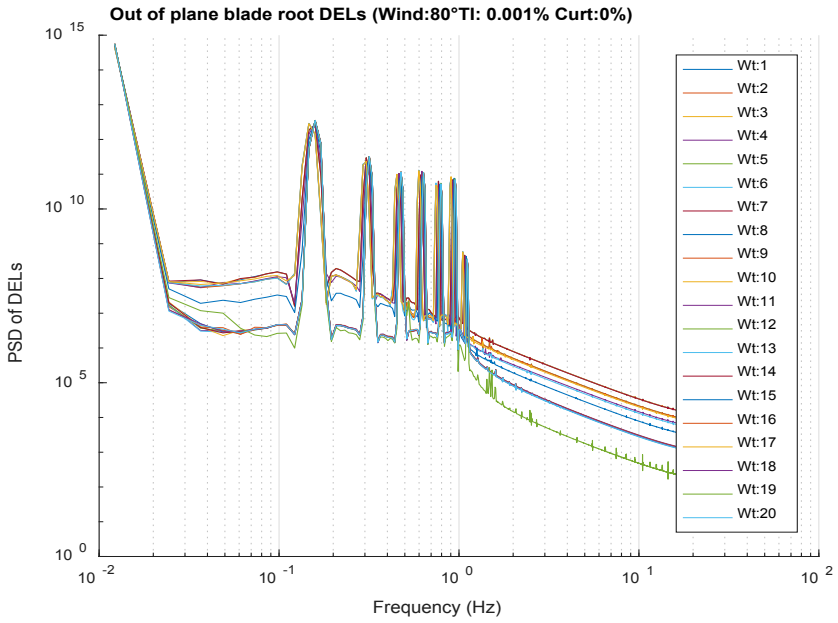


**Figure 17:** Power spectral density of out-of-plane blade root moment at the irregular layout. The conditions: 8m/s steady flow, 80 degrees, no curtailment.

### 3.1.3 Installed regular layout

For the installed regular layout, the suspicious behavior was spotted in the first row of wind turbines, which includes 1-4 machines. At zero angle wind flow direction the wind turbines in the first row are experienced by high fatigue loads compared to the different angle of wind flow. Figure 18 and Figure 19 show the installed regular layout at 15 m/s wind speed with 12% turbulence level for zero and 10 degrees wind flow angle, respectively.

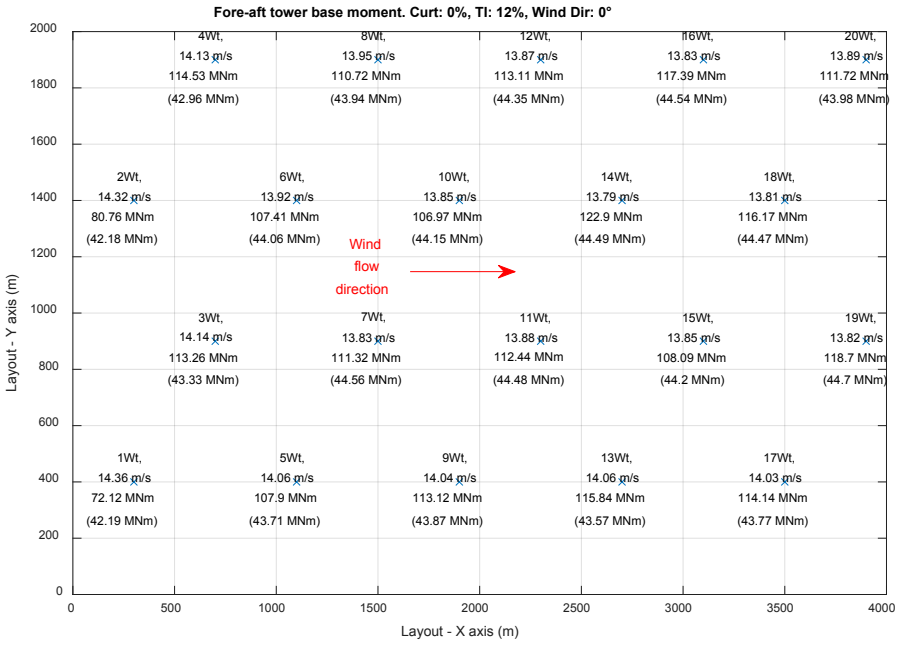

**Figure 18:** Installed regular layout with data of fore-aft tower base moment, 15 m/s steady flow and 0 degrees flow direction.

In Figure 18 the values of DELs at the wind turbines of the first row are almost double the values of DELs at same wind turbines in Figure 19. Possibly, this differences in DELs values is caused by the turbulence because there is no such difference in instantaneous loads at the steady wind flow.

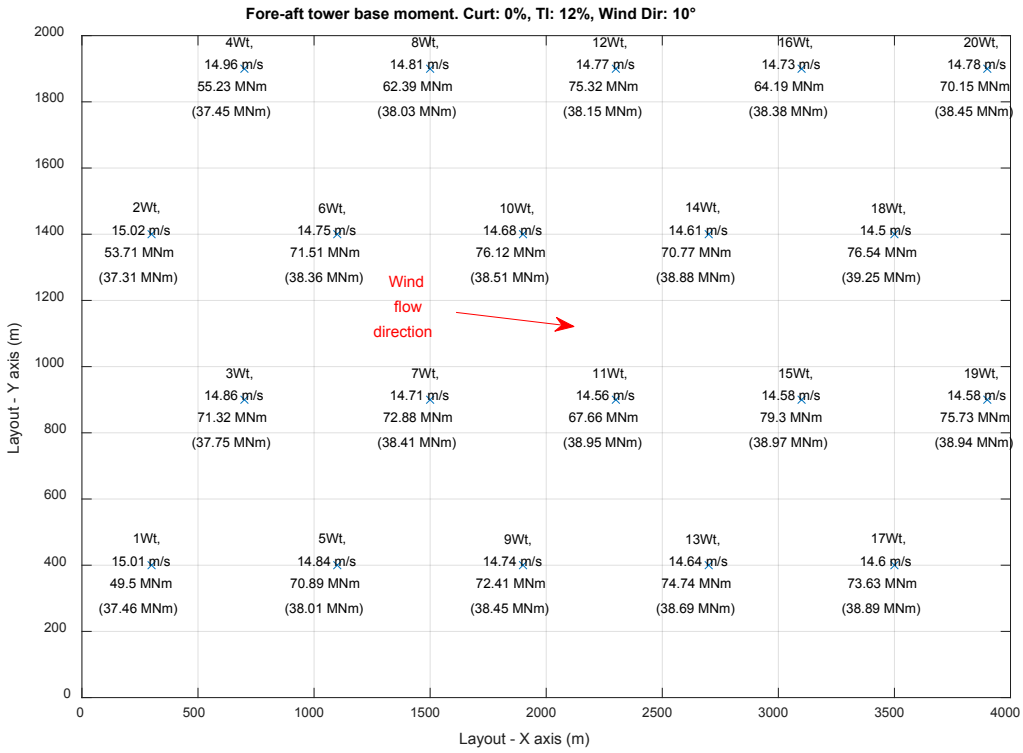


**Figure 19:** Installed regular layout with data of fore-aft tower base moment, 15 m/s steady flow and 10 degrees flow direction.

## 4.3. Effect of wind direction on the layouts

The three layouts in Figure 2 are considered here, with and without curtailment. The wind turbine with the maximum DELs is found within each layout for each direction of wind flow in Figure 3. For each layout, the out-of-plane and in-plane blade root DELs for Wohler coefficients 4 and 10 are estimated. The fore-aft and side-to-side tower base DELs for Wohler coefficients 4 is estimated. For each layout, the maximum DELs by wind direction are determined for four different conditions as shown below:

- Below rated wind speed (8 m/s) with turbulence (0.12 Iref.) and no curtailment.
- Below rated wind speed (8 m/s) with turbulence (0.12 Iref.) and 0.2 curtailment.
- Above rated wind speed (15m/s) with turbulence (0.12 Iref.) and no curtailment.
- Above rated wind speed (15m/s) with turbulence (0.12 Iref.) and 0.2 curtailment.

Each figure in this section highlights the wind turbine within the layout, which is experienced the highest DELs at the specific wind flow direction. The horizontal axis corresponds to the direction of inflow angle. The vertical axis stands to the number of wind turbine.

### 3.1.4 Regular layout

Figure 20 demonstrates the graphs corresponded to blade root DELs for Wolher coefficient 4 and 10. The fore-and-aft and side-to-side tower base DELs are shown in Figure 21. The graphs of Figure 20 and Figure 21 demonstrate that at below rated wind speed, the maximum DELs occur at 40 degrees inflow angle for all four variables. For the above rated wind speed without the curtailment, the highest DELs appeared mainly at 60 degrees apart the in-plane blade root DELs, which has the highest values at 20 degrees. For the above rated wind speed with the curtailment, the maximum DELs appear in range from 50 to 70 degrees depended on the variables. Thus, for the four variables the maximum DELs occurred in range from 40 to 70 degrees wind flow direction at the regular layout.

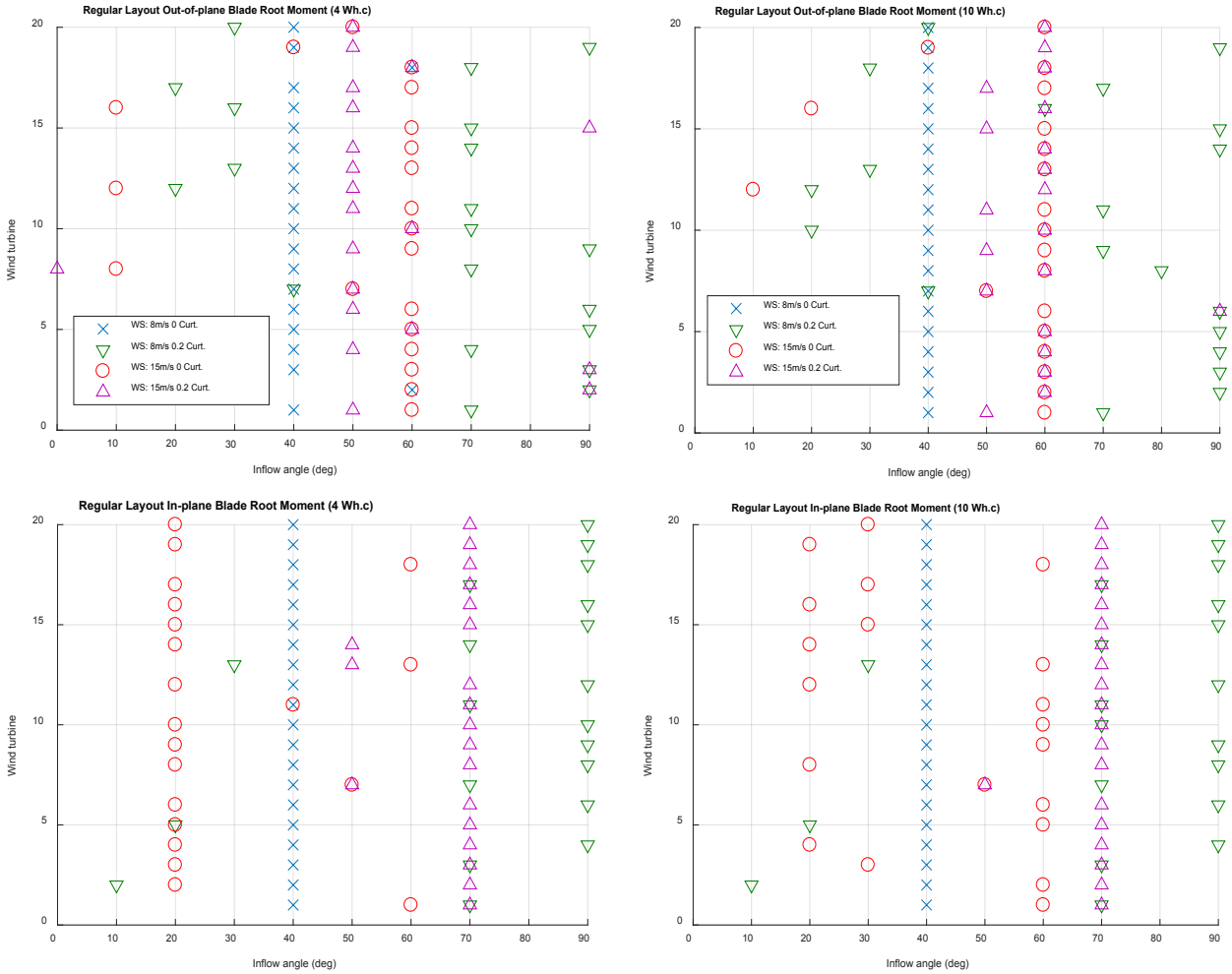


**Figure 20:** The highlighted wind turbine, which are experienced the maximum DELs of out-of-plane and in-plane blade root moments within the *regular layout*, at different wind flow direction angle (0:10:90°) and four different conditions (below or above rated and without/with curtailment) for Wohler confidents 4 and 10.

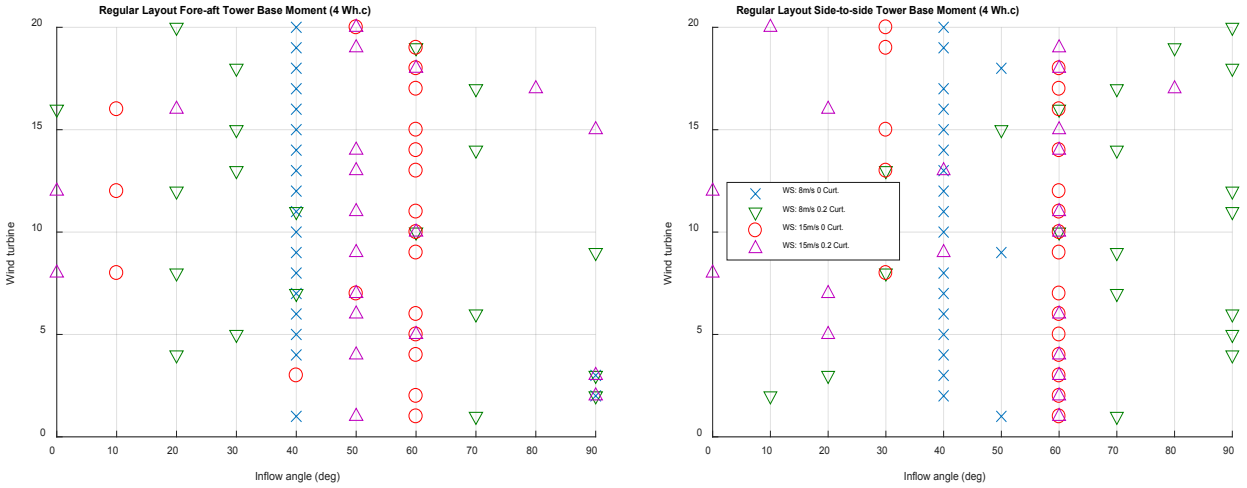


**Figure 21:** The highlighted wind turbines, which are experienced the maximum DELs of *fore-aft and side-to-side tower base moments* within the *regular layout*, at different wind flow direction angle (0:10:90°) and four different conditions (below or above rated and without/with curtailment).

### 3.1.5 Installed regular layout

Figure 22 and Figure 23 shows DELs for blade root (out-of-plane and in-plane) and tower base (fore-aft and side-to-side) DELs. For fore-aft tower base and out-of-plane blade root, the most of maximum DELs occur at 0, 60 and 70 wind direction angle. The highest DELs occur at 30, 50, 60, 70 degrees prevailing the wind flow angle for in-plane blade root moments at both Wohler coefficients. The highest side-to-side tower base DELs are more spread compared to other components. However, there are few prevailing wind flow direction, which are 0, 30, 60 and 70.

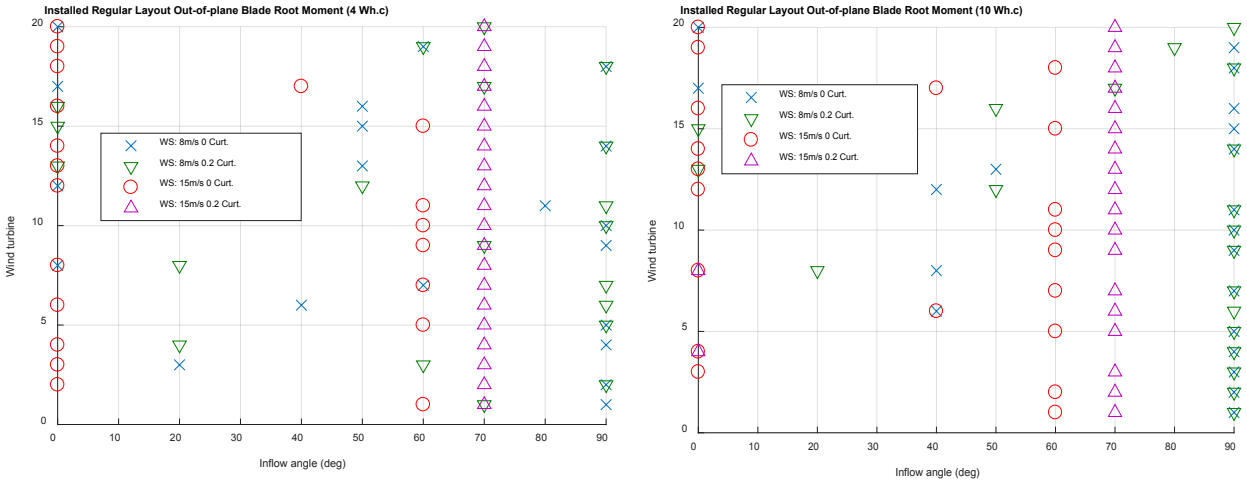

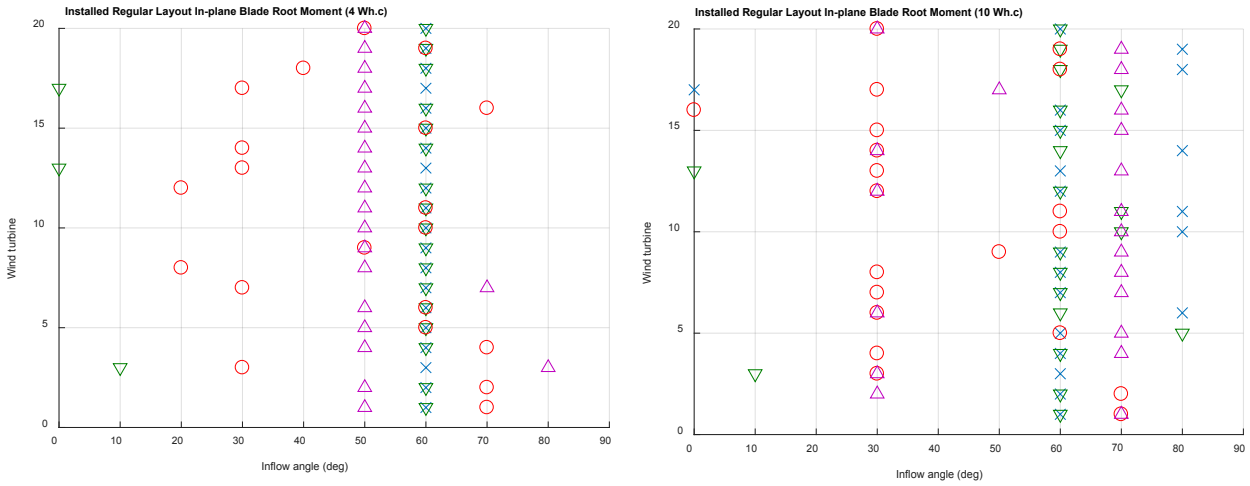


**Figure 22:** The highlighted wind turbine, which are experienced the maximum DELs of out-of-plane and in-plane blade root moments within the installed *regular layout*, at different wind flow direction angle (0:10:90°) and four different conditions (below or above rated and without/with curtailment) for Wohler confidents 4 and 10.

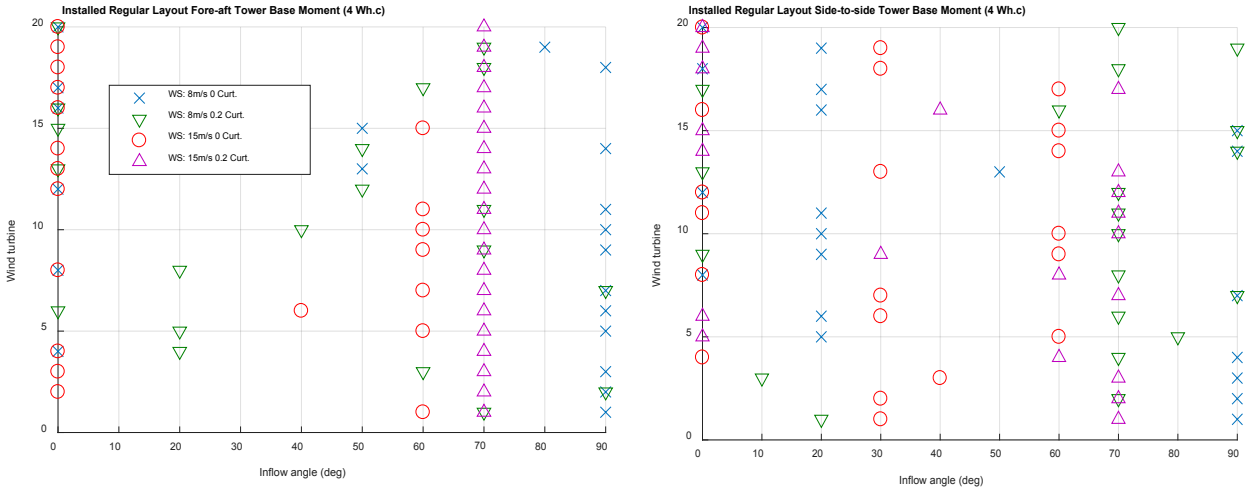


**Figure 23:** The highlighted wind turbines, which are experienced the maximum DELs of *fore-aft and side-to-side tower base moments* within the installed *regular layout*, at different wind flow direction angle (0:10:90°) and four different conditions (below or above rated and without/with curtailment).

### 3.1.6 Irregular layout

Figure 24 demonstrates the graphs corresponded to blade root DELs for Wolher coefficient 4 and 10. The fore-and-aft and side-to-side tower base DELs are shown in Figure 25. The wind flow directions, at 50 and 70 degrees produce the highest DELs for the out-of-plane and in-plane blade root. There are dissimilarities in wind flow direction, which produces the highest DELs, between out-of-plane and in-plane blade root. Therefore, the large amount of wind turbines, which are a power curtained, are experienced the highest out-of-plane blade root DELs at the above rated wind speed in the zero-

degree wind flow directions. The above rated wind speed with 90 degree flow direction produces the highest in-plane blade root DELs for the turbines with curtained power.

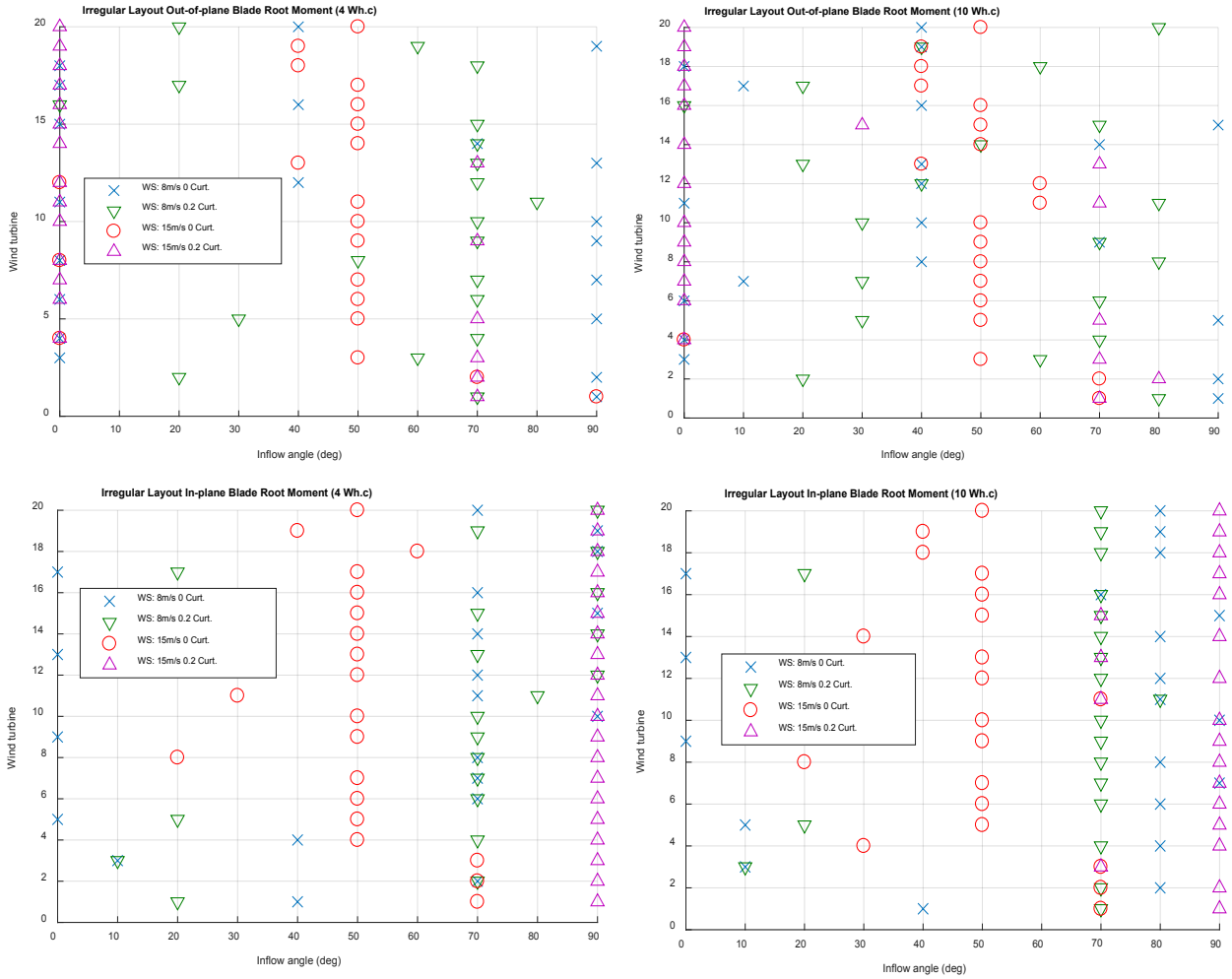


**Figure 24:** The highlighted wind turbine, which are experienced the maximum DELs of out-of-plane and in-plane blade root moments within the i*rregular layout*, at different wind flow direction angle (0:10:90°) and four different conditions (below or above rated and without/with curtailment) for Wohler confidents 4 and 10.

The fore-aft tower base DELs repeat almost the pattern of out-plane blade root DELs. Therefore, the fore-aft tower base DELs appear at 0, 50 and 70 wind flow direction. For the side-to-side tower base, the DELs are spread through among all wind flow directions. However, there are the three prevailing directions, which is 0, 60 and 70, as shown in Figure 25.

The regular and irregular layouts are almost similar apart from one row of wind turbines. However, there are dissimilates between the distribution of DELs in regular and irregular layouts. Possibly, there are statistical uncertainties in this study. It means that the simulation time and number of seeds can be increased in order to minimize the statistical uncertainties.

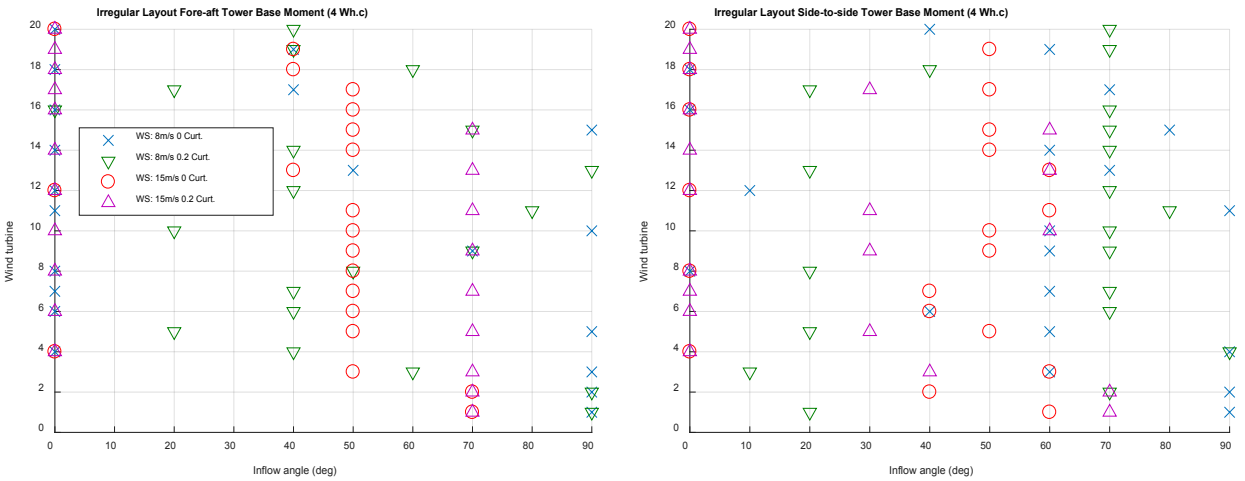


**Figure 25:** The highlighted wind turbines, which are experienced the maximum DELs of *fore-aft and side-to-side tower base moments* within the installed *regular layout*, at different wind flow direction angle (0:10:90°) and four different conditions (below or above rated and without/with curtailment).

## 4.4. Effect of wind direction on power production

In this section, the effect of wind flow direction on the power efficiency of a wind farm is investigated. The three layouts in Figure 2 and Figure 14 are again considered. The angle of wind flow direction varies from zero to 90 degrees in 10 degree increments. The power efficiency [9] of wind farm is calculated as in equation 2.

$$Eff_{power} = \frac{energy\ of\ whole\ wind\ farm}{(energy\ of\ one\ isolated\ turbine) * (number\ of\ Wts\ in\ farm)} \quad (2)$$

The power efficiency is calculated in below rated wind speed only as the wind speed deficit is not so significant in above rated region operation. For the above rated mean wind speed of 15 m/s chosen here, the measured minimum power efficiency is around 97.5%. Thus, only below rated wind speed is considered here. Figure 26 depicts the dependency of power efficiency on the wind flow direction for the three layouts (regular, installed regular and irregular). Figure 26 shows that the lowest power efficiency occurs at 10 degrees flow direction for the two layouts. For the irregular layout, 20 degrees wind demonstrate same low power efficiency as at 10 degrees. The curtailment does not have significant effect on the power efficiency as the trends of power efficiency with curtailment are similar, slightly shifted, to the trends without curtailment for the three layouts. For the regular layout, the graph of power efficiency is nearly symmetric about 45degrees, reflecting the symmetry of the layout, see Figure 1.

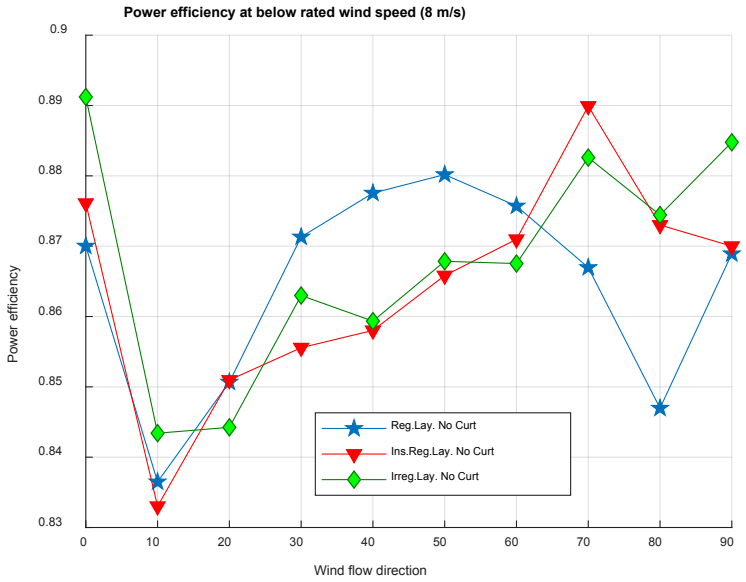


**Figure 26:** Changes power efficiency as a function different wind flow angle (0:10:90°) for the two layouts at below rated wind speed with/without curtailment.

In Lissaman et al. [10], It was shown that the geometry of turbine location and ambient turbulence intensity have high influence on power losses for a layout. Additionally, it was shown that, if the spacing among the turbines in the prevailing downwind direction is 10 diameters, then the power losses are below 10 %. In the regular layout in Figure 2 at zeros degree of prevailing wind direction, the spacing among turbines is eight diameters. In the perpendicular direction of wind flow direction, the spacing is five diameters between turbines. Figure 26 demonstrates that, with five and eight diameters spacing between turbines and a wind flow direction around 0 and 90 degrees, power efficiency is about 87%. That happens because wakes meander relative to the nominal direction of the wind, the extent, to which wakes from upstream turbines interact with a downstream turbine, varies randomly with time and the separation of the turbines, i. e. direction of wind speed. In addition, the turbulent wind speeds seen by each turbine varies randomly so that the mean wind speed seen be each turbine, also, varies randomly with its position in the array and direction of the wind speed. Consequently, due to the small number (6 seeds) and short duration of simulation runs, statistical uncertainty for each value plotted on Figure 26 remains substantial, implying that any estimation of direction of minimum power efficiency, with the same number and duration of runs as used here, would vary greatly. The shift of this estimate from the expected value of 0 degrees is thus not unexpected but gives some indication in the uncertainty in these results.

Additionally, the maximum power efficiency occurs with a prevailing wind flow direction of roughly 50 degrees for the regular layout. The highest DELs loads in below rated speed without curtailment occur at 40 degrees of wind flow direction as shown in Figure 20. For the irregular layout, the highest values of the power efficiency are at 0, 70 and 90 degrees. The flow direction at these directions produce the higher DELs. Therefore, the maximum power efficiency matches or coincides with the highest fatigue loads.

The highest power efficiency of the installed regular layout appears at 70 degrees. It again coincides with the maximum DELs in above rated wind speeds as shown in Figure 22. Therefore, there is correlation between the high power efficiency and the high DELs for the wind turbines within a layout.

## 5. Executive Summary

This study validates StrathFarm, which is a developed in-house wind farm modelling tool, and investigates the effect of wind flow direction on the fatigue loads on wind turbines within a wind farm, to determine the most critically loaded wind turbines for different wind farm layouts and their dependency on the direction of wind flow. Additionally, this study focusses on power efficiency in order to explore any correlation between the wind flow direction and the power efficiency of different layout. In this study, there are three layouts of the wind farm: regular, installed regular and irregular. Each layout is examined for four conditions: below and above rated wind flow with turbulence, 12% turbulence reference intensity, with and without curtailment (20% power curtailment in this study). The damage equivalent loads are used to calculate fatigue loads according to the IEC standards. The suspicious behaviors or key findings during the validation/examination of StrathFarm and the effect of wind flow direction for the three layouts:

- At the begging of the examination, StrathFram had issues with the changes of the flow direction. The specified angle of flow direction did not work accurate. That issues with the flow direction have been fixed. Currently, the flow direction works accurate.

- The suspicious data output was spotted for regular layout at 70 degrees wind direction flow as shown in Figure 7. The values of DELs are unexpectedly high for 1,2,5-7,9-11,12-15, 17-19 wind turbines compared to 3, 4, 8, 12, 20 machines. It was caused by the continuous wind changes for 1, 2, 5-7, 9-11, 12-15, 17-19 wind turbines. Possibly, the continuous wind changes are result of wake meandering, which produced by the upwind turbines.

- In the irregular layout at 8 m/s steady flow and 80-degree wind direction for 19th wind turbine is experienced unusual high wind speed. Possibly, the wake meandering of the upwind wind turbine, which is the 20th unit, produces the unusual high wind speed for the 19th wind turbine.

- In the installed regular layout at zero-degree flow direction, the first row of wind turbines, which includes 1-4 machines, are experienced by unusual high fatigue loads compared to the fatigue loads of same machine at the different angle of wind flow direction.

- The three layouts, which are considered in this study, demonstrate that the majority of the maximum fatigue loads occur at the range 40 and 70 degrees. Possibly, that is the consequences of the wake meandering through the propagation downwind within the layout and other influences such the extent of below and above rated operation. However, there are case, where the maximum loads appeared at 0 and 90 wind flow directions.

- The lowest power efficiency occurs at 10 degree flow direction angle for the three layouts. The regular layout is experienced same power efficiency (87%) at five and eight diameters spacing among turbine in the wind flow direction. The highest power efficiency occurs at wind flow angles, which corresponds to the angles, which produce the highest fatigue loads.

- The regular and irregular layouts are almost similar apart from one row of wind turbines. However, there are dissimilates between the distribution of DELs in regular and irregular layouts. Possibly, there are statistical uncertainties in this study. It means that the simulation time and number of seeds can be increased in order to minimize the statistical uncertainties.

Additional work is required to validate some of these results, particularly by direct comparison to the actual performance of a real wind farm with the same layout experiencing the same wind speed conditions.

## References


[1] I. E. Commission, "Wind Turbine—Part 1: Design Requirements, IEC 61400-1," Geneva, 2005.

[2] E. Bossanyi, "GH Bladed-User Manual, Version 4.4," *Garrad Hassan Bl.*, 2013.

[3] G. L. Rules, "Guidelines-IV Industrial Services-Part 2-Guideline for the Certification of Offshore Wind Turbines," 2012.

[4] M. Miner, "Cumulative damage in fatigue," *Appl. Mech.*, vol. 12, no. 3, pp. 159–164, 1945.

[5] P. Ragan and L. Manuel, "Estimation of Wind Turbine Fatigue Loads Using Time-Ragan, P., & Manuel, L. (2007). Estimation of Wind Turbine Fatigue Loads Using Time-Domain and Spectral Methods. 45th AIAA Aerospace Sciences Meeting and. Retrieved from http://arc.aiaa.org/doi/pdf/10.25," *45th AIAA Aerosp. Sci. Meet.*, 2007.

[6] S. Downing and D. Socie, "Simple rainflow counting algorithms," *Int. J. Fatigue*, vol. 4, no. 1, pp. 31–40, 1982.

[7] G. Glinka and J. Kam, "Rainflow counting algorithm for very long stress histories," *Int. J. Fatigue*, vol. 9, no. 4, pp. 223–228, 1987.

[8] ASTM E1049-85(2011)e1, "Standard Practices for Cycle Counting in Fatigue Analysis," West Conshohocken, PA, 2011.

[9] J. F. Manwell, J. G. McGowan, and A. L. Rogers, *Wind Energy Explained: Theory, Design and Application*. 2002.

[10] P. Lissaman, A. Zaday, G. G.-P. 4th I. S. on Wind, and undefined 1982, "Critical issues in the design and assessment of wind turbine arrays," *osti.gov*.

IOP Conf. Series: Journal of Physics: Conf. Series **1356** (2019) 012005 doi:10.1088/1742-6596/1356/1/012005

# Effect of wind flow direction on the loads at wind farm

**Romans Kazacoks, Lindsey Amos, Prof William Leithead**

Wind and Marine DTC, Strathclyde University, Glasgow, G1 1XW, United Kingdom

romans.kazacoks@strath.ac.uk; lindsey.amos@strath.ac.uk;

**Abstract**. This paper investigates the effect of wind flow direction on the fatigue loads on wind turbine within a wind farm, to determine the most critically loaded machines within the wind farm. The fatigue loads are calculated according IEC standards. In this study, the two layouts are considered. Additionally, this paper includes the effect of wind flow direction on the power efficiency of the wind farm for the two layouts. The simulations performed by StrathFarm, which is an in-house developed wind farm modeling tool, for the below and above rated wind speed flow with turbulence. In the regular and installed regular layouts at zeros degree of the prevailing wind flow direction, the spacing among turbines is eight diameters. At 90 degrees of wind flow direction the spacing between turbines is five diameters. The simulations demonstrate that the majority of the maximum fatigue loads occur at the range 40 and 70 degrees for the two layouts. However, there is small number of machines, which are experienced the highest fatigue loads at 90 degrees of wind flow direction. For the two layout the lowest power efficiency occurs at 10 degrees of wind flow direction. The regular layout is experienced same power efficiency at five and eight diameters spacing among turbine in the wind flow direction. The highest power efficiency occurs at wind flow angles, which produce the highest fatigue loads.

## 1. Introduction

The wind direction varies in time and space, which obviously has an effect on a wind turbine. There are many papers, which examine the effect of wind direction on efficiency or power production of a single wind turbine and wind turbines within a wind farm. However, there is little previous work, which examines the effect of variation of wind flow direction on the loads on wind turbines within a wind farm.

The purpose of this paper is to report an investigation of the effect of wind flow direction on the loads on wind turbines within a wind farm, to determine the most critically loaded wind turbines for different wind farm layouts and their dependence on the direction of wind flow; that is, the question being addressed is as follows:

- "How does the wind direction affect wind turbine loads within a wind farm?".

Additionally, this paper investigates the dependence of power efficiency in on wind flow direction and layout of the wind farm. Two different layouts of the wind farm are considered. The main goal is to examine the effect on loads, especially fatigue ones, of wind turbines within the wind farm because of changes in the wind flow direction. Therefore, extreme loads are beyond the scope of this study. In addition, the impact of curtailment on the wind turbine fatigue loads is investigated. The fatigue loads are calculated according to IEC 61400 standards [1].

StrathFarm, an in-house developed wind farm modelling tool, is applied to examine the fatigue loads and power efficiency of the wind turbines within the wind farm as result of the changes in wind flow

direction. StrathFarm was specifically developed for fast simulation of wind farms to enable estimation of performance over different mean wind speed, turbulence intensity and wind speed direction. Here the wind turbines are chosen to be the 5MW SuperGen turbines, which are similar to 5MW NREL wind turbine model.

## 2. Strathfarm overview

StrathFarm is an analysis and design wind farm model and simulation tool that meets the following requirements:

- Models wakes and wake interactions.
- Models the turbines in sufficient detail that tower, blade and drive train loads are sufficiently accurate to estimate the impact of turbine and farm controllers on loads.
- Includes commercial standard turbine controllers.
- Includes a wind farm controller.
- Provides very fast simulation of large wind farms; run in real time with 100 turbines.
- Complete flexibility of choice of farm layout, choice of turbines & controllers and wind conditions, direction, mean wind speed and turbulence intensity.

The tool comprises a MATLAB based interface, with user specified parameterisation of the wind farm simulation, through which a model of the wind farm is constructed from library blocks and a wind field time series is created. Different pitch regulated variable speed wind turbines can be represented by providing an appropriate parameterisation of both the wind turbine model and its controller.

### *2.1 Structure and Principles of the tool*

The wind farm model generated by the StrathFarm tool is a Simulink model consisting of appropriately connected C-code or Simulink library blocks. Each wind turbine is represented by an individual model library block, which feeds the thrust coefficient to the wind farm wake model. The wind field, which is represented by a pre-generated time series, is then adjusted for wake effects and local wind speed information input to each wind turbine model, thereby, providing the aerodynamic coupling of the turbines within the wind farm.

In the version of StrathFarm used to produce the results in this study, the wind turbine models are continuous Simulink block based models, with discrete controllers implemented as dlls. Each wind turbine controller includes a Power Adjusting Controller (PAC) [2], which provides the connection to a central wind farm controller and enables dynamic adjustment of power output. Each PAC communicates with the wind farm controller, a function-code dll library block, using a set of input and output flags.

### *2.2 Wind Turbine Model*

The overall dynamic performance of a wind turbine is due to a combination of the structural, powertrain and control system dynamics. The structural dynamics which are concerned with the motion of the blades and tower influence the transient loads on the structure of the wind turbine, and hence its fatigue life. The dynamics of the drivetrain influence the transient loads on the drivetrain components, such as the gearbox and they also influence the control system for a pitch regulated machine. The requirements for StrathFarm include a wind turbine model, which captures the key dynamics of the wind turbine system, whilst being computationally inexpensive. Lumped parameter models are used for the rotor, drivetrain and for representing a single blade. Reformulated BEM based aerodynamic coefficient models are used to determine the thrust and torque at the rotor, including dynamic induction lag.

### *2.2.1 Wind Turbine Model Components*

Aerodynamics: The rotor/wind field interaction employs an effective wind field model whose resolution is sufficient detailed to represent the interaction reasonable accurate up to 6P. Modified BEM based aerodynamic coefficient models are used to determine the thrust and torque at the rotor, whereby standard BEM is reformulated [2] to allow dynamic inflow effects to be modelled. The aerodynamic thrust and torques (in-plane and out-of-plane) are calculated using look up tables for aerodynamic coefficients of thrust, power and out-of-plane rotor torque, taking as inputs the pitch angle and tip-speed ratio calculated from wind turbine rotor speed and a combination of the correctly adjusted components of the wind field input.

Rotor and Tower Dynamics: The structural model of each turbine includes two blade modes and 2 tower modes [3]. Individual blade models use a lumped mass blade/hub model, which takes into consideration the distributed elastic properties of the blade with part of the mass and inertia of the blade incorporated into the hub. The fore-and-aft modes of the tower are incorporated into the rotor model and the fore-and-aft modes are incorporated into the drive-train model.

Drivetrain: the lumped parameter drivetrain model represents the rotor, hub, low-speed shaft, gearbox with damped compliant suspension, high speed shaft and generator rotor. The model is based on [3] and is represented by a linear, state-space system with two dynamic modes. The resulting dynamics are stiff.

### *2.2.2 Wind Turbine Model Validation*

The wind turbine used is the SuperGen 5MW exemplar turbine, which is similar to the 5MW NREL turbine [4]. It has a rotor diameter of 126m, a hub height of 90m, a maximum power coefficient of 0.4878 (at a tip-speed ratio of 7.5 and pitch angle of -0.011rad), rated speeds of 1.23 rad/s (rotor) and 120 rad/s (generator).

A DNV-GL Bladed aero-elastic model of the SuperGen 5MW turbine, that uses the same controller, has been used to validate the StrathFarm wind turbine model. The wind fields used by the models have the same mean wind speed and turbulence intensity, but the time series are not identical, as shown in the top two plots in Figure 1. The remaining plots are a selection of load power density spectra that demonstrate a good match between the key components of the loads represented, even with the non-identical wind input.

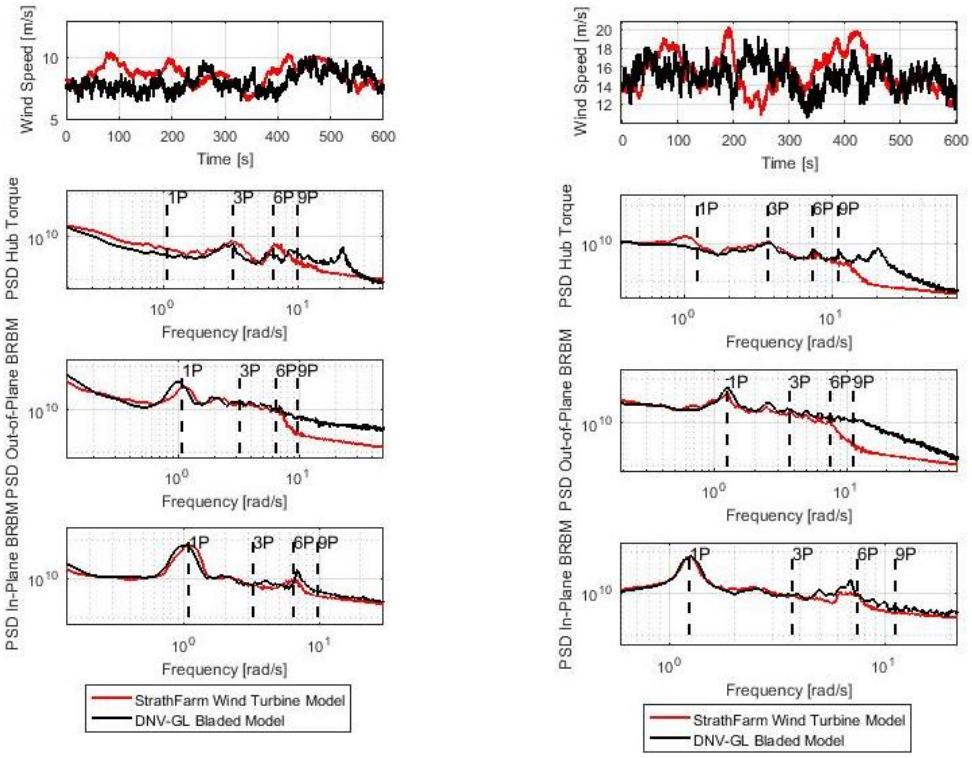


**Figure 1**: Comparison of the wind field time series, power density spectra of output hub torque, out-of-plane and in-plane blade root bending moments between 5MW Supergen model in StrathFarm and 5MW Supergen model in DNV-GL Bladed. Figure 1.a corresponds to a mean wind speed of 8 m/s and Figure 1.b to a mean wind speed of 15 m/s. All simulations use 10 % turbulence intensity.

### *2.3 Wind Field and Wake Modelling*

For each wind farm simulation in StrathFarm, the wind field is defined by inputs of mean wind speed, wind direction, turbulence intensity and surface roughness. The layout and dimensions of the wind farm are also inputs to the wind field and wake models. The wind field time series are pre-generated, stored in a file from which they are read during simulation. The wake model estimates the interaction of the turbines within the farm; to determine the wind speeds for each turbine at each time step.

#### *2.3.1 Time-Series Input Wind Field Components*

Two components of the wind field are calculated and input as time series to the StrathFarm simulation model. The first corresponds to the longitudinal and lateral turbulence time series with the required characteristics. The turbulent wind field model is based on the algorithm of Veers [5]. The second corresponds to an effective wind field model, local to the rotor for each turbine [6], representing the higher frequency components of the wind. In addition, deterministic components such as wind shear and tower shadow are also modelled components.

#### *2.3.2 Wind Field Simulation*

At each time step, the StrathFarm wake model determines a wind speed deficit, which is applied to the wind field. This represents the wakes of upwind turbines, and is effectively the proportion of wind available power experienced by each turbine compared to that would be experienced if there were no

wakes. A value of one for the deficit represents no wake effects. As well as a drop in effective wind speed seen by a downwind turbine, wake effects also produce an increase in relative turbulence. The time series representing the low frequency correlated turbulence wind field component is then combined with the higher frequency uncorrelated turbulence component local to each wind turbine to be used in the appropriate aerodynamic calculations.

### *2.3.3 Wake Model Description*

The wake deficits are calculated using the thrust coefficients of each wind turbine as inputs to a kinematic wake model. The kinematic wake model, based on the well-known model of Frandsen [7], uses a pre-generated lateral turbulence field to determine wake meandering, and analytically determined equations to calculate the wake diameters (wake expansion) and the effective reduction in available power experienced by downwind turbines (wake strength).

At each time step, the model iterates the wake effects downwind through the wind farm, combining the wakes of upwind wind turbines. The centre and diameter of each wind turbine wake determines which upwind turbines should be included in the deficit calculation for the downwind turbine. Partial wake cover and wake overlap is treated using a proportion based on the area of overlap between the rotor and a circle representing a wake.

## 3 Methodology

The effect of wind flow direction on the fatigue load distribution within the wind farm and power efficiency of the wind farm is investigated for two wind farm layouts (regular and installed regular), which are depicted in Figure 2. Each of these two layouts is examined for different angles of wind flow direction, from zero to 90 degrees in 10 degrees steps (wind direction angle $\in [0 : 10 : 90]$). Figure 3 shows the direction of the wind flow from zero to 90 degrees. At zeros degree, the wind flow goes from the west to the east. At 90 degrees, the wind flow goes from the north to the south. The wind flow direction rotates clockwise. Note the rotor of wind turbines are oriented towards the wind. Therefore, there is no yaw error for the wind turbines in StrathFarm simulation wind farm modelling tool.

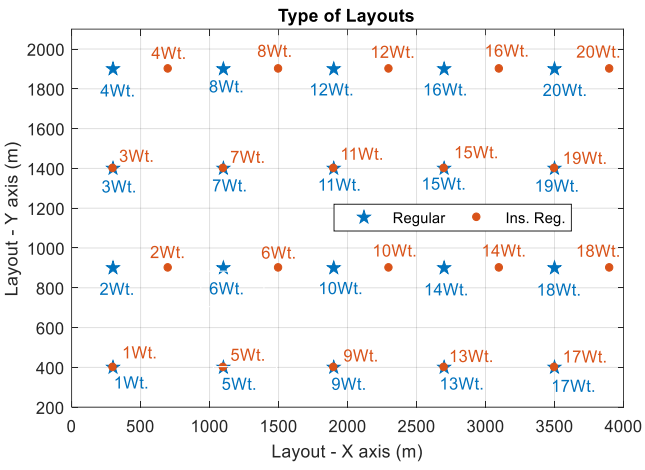


**Figure 2:** Two layouts of this study (Regular-blue star and Installed regular - red dot).

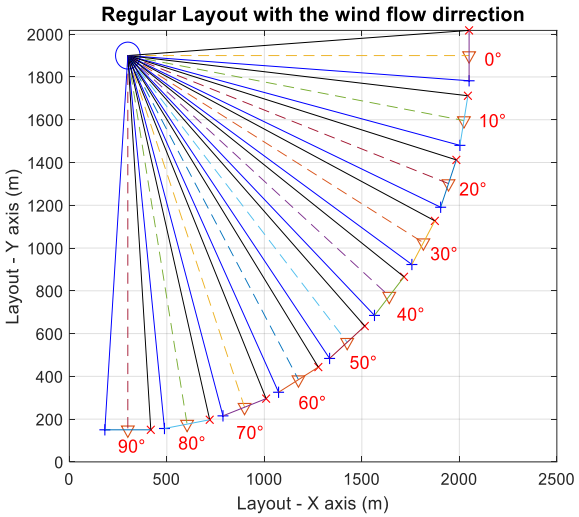


**Figure 3:** Orientation of wind flow direction for the wind turbines.

Additionally, the effect of power curtailment on loads is examined in this study. The power curtailment is applied at the wind farm level through wind farm controller. This study assumes a 20% power

curtailment. Therefore, each turbine within the layout has 20 % cut of power production. The effect of power curtailment on the loads is examined for each layout and wind flow direction.

### *3.1 Initial conditions*

The analysis was performed using two mean wind speed (8 and 15m/s) during normal power production conditions or design load case (DLC) 1.2 with normal turbulence model (NTM) set according to the IEC standards [1], i.e. turbulence intensity 0.12. The below rated region is represented by the 8 m/s wind speed and above rated region represented by 15 m/s. In-line with IEC standards, 6 different 'seeds' (i.e. random initiating points of the simulation) are employed per mean wind speed to reduce the uncertainty arising from the stochastic nature of the wind field.

### *3.2 Damage equivalent loads*

Damage equivalent loads (DELs) estimates are based on Palmgren-Miner linear cumulative damage theory [8], which assumes that fatigue damage increases linearly as a function of number of cycles, until it reaches the prescribed life exhausted of material [9]. Additionally, it assumes that only cycle load range contributes to fatigue damage, i.e. there is no contribution to fatigue damage from the mean value of cycles. Equation 1 shows the formula for the calculating DELs.

$$L_{DEL} = \left( \frac{\sum_{ip} \left( \sum_i^k n_i \, L_i^m \right)}{t_{sim} \, f} \right)^{\frac{1}{m}} \tag{1}$$

Where, $n_i$ is number of cycles, $L_i$is load range at bin, $m$ is Wöhler coefficient, $t_{\mathrm{sim}}$ is simulation time and $f$ is the reference frequency. The Rain flow counting (RFC) [10]–[12] is applied to count load range, mean and amount of cycles in a time series. According to the default calculation of DELs, the load range (maximum and minimum) contributes to fatigue.

### *3.3 Materials*

DELs are used to presents the fatigue loads in this study. For the calculations of the DELs, Wöhler coefficients of 4 and 10 are used. These coefficients characterise the gradient of a material's Wöhler SN curves. Wöhler coefficients of 4 and 10 are used for steel and composite materials, respectively. As the hub and bolts are made from steel, but the blades are from composites.

## 4 Results

This section investigates the effect of wind flow direction on the fatigue loads and power production for the two layouts. Manwell et al [13] mentioned that the wind turbine spacing, the number of turbines and size of the wind farm play a key role in terms loads and power production.

### *4.1 Effect of wind direction on fatigue loads*

The two layouts in Figure 2 are considered here, with and without curtailment. The wind turbine with the maximum DELs is found within each layout for each direction of wind flow in Figure 3. For each layout, the out-of-plane blade root DELs for Wohler coefficients 4 and 10 are estimated but not the in-plane blade roots DELs the latter are more dependent on gravity loads [13]–[16]. For each layout, the maximum DELs by wind direction are determined for four different conditions as shown below:

- Below rated wind speed (8 m/s) with turbulence (0.12 Iref.) and no curtailment.

- Below rated wind speed (8 m/s) with turbulence (0.12 Iref.) and 0.2 curtailment.
- Above rated wind speed (15m/s) with turbulence (0.12 Iref.) and no curtailment.
- Above rated wind speed (15m/s) with turbulence (0.12 Iref.) and 0.2 curtailment.

### *4.1.1 Regular layout*

For the regular layout, the results with Wöhler coefficients 4 and 10 are shown in Figure 4. Each figure depicts the wind turbines, which experienced the highest DELs at the specific wind flow direction. The horizontal axis is the direction of flow angle. The vertical axis is the number of the wind turbine in the layout. Figure 2 shows two layouts and how wind turbines are numbered within these two layouts.
In below rated wind speed, the maximum DELs mainly occur at 40, 70 and 90 degrees of the wind flow direction, see Figure 4. For the above rated wind speed without curtailment, the highest DELs occur mainly at 60 degrees. For the above rated wind speed with curtailment, the maximum DELs occur mainly at 50 and 60. Thus with the regular layout, the maximum DELs occurred in range from 40 to 70 and 90 degrees wind flow direction.

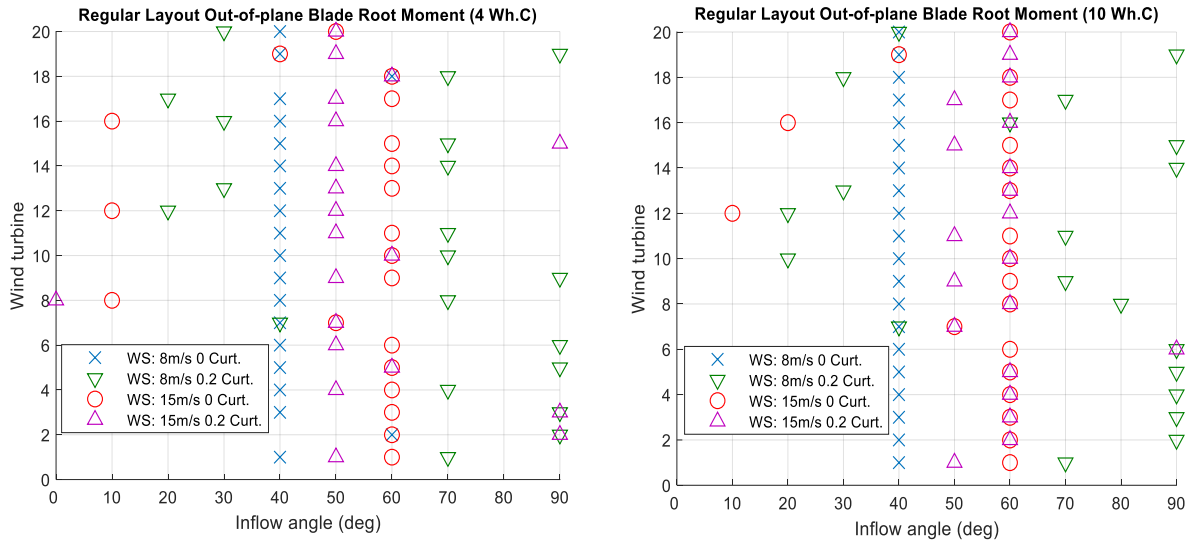


**Figure 4:** The highlighted wind turbines, which are experienced the maximum DELs of *out of plane blade root moment* within the *regular layout*, at different wind flow direction angle (0:10:90°). Graph A represents Wohler coefficient 4, graph B is for Wohler coefficient 10.

In the regular layout at zeros degree of prevailing wind flow direction, the spacing between turbines is eight diameters. The spacing, perpendicular to the prevailing direction, is five diameters. The spacing in the wind flow direction affects the downwind turbines, reducing the wind speed and increasing turbulence for the downwind wind turbines. As a result, the fatigue loads increase for the downwind machines when they are located in the wake of an upwind machine [13], [14]. Therefore, smaller spacing among wind turbine in the direction of wind flow produces higher fatigue loads for the downwind machines. There are a few machines, which are experienced higher DELs at 90 degrees of wind flow direction as shown in Figure 4. However, the majority of higher DELs are spread in range 40 and 70 degrees of wind flow direction. Possibly, that is the consequences of the wake meandering through the propagation of wake downwind and other influences such the extent of below and above rated operation.

### *4.1.2 Installed regular layout*

For the installed regular layout, the results with Wöhler coefficients 4 and 10 are shown in Figure 5. For Wöhler coefficient 4, the maximum DELs in below rated speed are more widely scattered throughout the layout than the maximum DELs in above rated wind speed, see Figure 5A. For Wöhler coefficient 10, the maximum DELs in below rated speed mainly occur at 90 degrees wind flow direction, see Figure 5B. The maximum DELs in the above rated speed mainly occur at 0, 60 and 70 degrees. The distribution of the maximum DELs with Wöhler coefficient 10 in above rated speed is the same as the maximum DELs for Wöhler coefficient 4.

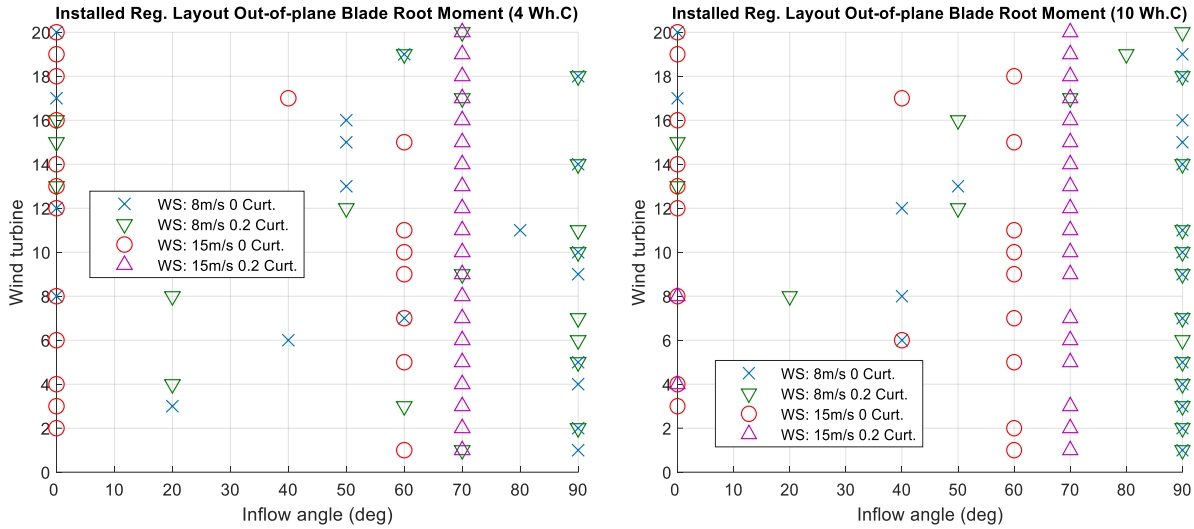


**Figure 5:** The highlighted wind turbines, which are experienced the maximum DELs of *out of plane blade root moment* within the *installed regular layout*, at different wind flow direction angle (0:10:90°). Graph A represents Wohler coefficient 4, graph B is for Wohler coefficient 10.

### *4.2 Effect of wind direction on fatigue loads*

In this section, the effect of wind flow direction on the power efficiency of a wind farm is investigated. The two layouts in Figure 2 are again considered. The angle of wind flow direction varies from zero to 90 degrees in 10 degree increments. The power efficiency [13] of wind farm is calculated as in equation (**2**.

$$Eff_{power} = \frac{energy\ of\ whole\ wind\ farm}{(energy\ of\ one\ isolated\ turbine) * (number\ of\ Wts\ in\ farm)} \quad (2)$$

The power efficiency is calculated in below rated wind speed only as the wind speed deficit is not so significant in above rated region operation. For the above rated mean wind speed of 15 m/s chosen here, the measured minimum power efficiency is around 97.5%. Thus, only below rated wind speed is considered here. Figure 6 depicts the dependency of power efficiency on the wind flow direction for the two layouts (regular are installed regular). Figure 6 shows that the lowest power efficiency occurs at 10 degrees flow direction for the two layouts. The curtailment does not have significant effect on the power efficiency as the trends of power efficiency with curtailment are similar, slightly shifted, to the trends without curtailment for both layouts. For the regular layout, the graph of power efficiency is nearly symmetric about 45 degrees, reflecting the symmetry of the layout, see Figure 2.

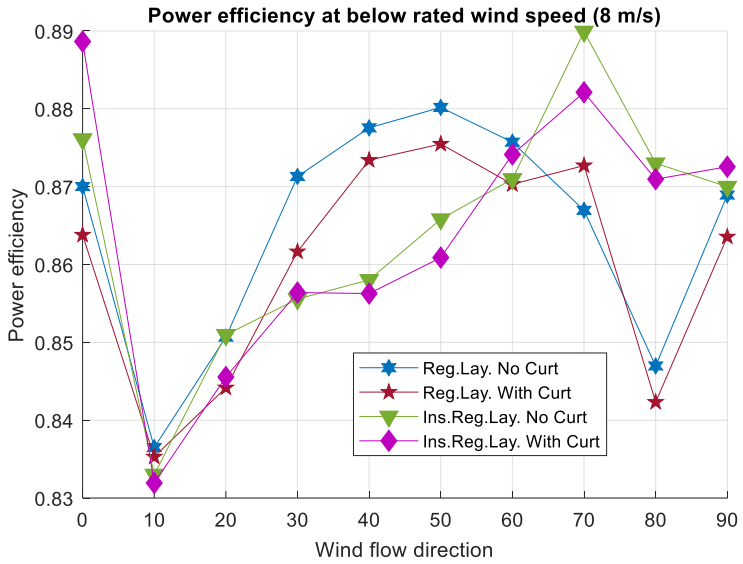


**Figure 6:** Changes power efficiency as a function different wind flow angle (0:10:90°) for the two layouts at below rated wind speed with/without curtailment.

In Lissaman et al. [17], It was shown that the geometry of turbine location and ambient turbulence intensity have high influence on power losses for a layout. Additionally, it was shown that, if the spacing among the turbines in the prevailing downwind direction is 10 diameters, then the power losses are below 10 %. In the regular layout in Figure 2 at zeros degree of prevailing wind direction, the spacing among turbines is eight diameters. In the perpendicular direction of wind flow direction, the spacing is five diameters between turbines. Figure 6 demonstrates that, with five and eight diameters spacing between turbines and a wind flow direction around 0 and 90 degrees, power efficiency is about 87%. That happens because wakes meander relative to the nominal direction of the wind, the extent, to which wakes from upstream turbines interact with a downstream turbine, varies randomly with time and the separation of the turbines, i. e. direction of wind speed. In addition, the turbulent wind speeds seen by each turbine varies randomly so that the mean wind speed seen be each turbine, also, varies randomly with its position in the array and direction of the wind speed. Consequently, due to the small number (6 seeds) and short duration of simulation runs, statistical uncertainty for each value plotted on Figure 6 remains substantial, implying that any estimation of direction of minimum power efficiency, with the same number and duration of runs as used here, would vary greatly. The shift of this estimate from the expected value of 0 degrees is thus not unexpected but gives some indication in the uncertainty in these results.
Additionally, the maximum power efficiency occurs with a prevailing wind flow direction of roughly 50 degrees for the regular layout. The highest DELs loads in below rated speed without curtailment occur at 40 degrees of wind flow direction as shown in Figure 4. Therefore, the maximum power efficiency matches or coincides with the highest fatigue loads.
The highest power efficiency of the installed regular layout appears at 70 degrees. It again coincides with the maximum DELs in above rated wind speeds as shown in Figure 5. Therefore, there is correlation between the high power efficiency and the high DELs for the wind turbines within a layout.

## 5 Conclusion

This paper investigates the effect of wind flow direction on the fatigue loads on wind turbines within a wind farm, to determine the most critically loaded wind turbines for different wind farm layouts and

their dependency on the direction of wind flow. Additionally, this paper focusses on power efficiency in order to explore any correlation between the wind flow direction and the power efficiency of different layout. In this study, there are two layouts of the wind farm: regular and installed regular.
Each layout is examined for four conditions: below and above rated wind flow with turbulence, 12% turbulence reference intensity, with and without curtailment (20% power curtailment in this study). The damage equivalent loads are used to calculate fatigue loads according to the IEC standards. The calculations performed by StrathFarm, which is the in-house wind farm-modelling tool.
The two layouts demonstrate that the majority of the maximum fatigue loads occur at the range 40 and 70 degrees. In the regular layout at zeros degree the spacing among turbines is eight diameters. The spacing, at 90 degrees is five diameters among turbines. In Manwell et al [8] and Burton et al [9], it is observed that the spacing in the prevailing direction affects the loads on the downwind turbines. The upwind turbines reduce the wind flow speed and increase turbulence for the downwind wind turbines. As result of increased turbulence, the fatigue loads increase for the downwind machines. Therefore, the highest fatigues loads should for a prevailing wind direction of 90 degrees. There are a few machines, which experience the highest fatigue loads at 90 degrees, but the majority with highest fatigue loads occur at 40, 50, 60 degrees. Possibly, that is the consequences of the wake meandering through the propagation downwind within the layout and other influences such the extent of below and above rated operation. To clarify this and reduce statistical uncertainty concerning all estimated values, it is clear that a greater number of simulation runs at each mean wind speed and for a larger set of mean wind speeds is required.
The lowest power efficiency occurs at 10 degrees flow direction angle for the two layouts. The regular layout is experienced same power efficiency (87%) at five and eight diameters spacing among turbine in the wind flow direction. The highest power efficiency occurs at wind flow angles, which corresponds to the angles, which produce the highest fatigue loads.

Additional work is required to validate some of these results, particularly by direct comparison to the actual performance of a real wind farm with the same layout experiencing the same wind speed conditions such as: turbulence, wind shear, air density and so on.

**Acknowledgment**
With thanks to the contributions of Adam Stock, Victoria Neilson, Lourdes Gala Santos, Saman Poushpas, Sung-Ho Hur, Giorgio Zorzi and Velissarios Kourkoulis from the University of Strathclyde.

The work has been funded by EPSRC EP/G037728/1 DTC Wind Energy Systems; EPSRC EP/L016680/1 DTC Wind and Marine Energy Systems; EPSRC EP/H018662/1 Supergen Wind Phas2; EPSRC EP/N006224/1 MAXFARM; FP-ENERGY-2013.10.1.6: 609795 IRPWind

**References**
[1] I. E. Commission, “Wind Turbine—Part 1: Design Requirements, IEC 61400-1,” Geneva, 2005.
[2] A. Stock, B. Leithead, and H. Yue, “Augmented control for flexible operation of wind turbines,” 2015.
[3] W. Leithead, M. R.-W. Engineering, and undefined 1996, “Drive-train characteristics of constant speed HAWT’s: Part I–Representation by simple dynamic models,” *JSTOR*.
[4] J. Jonkman, S. Butterfield, W. Musial, G. S.-N. R. Energy, and undefined 2009, “Definition of a 5-MW reference wind turbine for offshore system development,” *nrel.gov*.
[5] P. S. Veers, “Three-Dimensional Wind Simulation,” *J. Geophys. Res.*, vol. 92, no. A3, p. 2289, 1987.
[6] M. Santos, “Aerodynamic and wind field models for wind turbine control,” 2018.

[7] S. Frandsen, "Turbulence and turbulence-generated structural loading in wind turbine clusters," Technical University of Denmark, 2007.
[8] M. Miner, "Cumulative damage in fatigue," *Appl. Mech.*, vol. 12, no. 3, pp. 159–164, 1945.
[9] P. Ragan and L. Manuel, "Estimation of Wind Turbine Fatigue Loads Using Time-Ragan, P., & Manuel, L. (2007). Estimation of Wind Turbine Fatigue Loads Using Time-Domain and Spectral Methods. 45th AIAA Aerospace Sciences Meeting and. Retrieved from http://arc.aiaa.org/doi/pdf/10.25," *45th AIAA Aerosp. Sci. Meet.*, 2007.
[10] S. Downing and D. Socie, "Simple rainflow counting algorithms," *Int. J. Fatigue*, vol. 4, no. 1, pp. 31–40, 1982.
[11] G. Glinka and J. Kam, "Rainflow counting algorithm for very long stress histories," *Int. J. Fatigue*, vol. 9, no. 4, pp. 223–228, 1987.
[12] ASTM E1049-85(2011)e1, "Standard Practices for Cycle Counting in Fatigue Analysis," West Conshohocken, PA, 2011.
[13] J. F. Manwell, J. G. McGowan, and A. L. Rogers, *Wind Energy Explained: Theory, Design and Application*. 2002.
[14] T. Burton, N. Jenkins, D. Sharpe, B. Ervin, and D. Sharpe, *Wind Energy Handbook*. John Wiley & Sons, Inc., 2011.
[15] M. O. L. Hansen, *Aerodynamics of wind turbines*, 2nd ed. London: Earthscan, 2008.
[16] R. Gasch and T. Jochen, *Wind Power Plants: Fundamentals, Design, Construction and Operation*, Second. Springer, 2012.
[17] P. Lissaman, A. Zaday, G. G.-P. 4th I. S. on Wind, and undefined 1982, "Critical issues in the design and assessment of wind turbine arrays," *osti.gov*.


# Investigation and Assessment of the Benefits For Power Systems From Wind Farm Control

Matthew D. Cole, Professor William E. Leithead, Dr Olimpo Anaya-Lara,
Dr. Julian Feuchtwang & Lindsey J. Amos
Industrial partner - SgurrControl
University of Strathclyde - Wind and Marine Energy Systems CDT

November 30, 2018


# Chapter 4

# Work completed

In order to provide ancillary services using wind farm control the first step needs to be developing a wind farm level controller which is able to request a power output from the wind farm.

## 4.1 work done

### 4.1.1 Wind Farm controller

The initial starting point for this research was a controller which could achieve delta control. The initial step was to design a controller which could achieve set-point regulation at the wind farm level. This had already been shown in [7], However, this was in continuous time and due to the heavy computational cost of a model of this type a new approach was required. Discrete time has the advantage that it is less computationally expensive and will therefore simulate more quickly helping to fulfill Strathfarms ethos of running on a standard desktop PC.

The approach chosen here was the same as [7]beginning with a PI controller.

The wind farm controler used began from the one used in [7] in the s-domain form of:

$$\Delta P = k_p(P_d(t) - P(t)) + k_i \int (P_d(t) - P(t))dt \tag{4.1}$$

where $P_d$ is the demanded power and $P(t)$ is the power output of the wind farm. This

can be considered in the Laplace domain in the form and substituting $P_s = P_d(t) - P(t)$:

$$= (k_p + \frac{k_i}{s})P_s \tag{4.2}$$

which can be considered in discrete time as:

$$= (k_p + k_i\frac{T}{2}\frac{1+z^{-1}}{1-z^{-1}})P_s \tag{4.3}$$

Where $T$ is the time-step.

$$= (\frac{k_p(1-z^{-1}) + k_i\frac{T}{2}(1+z^{-1})}{1-z^{-1}})P_s \tag{4.4}$$

$$= (\frac{k_p + k_i\frac{T}{2} + (k_i\frac{T}{2} - k_p)z^{-1})}{1-z^{-1}})P_s \tag{4.5}$$

$$= (k_p + k_i\frac{T}{2} + \frac{k_iTz^{-1}}{1-z^{-1}})P_s \tag{4.6}$$

This can be considered in incremental form as:

$$\Delta P[n+1] \;=\; \Delta P[n] + (k_p + k_i\frac{T}{2})P_s[n+1] - (k_p + k_i\frac{T}{2})P_s[n] + k_iP_s[n]T \tag{4.7}$$

$$\Delta P[n+1] \;=\; \Delta P[n] + K_p(P_s[n+1] - P_s[n]) + K_i\frac{T}{2}(P_s[n+1] + P_s[n]) \tag{4.8}$$

### 4.1.2 Anti-windup

In practice there are limits to the operation of the wind turbines in terms of how much curtailment can be delivered based on the operational status of the wind turbine. When a turbine is requested to go beyond these limits it will saturate resulting in the controller failing to accurately track the wind farm set-point. Saturation occurs in both the level of curtailment which a wind turbine can deliver, which varies depending on its location on the torque speed plane, and also in the rate at which it can vary its level of curtailment.

The limits on the level of curtailment are chosen based on a series of "traffic Light" flags which are conveyed from the PACs to the WFC and indicate how far each wind turbine has deviated from its default operational strategy with green flags being closest, amber slightly further and red the furthest away. The limits used in Strathfarm can be seen in Figure(4.1).

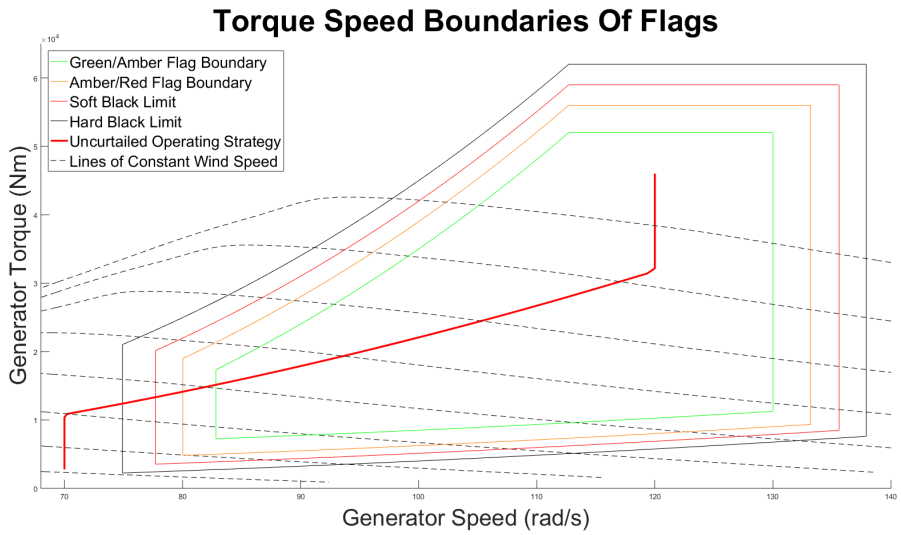


Figure 4.1: The traffic light boundaries in Strathfarm

The lower bounds of curtailment which [13] recommends are

1. -2.5MW for green flags
2. -1.5MW for amber flags
3. 0MW for red flags

In addition to these limits the PAC also has a limit on the rate of change of curtailment that a wind turbine can deliver. These limits however do not vary with the traffic light flags.

The solution to this saturation used in Strathfarm's WFC is to consider the saturation at both the total windfarm wide level and then again at the wind turbine level.

Initially the WFC uses the status flags of all of the wind turbines and then finds the total upper and lower bounds of the windfarm for both the total level of curtailment and

the rate of change of curtailment. using these limits a back-calculation based approach to anti-windup is used.

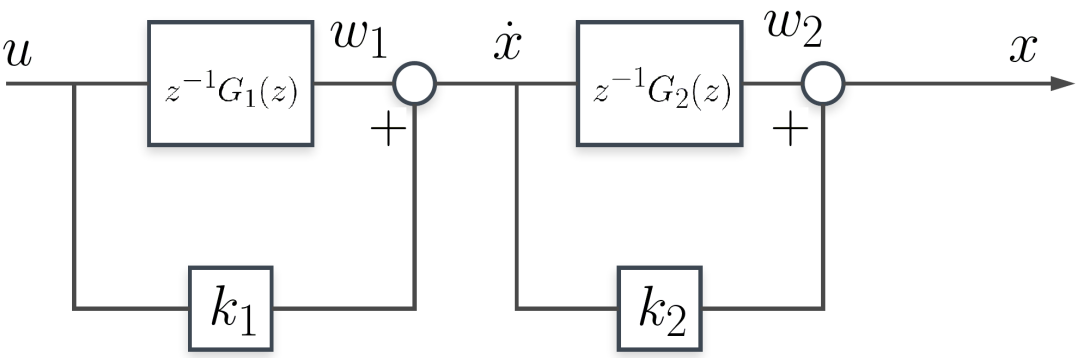


Figure 4.2: A generic form block diagram of the wind farm controller.

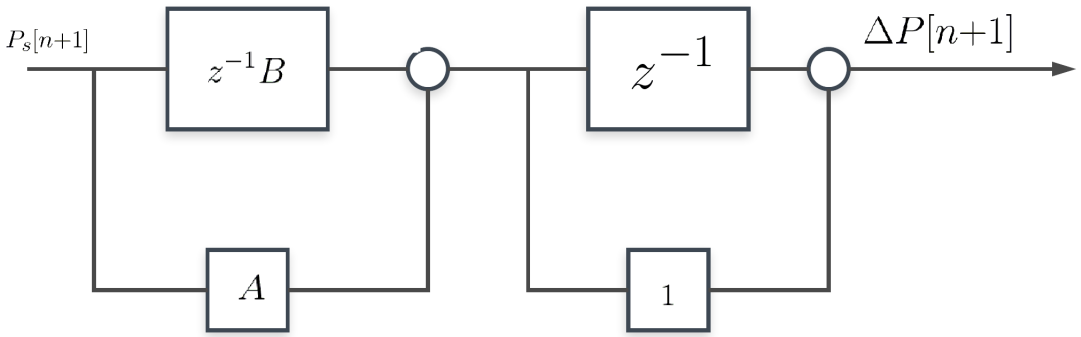


Figure 4.3: A block diagram of the wind farm controller.

Figure (4.2) shows the generic form of the controller and Figure (4.3) shows the specific form where

$$A = k_p + \frac{Tk_i}{2} \tag{4.9}$$

and

$$B = -k_p + \frac{Tk_i}{2} \tag{4.10}$$

The $z^{-1}$ blocks act as a lag of one iteration. In the case of this controller the top left block outputs the $n$th iteration's power error multiplied by $B$ , which when combined

with the output of the bottom left block gives

$$K_p(P_s[n+1] - P_s[n]) + K_i\frac{T}{2}(P_s[n+1] + P_s[n]) \tag{4.11}$$

which Equation (4.8) shows is the change in $\Delta P$. The right two blocks show that the block diagram is equivalent to Equation (4.8) as the top right block outputs the previous iteration of $\Delta P$ and the new iteration is found by adding the rate of change found from the left two blocks. The controller first checks whether $\Delta P[n+1]$ is saturated, if $\Delta P[n+1]$ is saturated it is set to be equal to the saturation limit and $P_s[n+1]$ is subsequently back calculated. The controller then checks if the rate ($\dot{x}$) is saturated, if $\dot{x}$ is saturated $P_s[n+1]$ back calculated and then both values are used to find an updated value for $\Delta P[n+1]$.

A change that has been made in the implementation of th wind farm controller is to remove the governing of these limits from the PACs and doing it in the allocation at the wind farm level as controlling it at a higher level means that curtailment can be allocated in such a way that when there is a change in flag status at one turbine the rate of change of power is matched by the unchanged wind turbines. This is required as there are limits to how fast the PAC can change the level of curtailment of a turbine.

### 4.1.3 Recovery flags

When a wind turbine deviates too far from its operational strategy to the extent that it is no longer stable it is allocated a recovery flag. In this case the allocation of curtailment to that wind turbine is reduced to zero and the rest of the wind turbines compensate for it. The anti-windup limits have been modified to allow a discontinuity in the total level of curtailment of the wind farm in this case as the wind turbine. The result of this implementation is that there is no noticeable change in the power output of the wind farm as can be seen by the results in this report.

### 4.1.4 Curtailment Reallocation

After curtailment has been found at the wind farm level it is then distributed across the wind turbines.

As there are two types of saturation they can at times not both be prevented. For example if a turbine has a flag change from amber to red it can and was being allocated a curtailment of 1MW it cannot possibly satisfy its limit on the total level of curtailment and the rate of change of curtailment. The WFC controller prevents this by where possible reallocating any changes in curtailment which cannot be provided due to saturation to wind turbines which are not saturated. If reallocation of all of the request curtailment cannot be provided a final back calculation is done so that there is not a discontinuity between the controller limits and the system.

However, using the controller parameters from [7] does not produce curtailment in the wind farm so the controller has required tuning.

The tuning was done for a wind farm with ten turbines arranged in a row perpendicular to the direction of the wind to prevent and wake effects.

The controller has been tuned in turbulence free wind fields at below near and above rated wind speeds of 9m/s,11.5m/s and 14 m/s. As the wind farm has anti-windup the overshoot is removed but there can be a long settling time if the integral gain is too high. If the gain of the controller is too high it can negatively interact with the PAC due to there being a small lag applied to the estimated power without the PAC which causes the controller to act on an error which it should ignore. The tuned parameters for the WFC are $K_P = 1$ and $K_I = 4$

Following this step the WFC then allocates the level of curtailment to each turbine based on the flag status of each turbine. The initial distribution of allocating curtailment was proposed by [7] as

$$\Delta P_i = \frac{\Delta P f_i}{\sum_{i=1}^{N_t} \hat{f}_i} \tag{4.12}$$

where $\Delta P_i$ is the requested curtailment of the $i$th turbine,$\Delta P$ is the total requested curtailment of the wind farm, $f_i$ is the status flag of the $i$th turbine and $N_t$ is the

number of wind turbines in the wind farm. Following this allocation the WFC then checks to see if it will result in any wind turbines become saturated due to either the limits on how much curtailment each turbine can be allocated based on its status flag or if it will result in a wind turbine having a change in curtailment allocation greater than the PAC limit. In the event that a wind turbine is going to become saturated the curtailment which cannot be realised is, where possible, allocated to unsaturated wind turbines.

### 4.1.5 The PAC Rate Limit

The limit at which the PAC can change the level of curtailment in a wind turbine is limited. When this limit is increased above the default rate of 50kw/s there is at times unintended interactions in the model. This is best seen in the wind speed estimator which changes when the requested rate of change of curtailment is high.

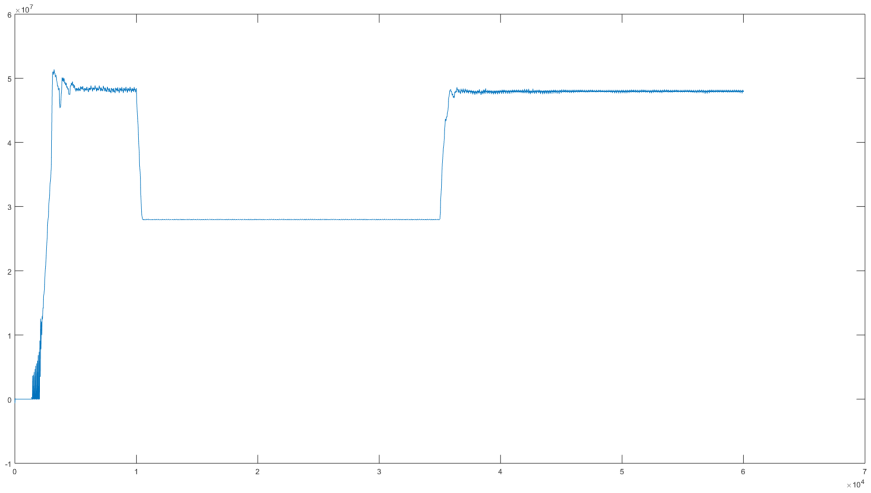

Figure 4.4: An example of a tuning wind farm power output.

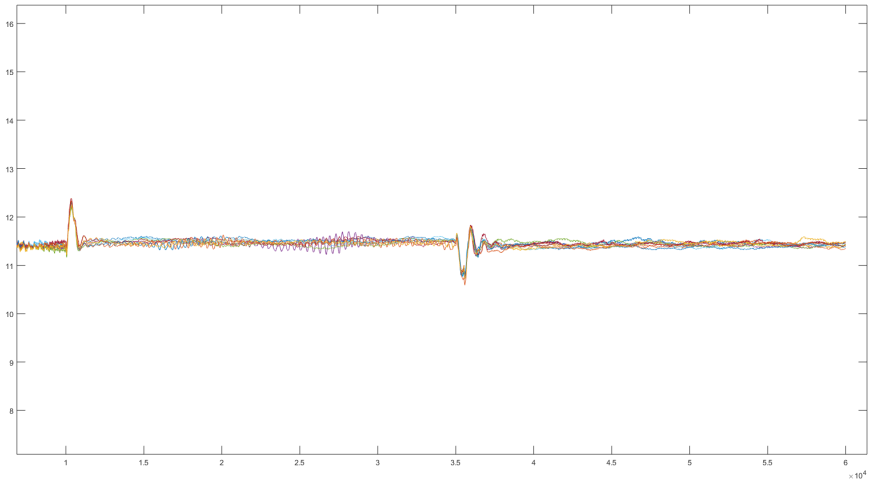


Figure 4.5: The change in the wind speed estimates when the PAC rate limits are increased to 50 KW/s corresponding to Figure (4.4).

As the wind speed estimate is used for calculating the uncurtailed power estimate changes like these can create great instability in Strathfarm.

However, if a stable set-point output power from the wind farm is required as it is here the default rate in the PAC is inadequate as such a low rate of change results cannot react sufficiently to changes in the wind field across the farm. However the larger the wind farm the smaller this value can be as the relative variation in the total uncurtailed power of the wind farm reduces as the number of wind turbines increases.

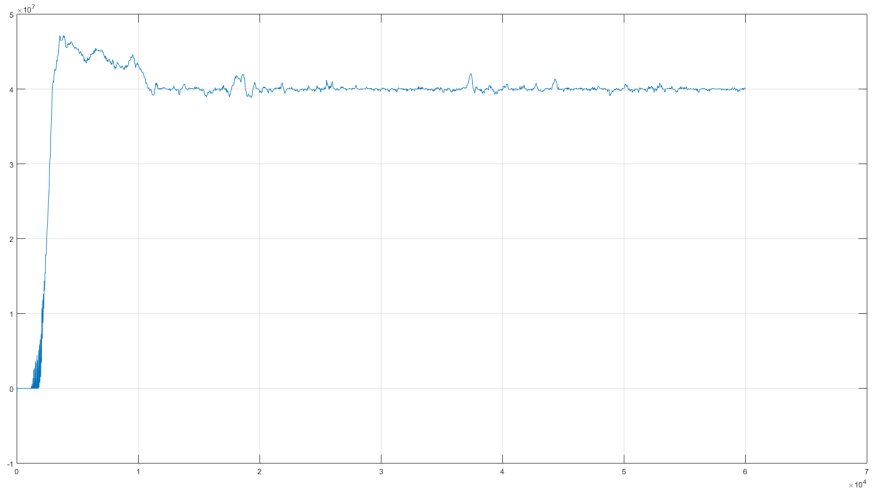

Figure 4.6: An example of a wind farm with 10 wind turbines being curtailed to a set-point with a rate limit of 50 KW/s

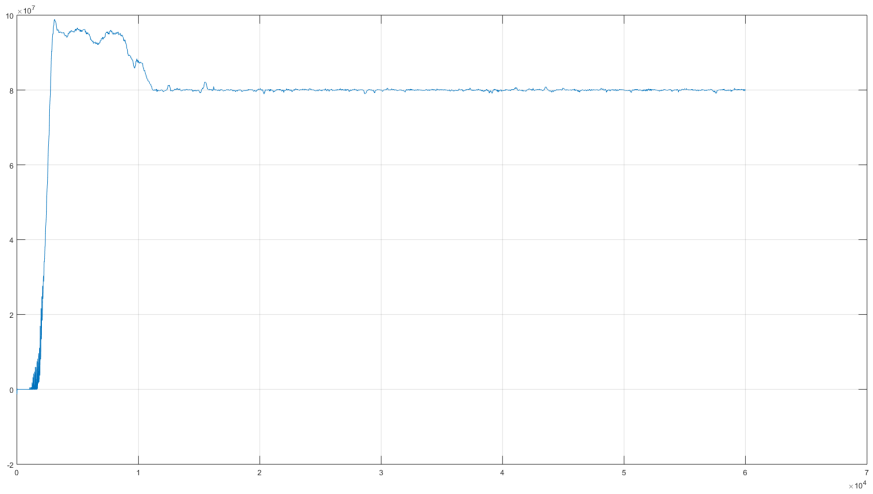

Figure 4.7: An example of a wind farm with 20 wind turbines being curtailed to a set-point with a rate limit of 50 KW/s

Figure (4.6) and Figure (4.7) show that as would be expected when there are more wind turbines in a wind farm the less impact the rate limits on the wind turbines has. By comparing the two simulations it can be seen that as expected adding more turbines to the wind farm increases the effectiveness of the controller when the rate at which

the wind turbines can change their level of curtailment allocation is 50kw/s.

As a compromise the results generated later in this report use a maximum rate of change of 150kw/s

## 4.2 Wind Farm Damage equivalent loads

A requirement of any wind farm curtailment strategy is to ensure that it does not have an adverse impact on the fatigue of the wind farm. This section will detail the validation of [7]'s approach in this new version of a wind farm controller using discrete time and showing that it can be further improved through using the estimated wind speed from the PAC as an input to the curtailment allocation equation.

### 4.2.1 Damage equivalent loads

The damage equivalent load which are to be considered are the fore-aft tower root being moment and the out of plane root bending moment. These were chosen as the moments which the research has focused on as when power is curtailed from a turbine fitted with the PAC the means of reduction is to pitch the blades. This pitching changes the forces on on the blades resulting in a change in the out-of plane bending moment. This change is then transmitted to the tower through the hub resulting in a change in the fore-aft bending moment. The damage equivalent loads (DELs) have been calculated using a rainflow counting method proposed by [10] which considers the variation in the moment by breaking the time series into a series of half cycles using rainflow counting. By comparing these half cycles using an S-N curve based approach a single damage equivalent load can be found.

Using this approach means that the goal of the wind farm control systems should not be to always minimize the bending moments experienced by the components of the wind turbines but instead to reduce any changes to them. This means that at times it may be beneficial to not curtail a wind turbine experiencing high bending moments and at times it may be beneficial, at least hypothetically, to request more power from a turbine in order to maintain the bending moments or at lead to minimize any changes to them.

What has been considered for the research presented here is how the static moments change as a wind turbine experiences different wind speeds. As the primary focuses of a wind turbine's control strategy is to maximise power output below the rated wind speed and then maintain rated power above the rated wind speed there is no consideration of how this affects the bending moments of the blades and tower.

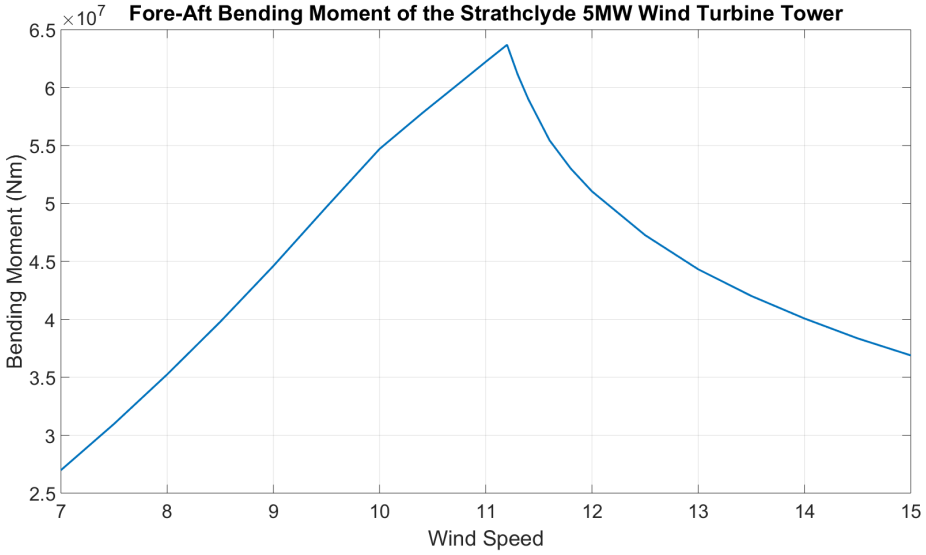


Figure 4.8: The fore-aft tower bending moment of the University of Strathclyde exemplar wind turbine over a range of wind speeds

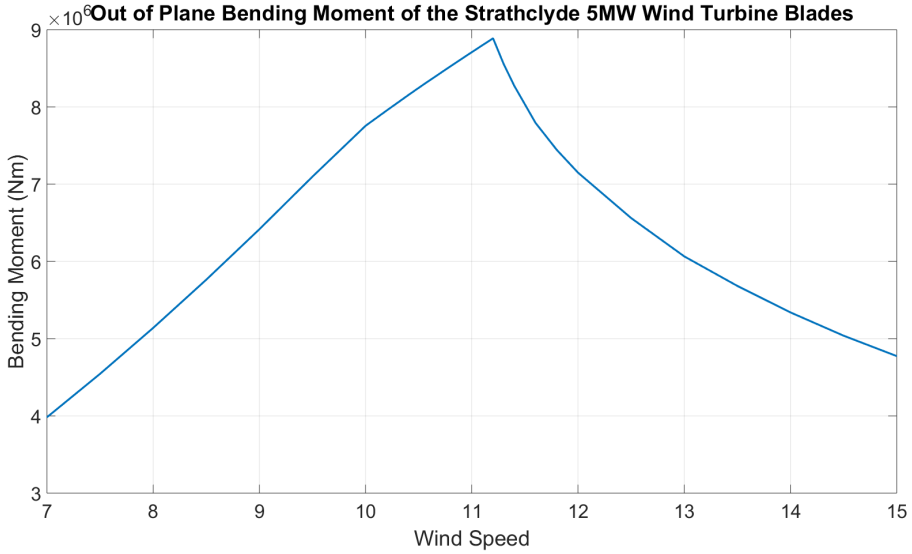


Figure 4.9: The out of plane blade bending moment of the University of Strathclyde exemplar wind turbine over a range of wind speeds

Figure (4.8) and Figure (4.9) show the bending moments of the University of Strathclyde exemplar 5MW wind turbine used in Strathfarm over a range of wind speeds. What can be seen in both profiles is that below rated the moments increase as the wind speed increases but above rated when the blades are pitched to maintain rated power there is a reduction in the moments as the wind speed increases. As this has shown the large impact which pitching the blades has on the moments of the structural components of the wind turbine the obvious next step is to consider how curtailing the wind turbine using the PAC, which reduces power output through pitching, has on these moments.

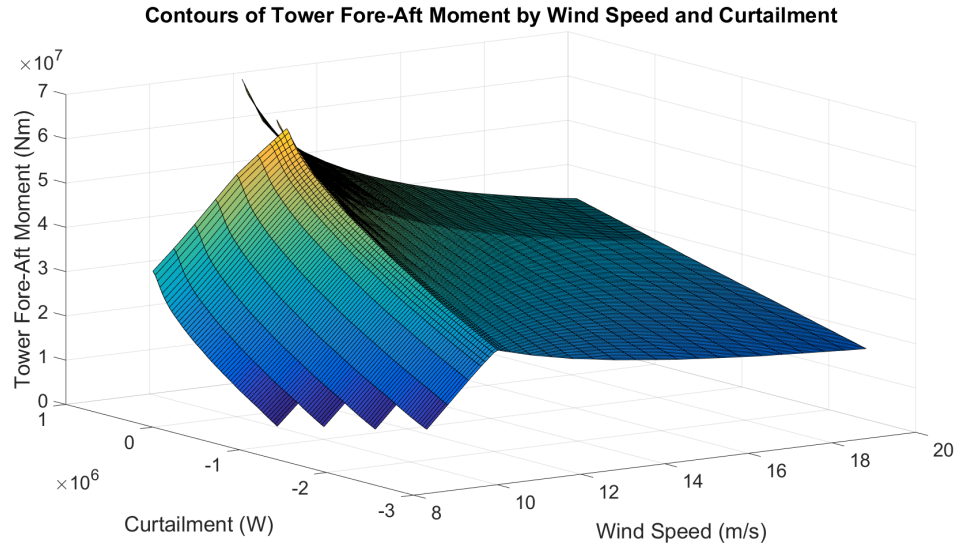


Figure 4.10: A plot of the fore-aft tower bending moment of the University of Strathclyde exemplar wind turbine by wind speed and level of curtailment.

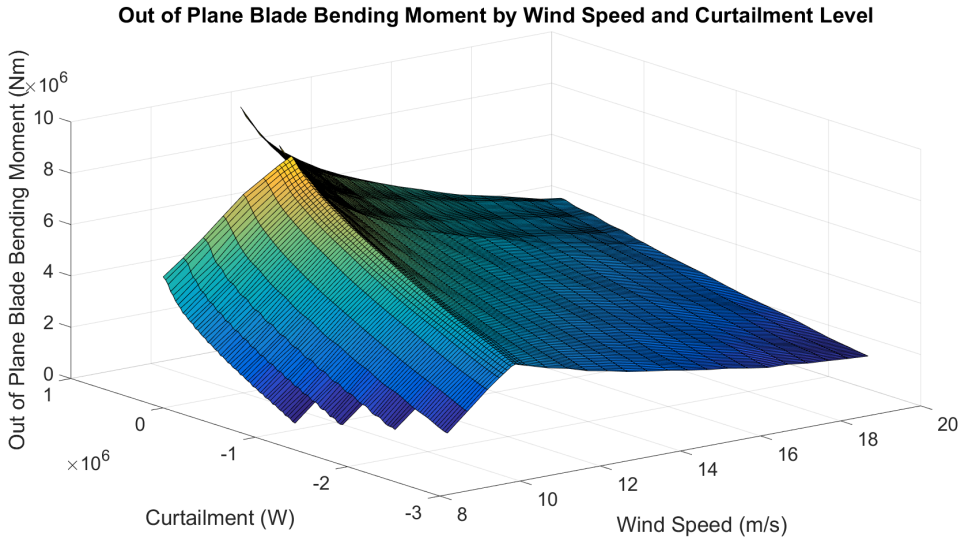


Figure 4.11: A plot of the out of plane root bending moment of the University of Strathclyde exemplar wind turbine by wind speed and level of curtailment.

Figure(4.10) and Figure(4.11) show how the static moment of the tower and blades change as the level of curtailment is changed.

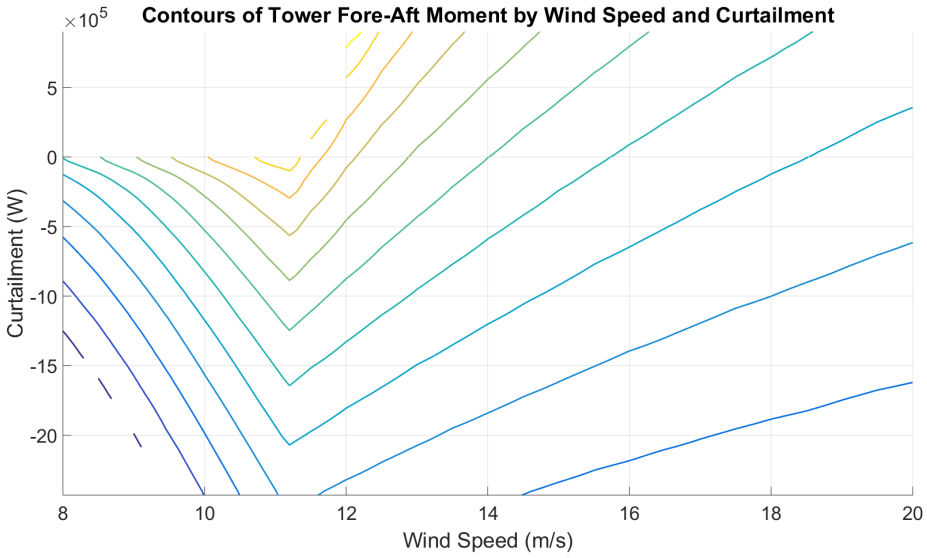


Figure 4.12: A contour plot of the fore-aft tower bending moment of the University of Strathclyde exemplar wind turbine by wind speed and level of curtailment.

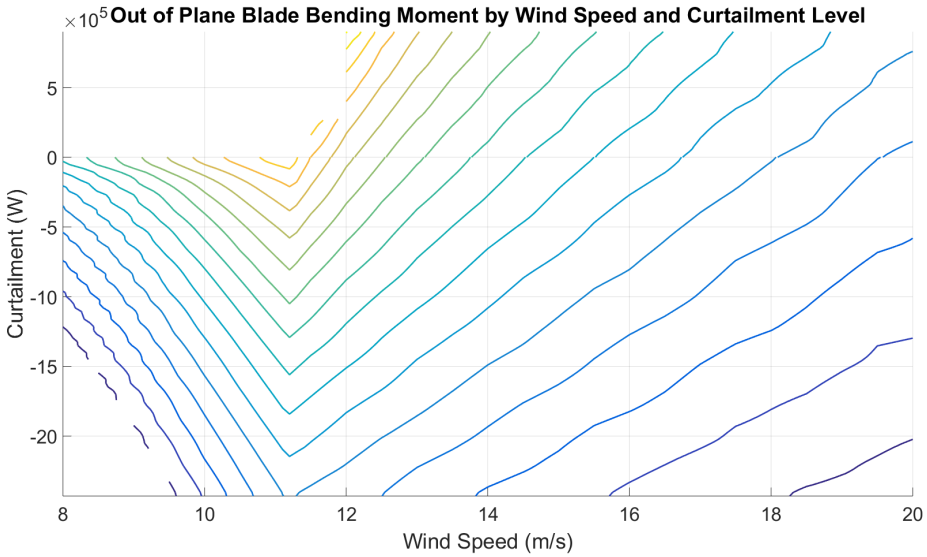


Figure 4.13: A contour plot of the out of plane root bending moment of the University of Strathclyde exemplar wind turbine by wind speed and level of curtailment.

Figure(4.12) and Figure(4.13) show contour plots of Figure(4.10) and Figure(4.11) respectively.

While historically wind turbines have been seen in isolation and maximising power

output was the main goal with wind farm control the array can be seen as a whole in its operation. With this in mind and given the aim of this research to look at strategies of wind farm control to reduce wind farm fatigue the follow solution is proposed. Given that fatigue is caused by variations in bending moments what happens if curtailment of a wind farm is allocated to maintain the bending moments of the wind turbines. As it has been shown that in a single wind turbines operation it will experience a variation in bending moments as the wind speed changes and there is scope to derate wind farms as part of grid requires such as providing droop control and genral wind power curtailment the curtailment across the wind farm can be allocated using the wind speed estimate to maintain a single baseline bending moment across all wind turbines.

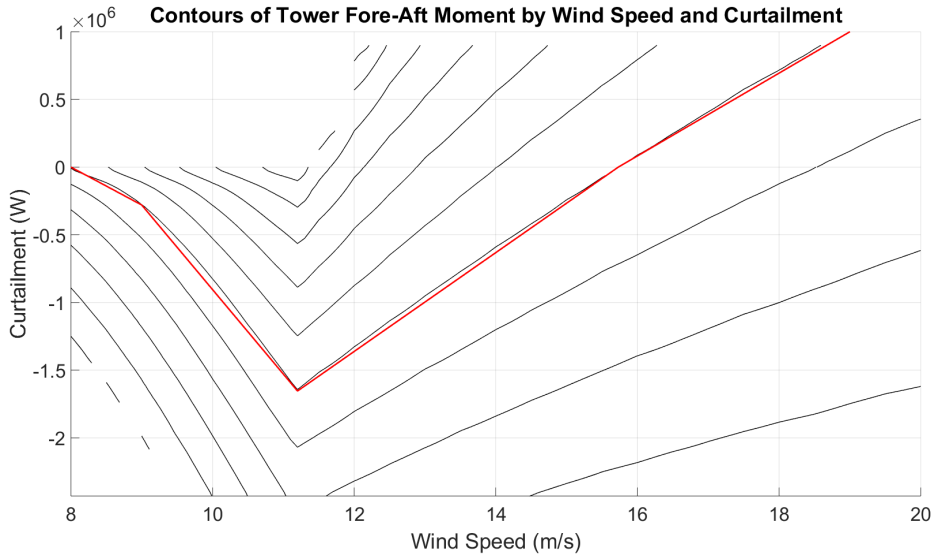


Figure 4.14: A plot of contours of constant tower fore-aft moment by curtailment and wind speed with the proposed baseline curtailment strategy.

Figure(4.14) Shows the new baseline strategy for power allocation in the wind farm. Initially each turbine is curtailed to this line and then any difference in power is allocated to the wind turbines by the square of the estimated wind speed. The square of the estimated wind speed was chosen as the higher the wind speed the lower the gradient of the moments. As shown in Figure(4.14) wind turbines are at times allocated positive curtailment levels in order to maintain the tower moment.

## 4.3 Results

The results presented in this section are designed to show that the wind farm controller can operate in a variety of wind conditions and wind farm layouts. For comparison other strategies than the one discussed in the previous section are tested. The flag based allocation system is the one proposed by [7] based on the PAC's traffic light system with turbines with curtailment being allocated in a ratio of 3:1:0 for turbines with green, amber and red flags respectively. Allocation by uncurtailed power is also included as it has been used as a curtailment strategy in some research. When the uncurtailed power is used directly in the allocation of curtailment the system becomes unstable so the estimated wind speed has been used in its place . To allocate proportionally by uncurtailed power the level of curtailment was allocated by the ratios of the estimated wind speed cubed below rated and as the cube of the rated wind speed above rated. .Finally in some cases only the front row of turbines has been curtailed to show the impact of wakes within the wind farm.

### 4.3.1 Below Rated

#### Model One

The first model used in this report was a 9m/s windfield at a turbulence intensity of 0.1. 20 turbines were simulated with the arrangement being a row of all twenty turbines perpendicular to the flow of the wind.

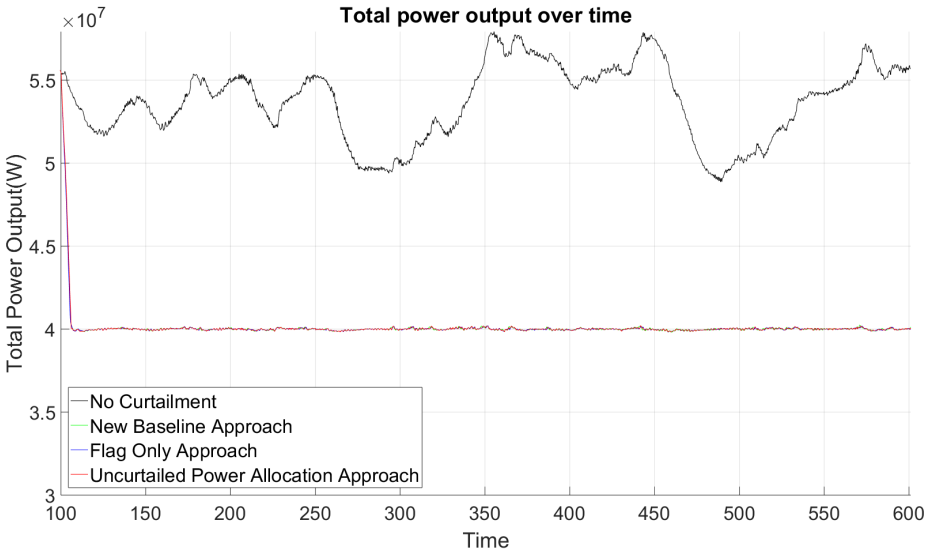


Figure 4.15: Power output from the wind farm when it is curtailed to 40MW in Model One

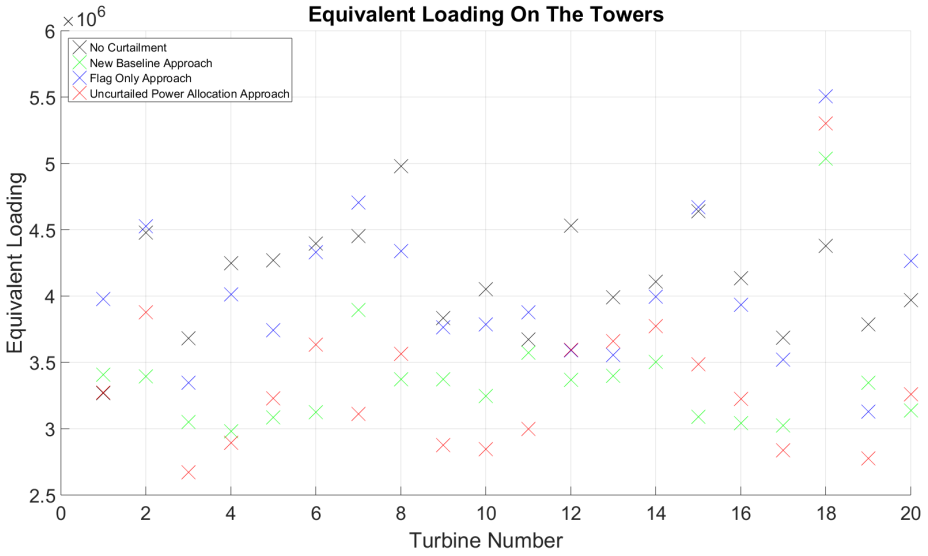


Figure 4.16: DELs for the fore-aft tower moments from the wind turbines when the wind farm is curtailed to 40MW in Model one


Figure 4.17: DELs for the out of plane blade bending moments from the wind turbines when the wind farm is curtailed to 40MW in Model one

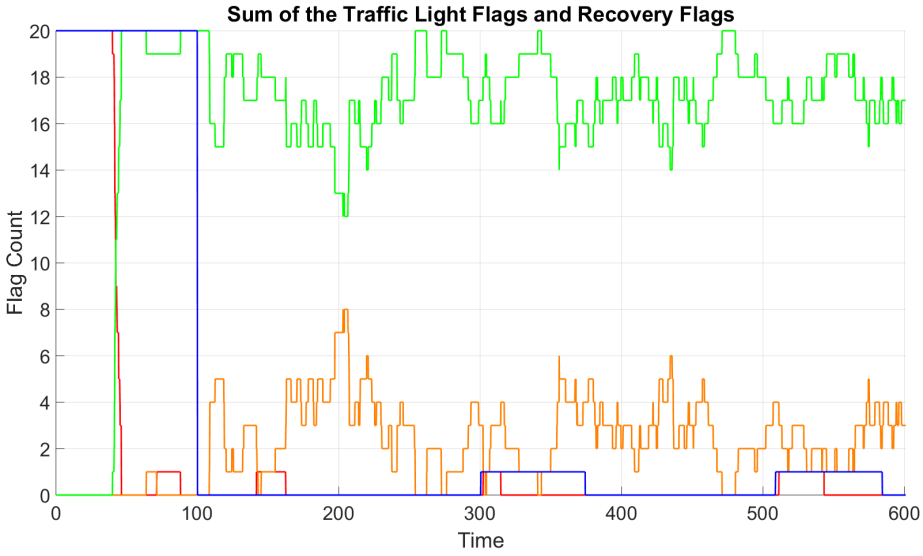


Figure 4.18: Sum of the traffic light flags using the flag based curtailment strategy at a set-point power output of 40MW in Model One.

Figure(4.18) Shows that at this level of curtailment the wind farm is reaching the limits of the PAC as the level of curtailment is so high that the turbines are being forced into the lower amber limit. It can also be seen that the wind speed flag is being

activated on two occasions. This is due to the wind speed being too low for the PAC to operate resulting in the PAC temporarily turning off.

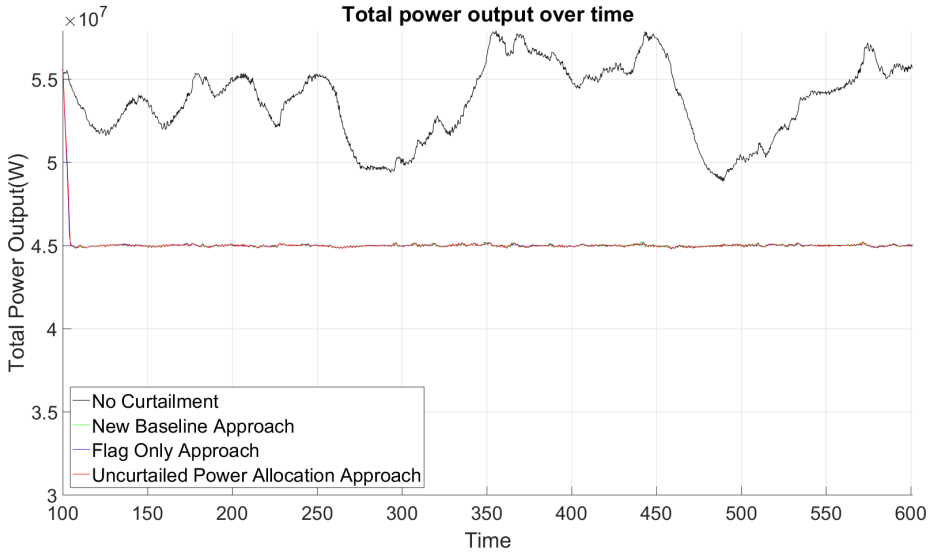


Figure 4.19: Power output from the wind farm when it is curtailed to 45MW in Model One

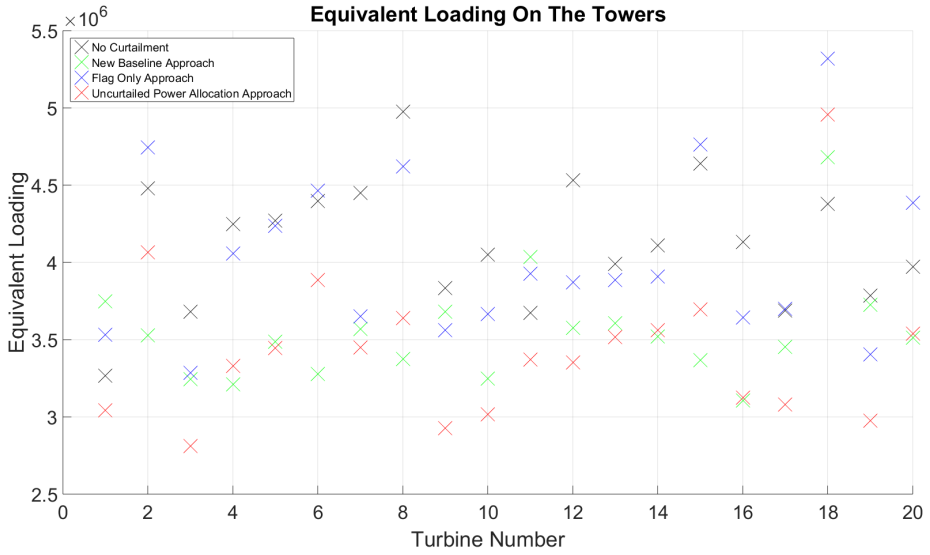


Figure 4.20: DELs for the fore-aft tower moments from the wind turbines when the wind farm is curtailed to 45MW in Model One


Figure 4.21: DELs for the out of plane blade bending moments from the wind turbines when the wind farm is curtailed to 45MW in Model One

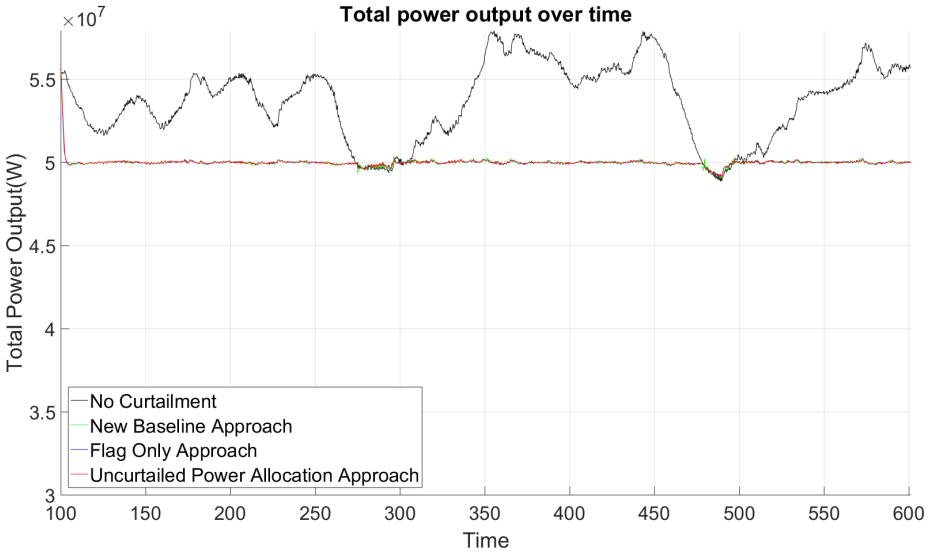


Figure 4.22: Power output from the wind farm when it is curtailed to 50MW in Model One

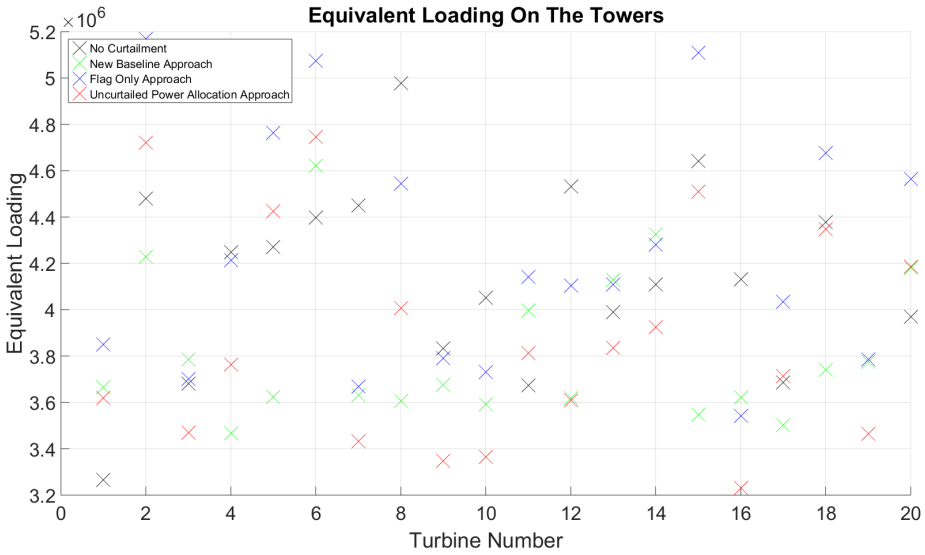


Figure 4.23: DELs for the fore-aft tower moments from the wind turbines when the wind farm is curtailed to 50MW in Model One

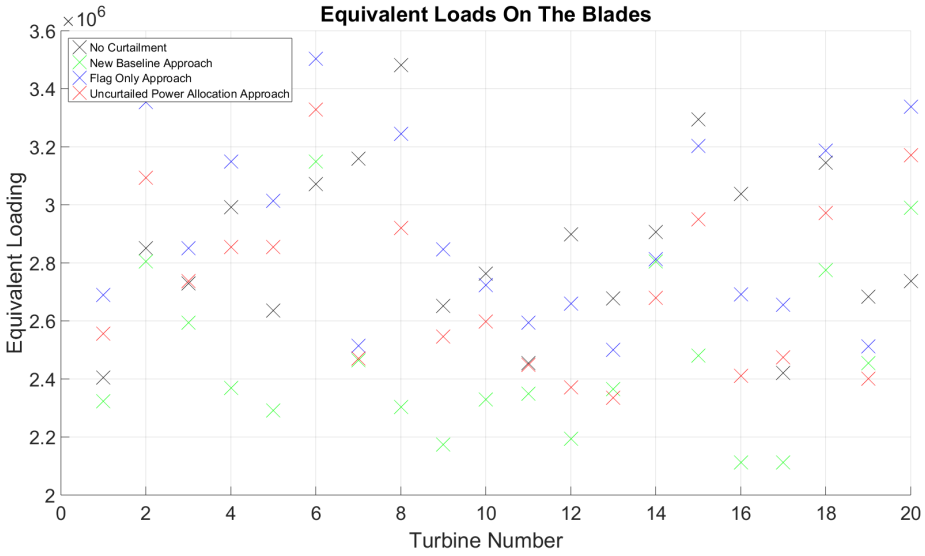


Figure 4.24: DELs for the out of plane blade bending moments from the wind turbines when the wind farm is curtailed to 50MW in Model One

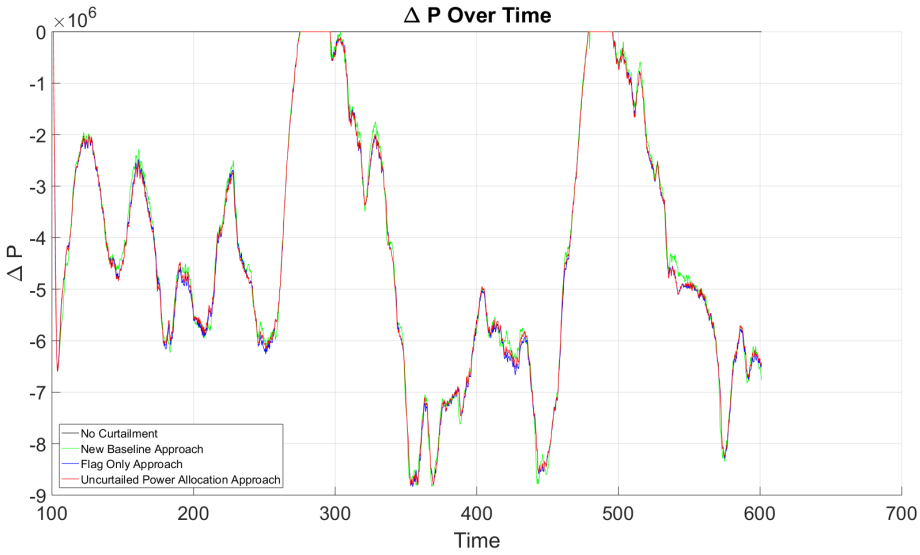


Figure 4.25: The total level of curtailment across the wind farm for each of the curtailment allocation strategies when the wind farm is curtailed to 50MW in Model One

Figure(4.25) shows that the wind turbines are never allocated an above rated curtailment. This is deliberate as at low wind speeds there is very little energy stored in the rotor and so there is very little to be gained from using this approach. In addition to this the small amount of energy stored in the rotor should be saved for a frequency response if it is required.

| Allocation | 40 MW | 45 MW | 50 MW |
|---|---|---|---|
| New Baseline Allocation | 17.67% | 13.11% | 6.67% |
| Flag Based Allocation | 2.15 % | 2.23% | -3.11% |
| Uncurtailed power based allocation | 18.82% | 16.52% | 5.70% |

Table 4.1: Change in mean damage equivalent load to the fore-aft tower moment in Model One

| Allocation | 40 MW | 45 MW | 50 MW |
|---|---|---|---|
| New Baseline Allocation | 28.51% | 25.82% | 12.68% |
| Flag Based Allocation | 9.90 % | 5.30% | -2.32% |
| Uncurtailed power based allocation | 21.66% | 16.49% | 4.43% |

Table 4.2: Change in mean damage equivalent load to the out-of-plane bending moment in Model One

Table(4.1) and Table(4.2) show that there is a significant reduction in the DELs of both the tower and the blades when the wind farm is curtailed, even when the curtailment level is low. The increase in the DELs when the flag based strategy is used is caused by the turbines being curtailed and uncurtailed over the steepest part of the moment slope. As the other strategies aim to avoid operating on the steepest section of the the slope they do not experience as much fatigue.

### Model Two

The second set of below rated simulations have been run in a 10m/s windfield at a turbulence intensity of 0.1. 20 turbines were simulated with the arrangement being in two rows of ten turbines perpendicular to the flow of the wind.

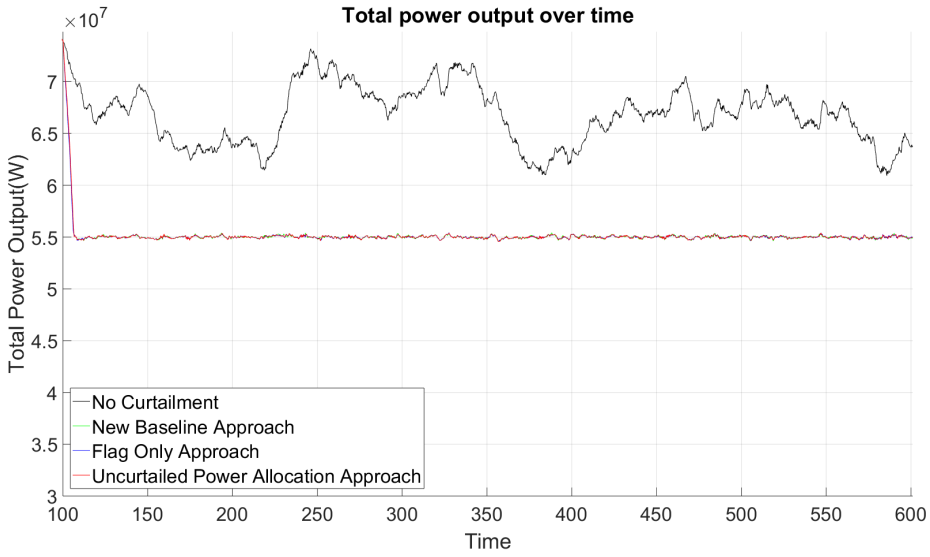


Figure 4.26: Power output from the wind farm when it is curtailed to 55MW in Model Two.

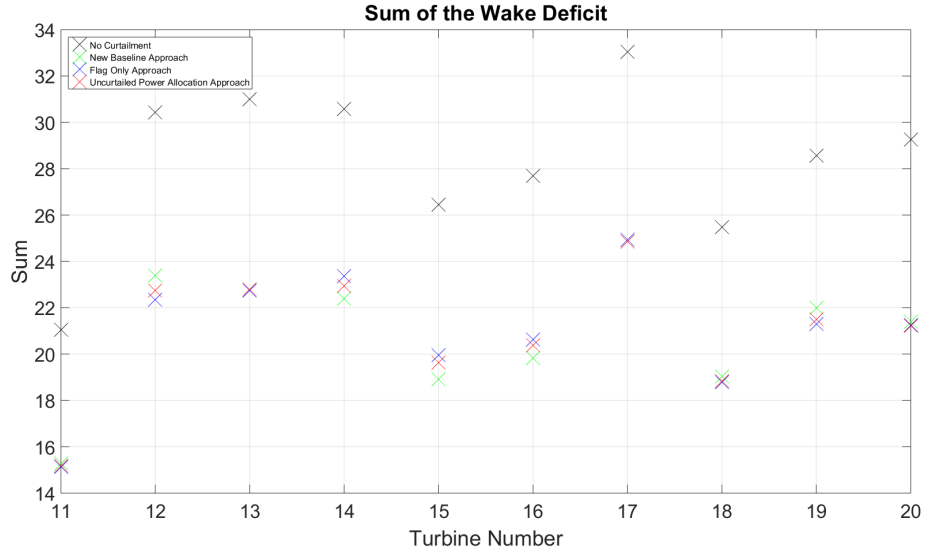


Figure 4.27: Sum of the wake deficits in the second row of wind turbines in Model Two.

Figure(4.27) shows the sum of the wake deficit for all of the back row of wind turbines. What can clearly be seen is that all three curtailment strategies reduce the wake deficit in approximately equal measure. For comparison a simulation only curtailing the front row of wind turbines has been included and can be seen to have the lowest levels of wake deficit.

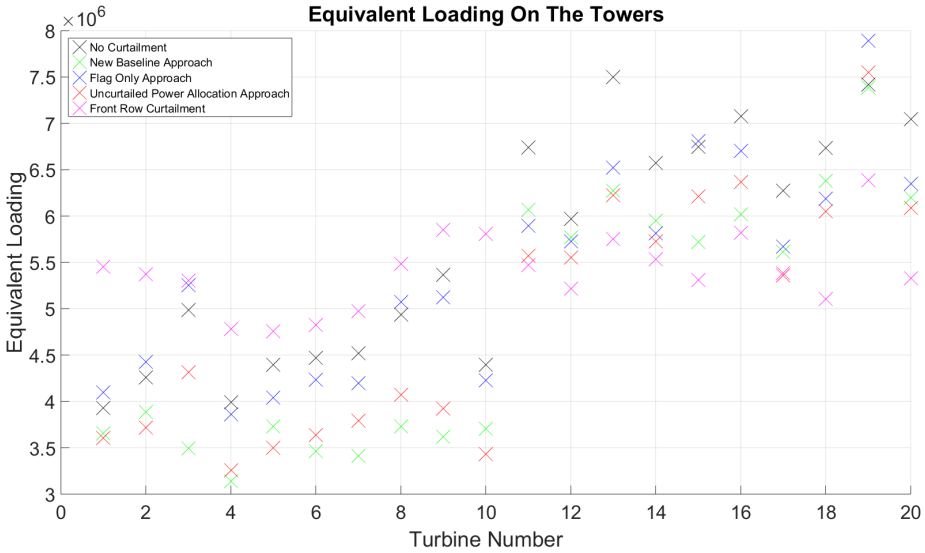


Figure 4.28: DELs for the fore-aft tower moments from the wind turbines when the wind farm is curtailed to 55MW in Model Two.

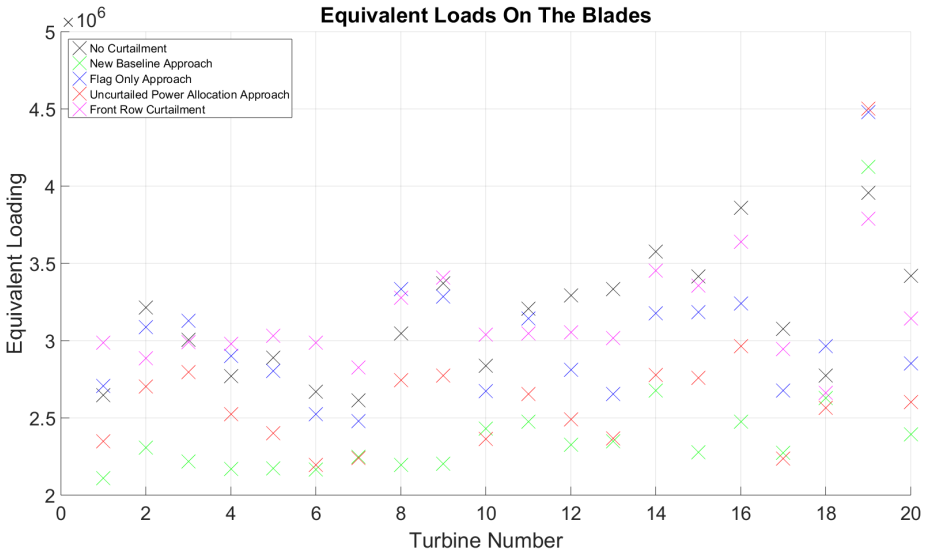


Figure 4.29: DELs for the out of plane blade bending moments from the wind turbines when the wind farm is curtailed to 55MW in Model Two.

Wakes have been known to contribute to wind turbine fatigue. This can be seen in Figure (4.28) and Figure (4.29). However, when the control strategy aims to maximise wake reduction the results were a much smalled reduction in damage equivalent loads than the other strategies as whilst the level of fatigue of the towers for the back row decreased the level of damage to the back row increased.

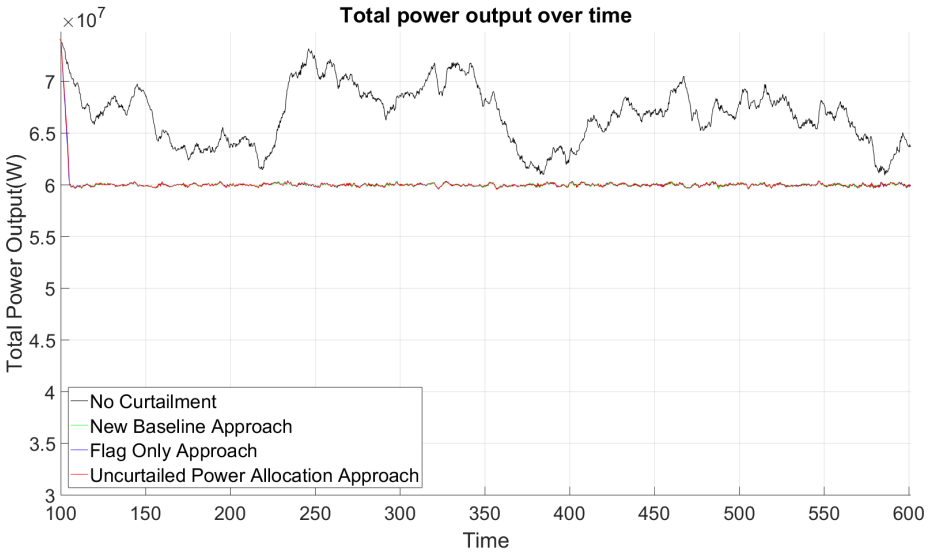


Figure 4.30: Power output from the wind farm when it is curtailed to 60MW in Model Two.

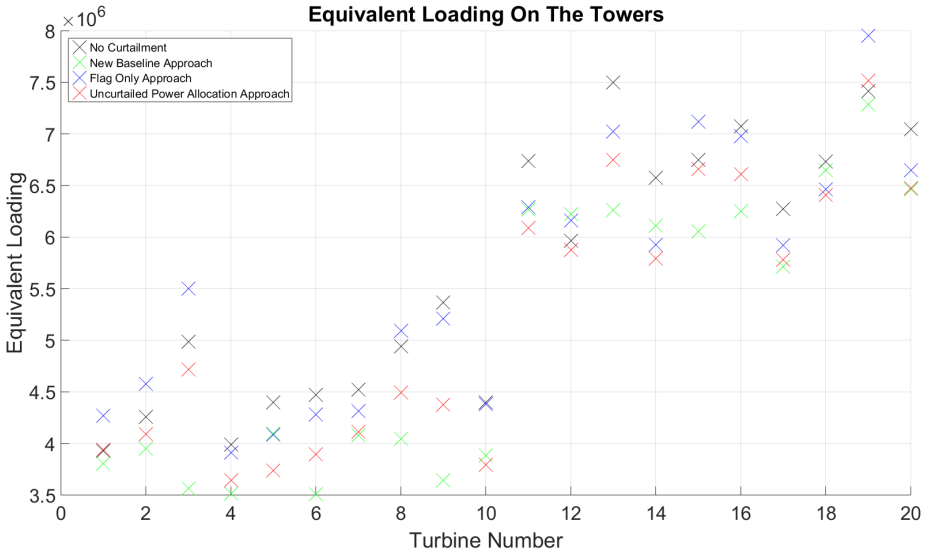


Figure 4.31: DELs for the fore-aft tower moments from the wind turbines when the wind farm is curtailed to 60MW in Model Two.


Figure 4.32: DELs for the out of plane blade bending moments from the wind turbines when the wind farm is curtailed to 60MW in Model Two.

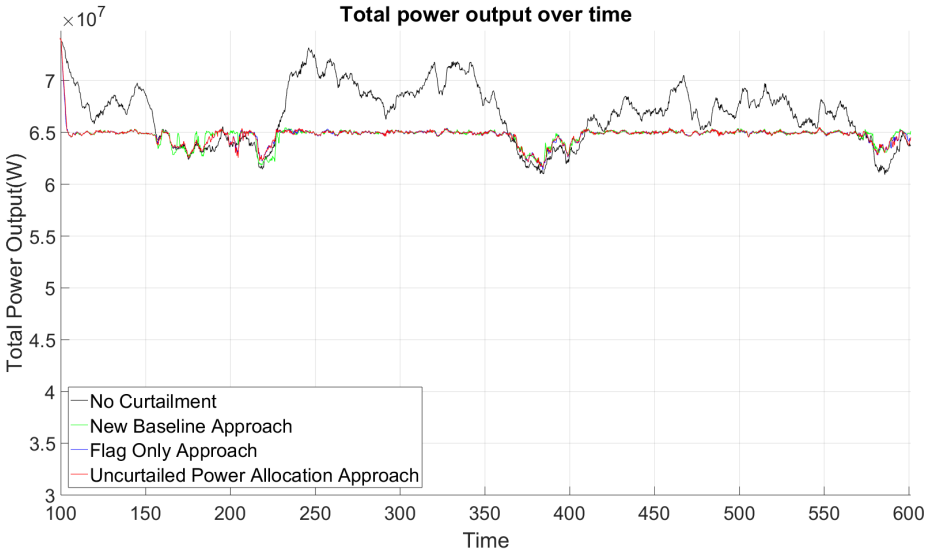


Figure 4.33: Power output from the wind farm when it is curtailed to 65MW in Model Two.

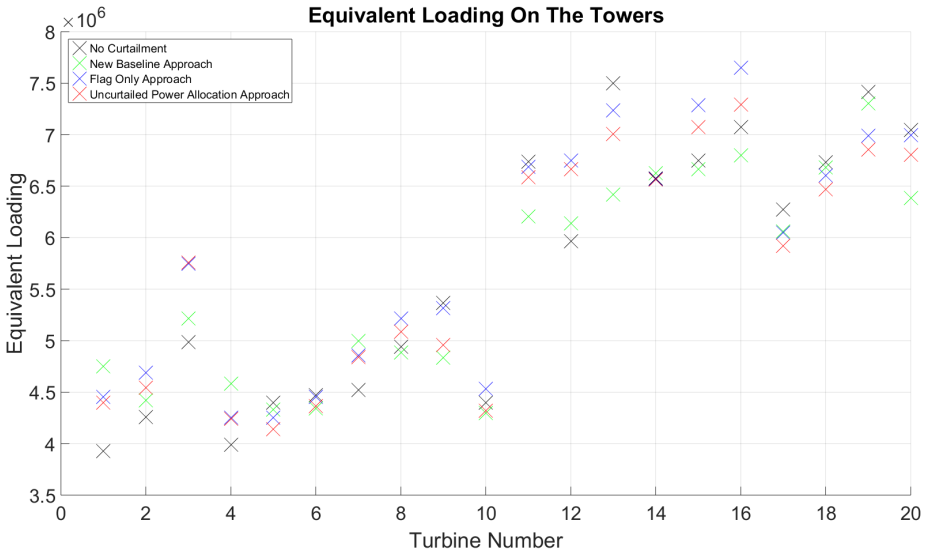


Figure 4.34: DELs for the fore-aft tower moments from the wind turbines when the wind farm is curtailed to 65MW in Model Two.

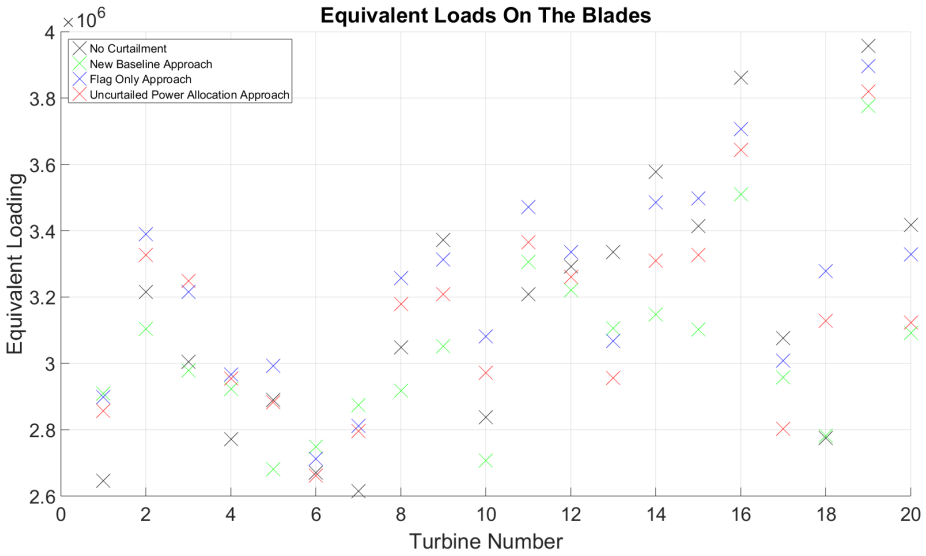


Figure 4.35: DELs for the out of plane blade bending moments from the wind turbines when the wind farm is curtailed to 65MW in Model Two.

Figure (4.34) and Figure (4.35) show that there are some wind turbines which are experiencing increased damage equivalent loads when the wind farm is curtailed to 65MW. The cause of this is that when the wind turbines use there inertia to maintain the set-point power there can be increases in the DELS.

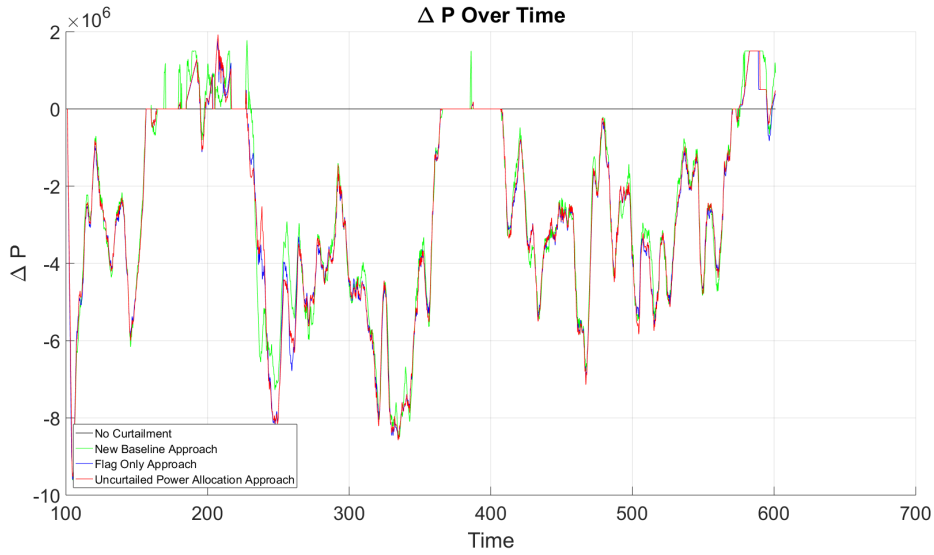


Figure 4.36: The total level of curtailment of the wind farm in in Model Two when it is curtailed to 65MW by the three curtailment strategies.

Figure(4.36) shows that compared to the previous wind field there are some turbines which are at above rated wind speeds so the controller is attempting positive curtailment to maintain the set-point. However, as the wind speeds are still quite low there is above rated set point tracking cannot be achieved by any strategy.

| Allocation | 55 MW | 60 MW | 65 MW |
|---|---|---|---|
| New Baseline | 14.9669 % | 10.9634% | 0.0807% |
| Flag Based | 4.1174% | 0.7643% | -3.4875 % |
| Uncurtailed power based | 14.1510% | 7.8221% | -1.1447% |

Table 4.3: Change in mean damage equivalent load to the fore-aft tower moment in Model Two.

| Allocation | 55 MW | 60 MW | 65 MW |
|---|---|---|---|
| New Baseline | 23.2143 % | 16.7617% | 2.7853% |
| Flag Based | 4.3062% | -0.0380% | -3.2246 % |
| Uncurtailed power based | 15.8376% | 8.6528% | -0.2661% |

Table 4.4: Change in mean damage equivalent load to the out-of-plane bending moment in Model Two.

Table(4.3) and Table(4.4) show that the largest reduction in the DELs of the wind

turbines comes from the proposed new strategy.

### 4.3.2 Near Rated

#### Model Three

These first near rated simulations were run in a 12m/s wind feild at 0.1 TI . 20 turbines were simulated with the arrangement being in two rows of ten turbines perpendicular to the flow of the wind.

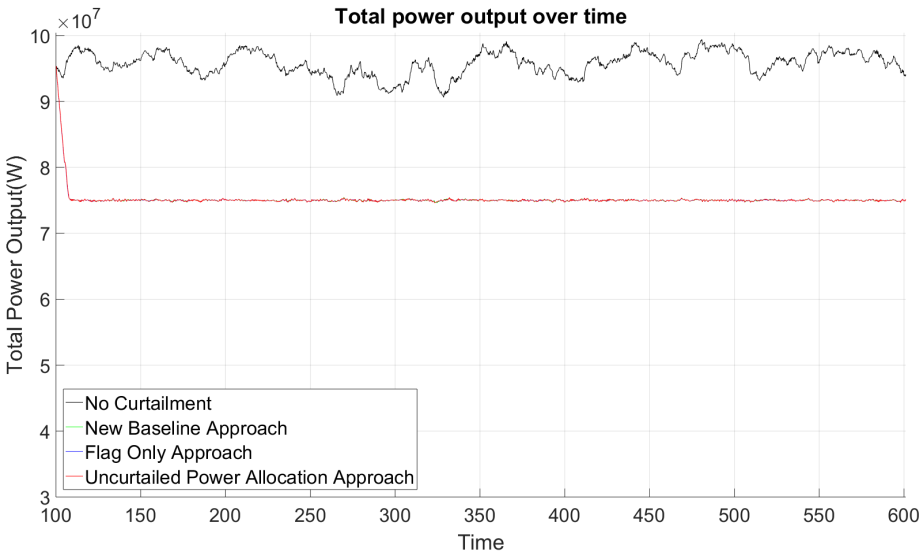


Figure 4.37: Power output from the wind farm when it is curtailed to 75MW in Model Three

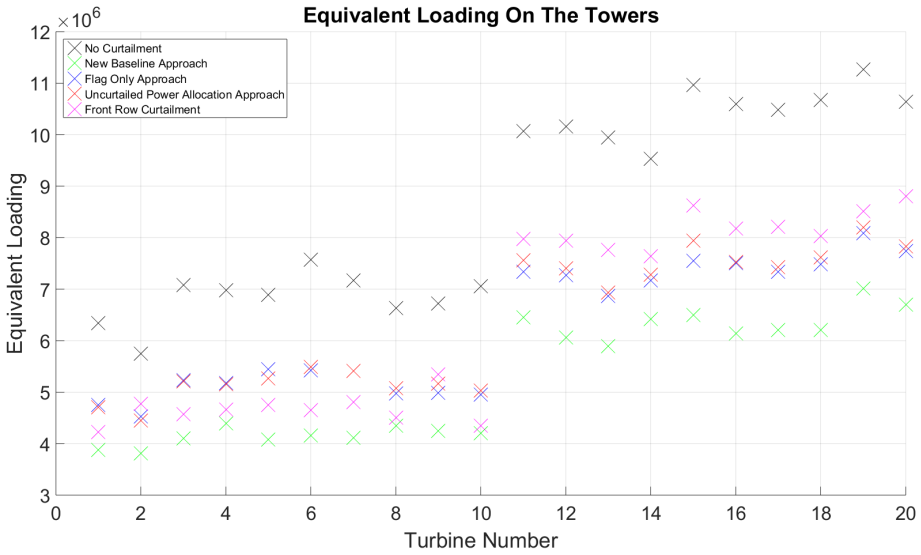


Figure 4.38: DELs for the fore-aft tower moments from the wind turbines when the wind farm is curtailed to 75MW in Model Three.

Figure(4.38) shows that the proposed new strategy has results in the largest reduction in tower DELs for all twenty wind turbines and is also more effective at this than when the only the front row of turbines is curtailed even though, as Figure (4.54) shows that, curtailing the front row of wind turbines results in the lowest wake deficits of all of the strategies.

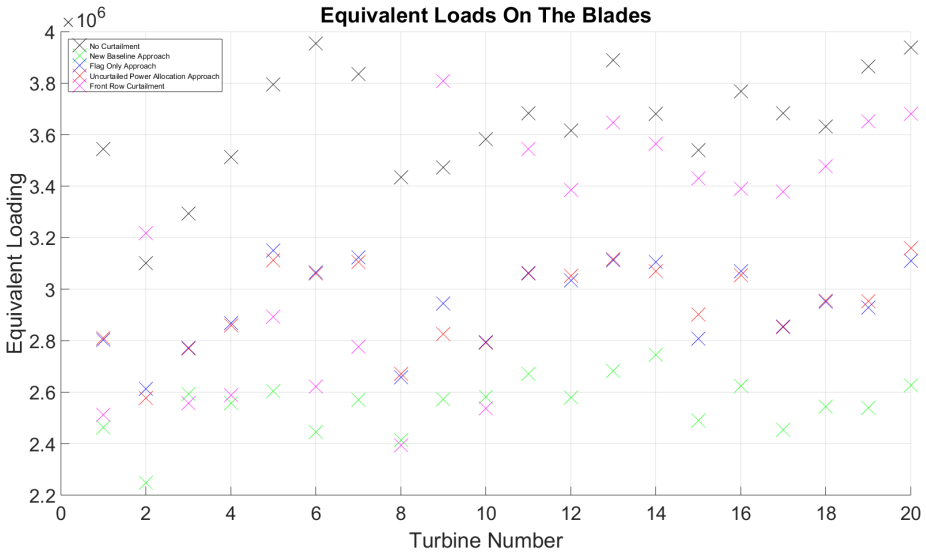


Figure 4.39: DELs for the out of plane blade bending moments from the wind turbines when the wind farm is curtailed to 75MW in Model Three.

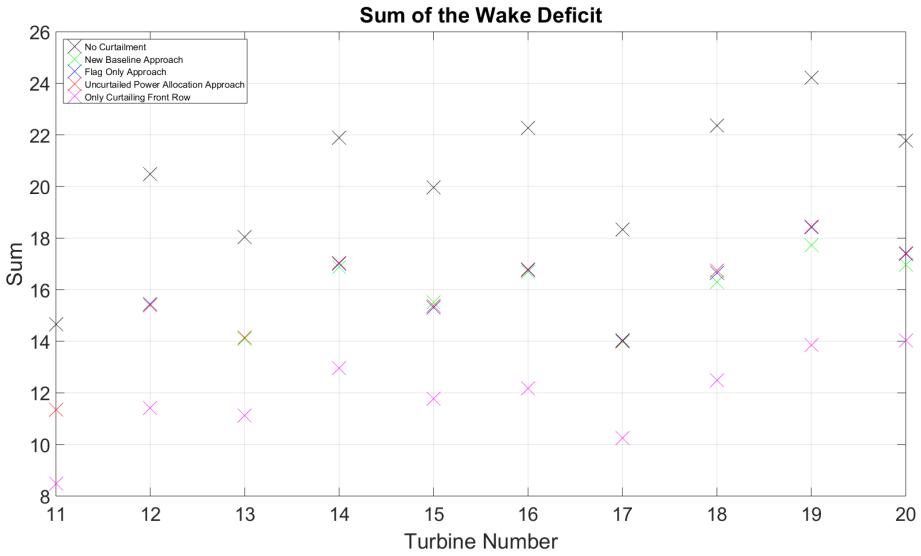


Figure 4.40: Sum of the wake deficits in the second row of wind turbines when the wind farm is curtailed to 75MW in Model Three.

Figure(4.54) shows that by only curtailing the front row of wind turbines there is a large reduction in the wake deficits. However, counter-intuitively this results in higher damage equivalent loads for the back row of wind turbines that the other strategies. The reason for this is that as the back row of wind turbines are not being curtailed they

will experience variation in their tower and blade moments as the wind speed varies and as they are at zero curtailment this variation is at its highest.

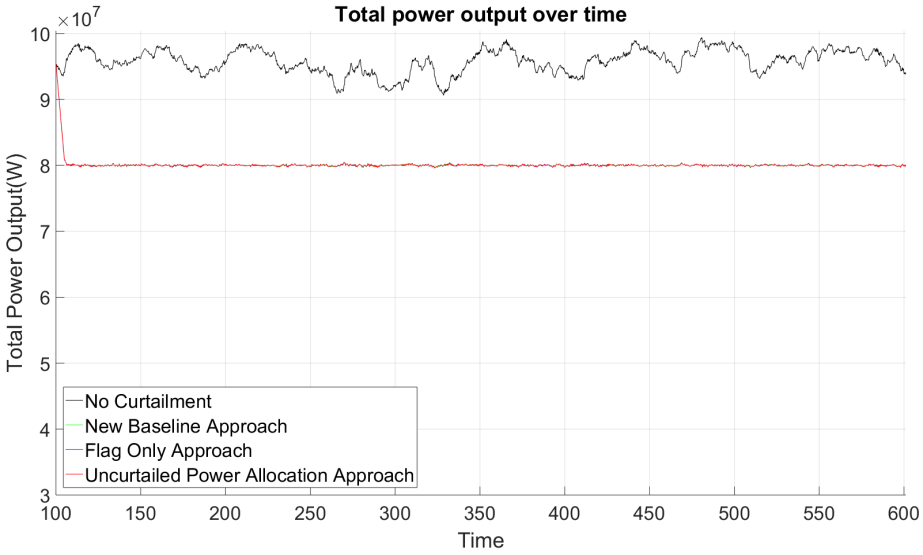


Figure 4.41: Power output from the wind farm when it is curtailed to 80MW in Model Three.

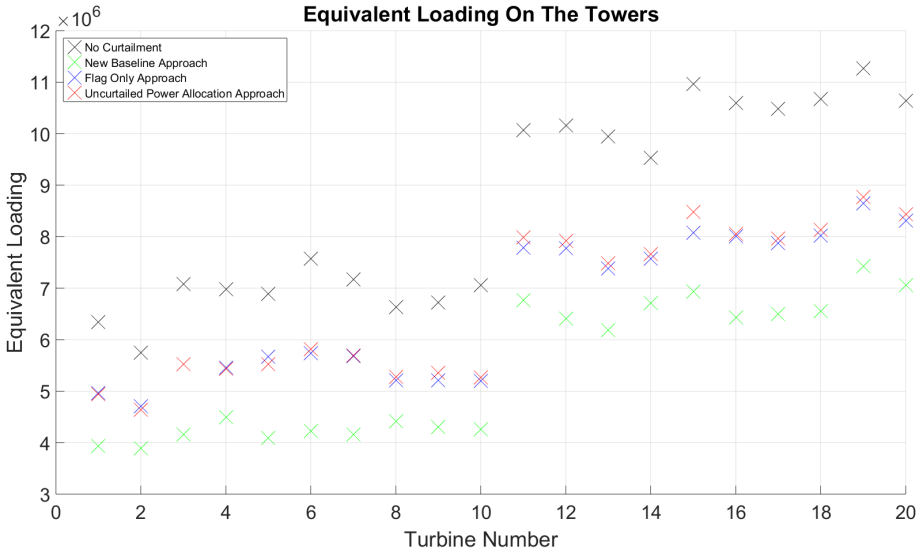


Figure 4.42: DELs for the fore-aft tower moments from the wind turbines when the wind farm is curtailed to 80MW in Model Three.

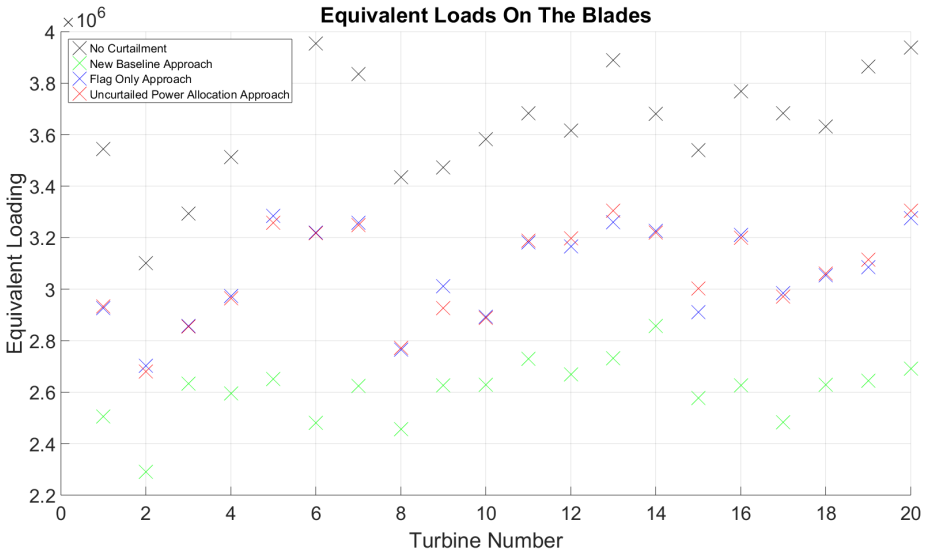


Figure 4.43: DELs for the out of plane blade bending moments from the wind turbines when the wind farm is curtailed to 80MW in Model Three.

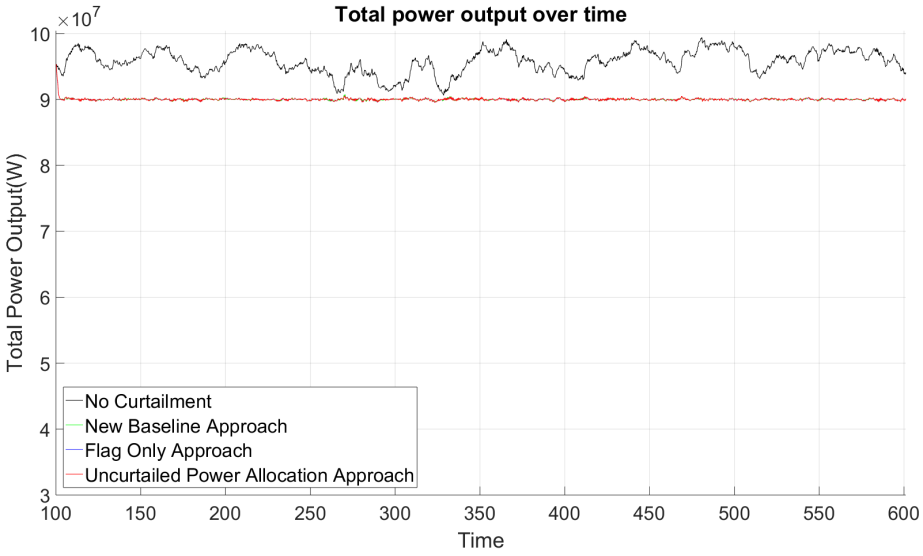


Figure 4.44: Power output from the wind farm when it is curtailed to 90MW in Model Three.

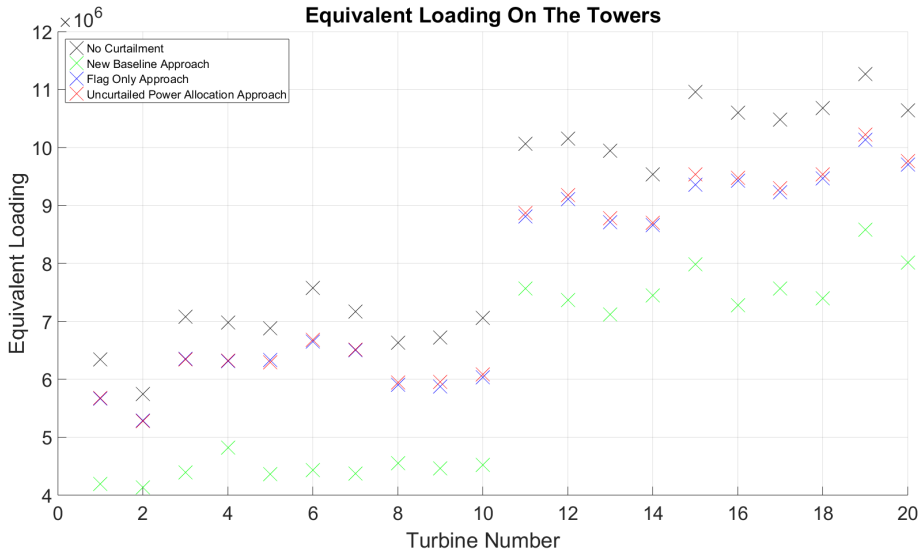


Figure 4.45: DELs for the fore-aft tower moments from the wind turbines when the wind farm is curtailed to 90MW in Model Three.

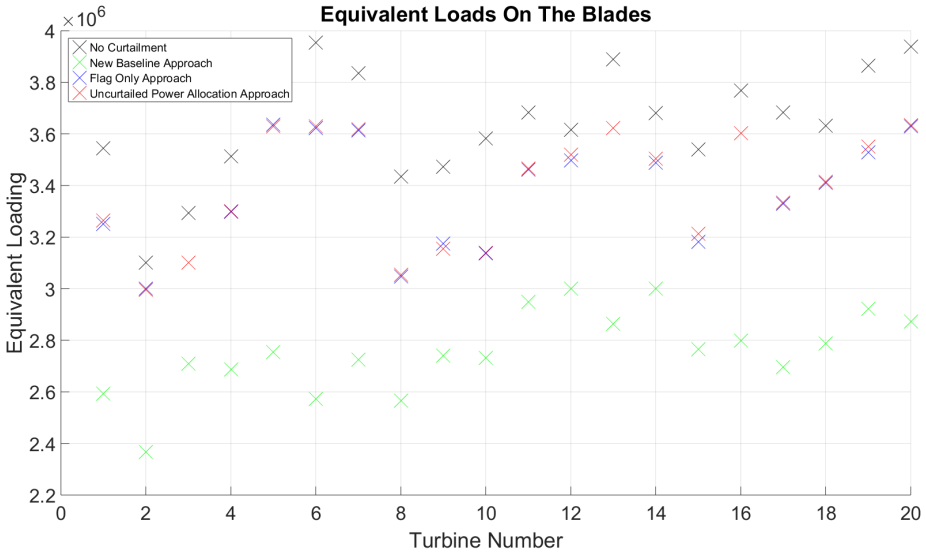


Figure 4.46: DELs for the out of plane blade bending moments from the wind turbines when the wind farm is curtailed to 90MW in Model Three.

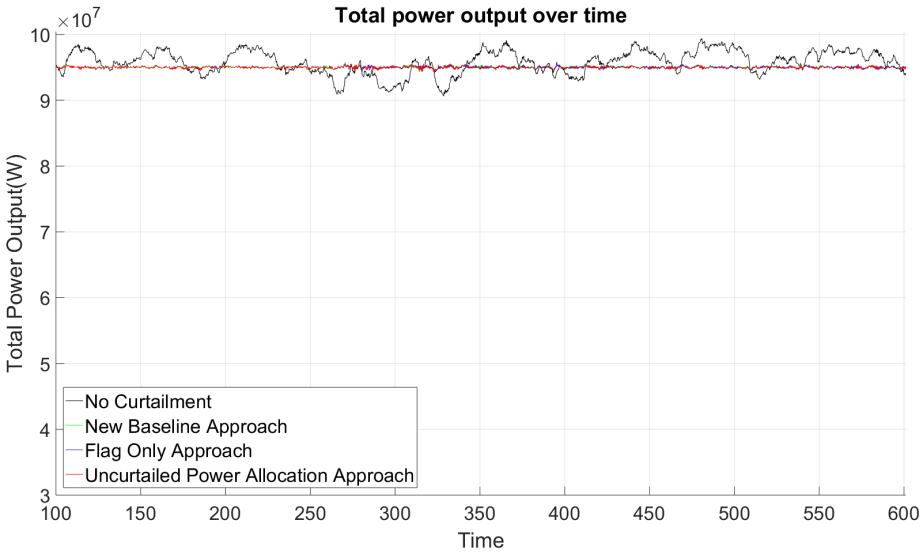


Figure 4.47: Power output from the wind farm when it is curtailed to 95MW in Model Three.

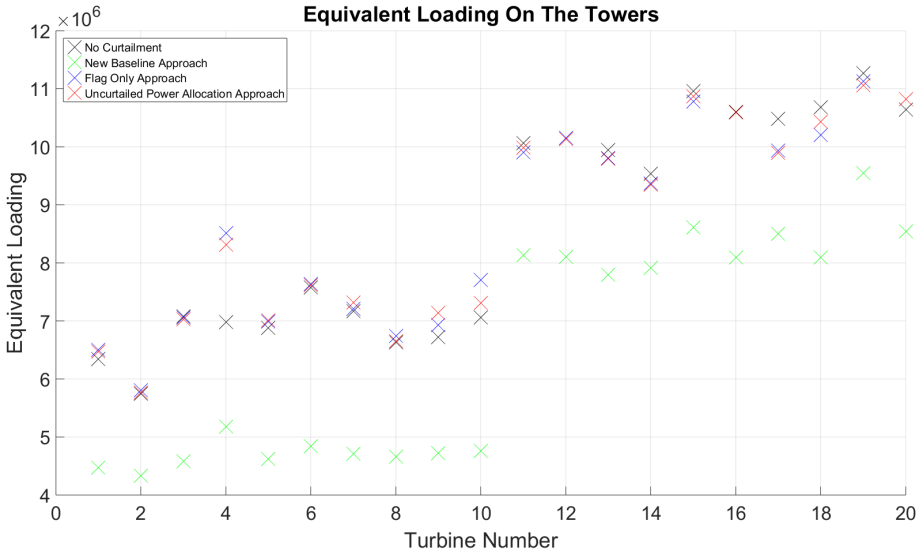


Figure 4.48: DELs for the fore-aft tower moments from the wind turbines when the wind farm is curtailed to 95MW in Model Three.

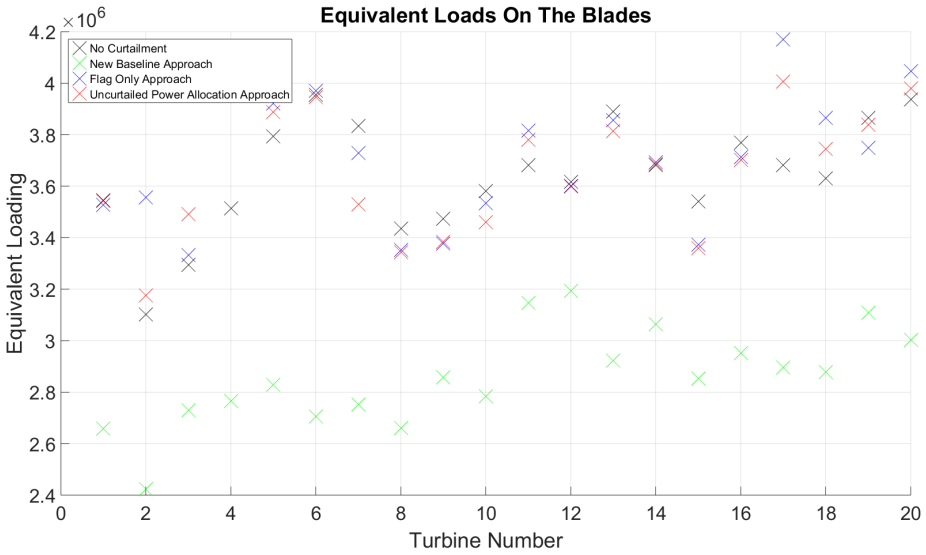


Figure 4.49: DELs for the out of plane blade bending moments from the wind turbines when the wind farm is curtailed to 95MW in Model Three.

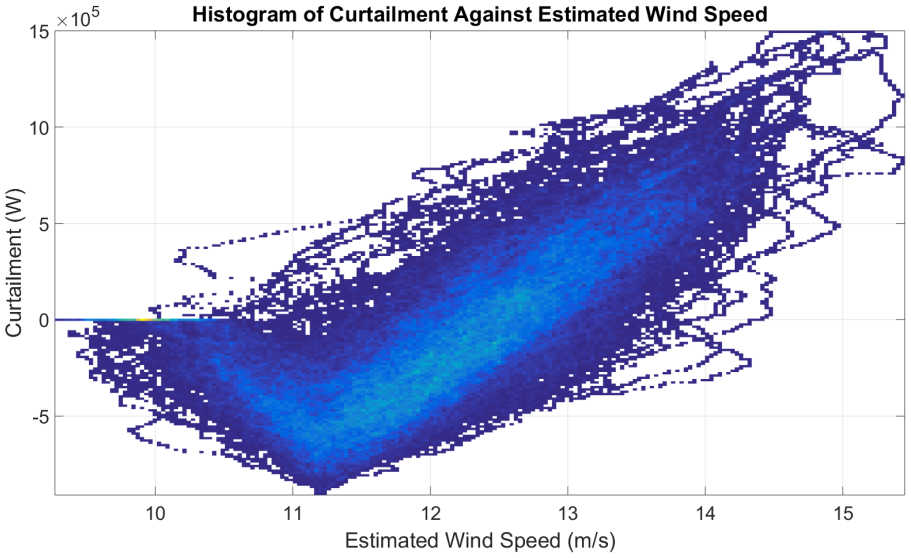


Figure 4.50: A histogram of the level of curtailment against the estimated wind speed when the New Baseline strategy is used and the wind farm is curtailed to 95MW in Model Three.

| Allocation | 75 MW | 80 MW | 90 MW | 95MW |
|---|---|---|---|---|
| New Baseline | 39.0714 % | 37.0105 % | 30.8308% | 25.5851% |
| Flag Based | 26.9845 % | 22.7368 % | 10.8973% | -1.3208% |
| Uncurtailed power based | 26.2650 % | 21.9763 % | 10.4311% | -1.1002% |

Table 4.5: Change in mean damage equivalent load to the fore-aft tower moment in Model Three

| Allocation | 75 MW | 80 MW | 90 MW | 95MW |
|---|---|---|---|---|
| New Baseline | 29.8090 % | 28.2637 % | 24.2163% | 21.3699% |
| Flag Based | 19.1523 % | 15.8531 % | 7.1148% | -2.0382% |
| Uncurtailed power based | 19.2559 % | 15.7853 % | 6.9554% | -0.6282% |

Table 4.6: Change in mean damage equivalent load to the out-of-plane bending moment in Model Three

Table (4.5) and Table (4.6) show that over all levels of curtailment the new baseline sytratergy produces the largest reduction in DELs. The reductions in the DELs when the wind farm is curtailed to 95MW show that the new baseline strategy can significantly reduce wind turbine fatigue around rated win speeds while maintaining a set-point power output comparable to the uncurtailed power output of the wind farm

### Model Four

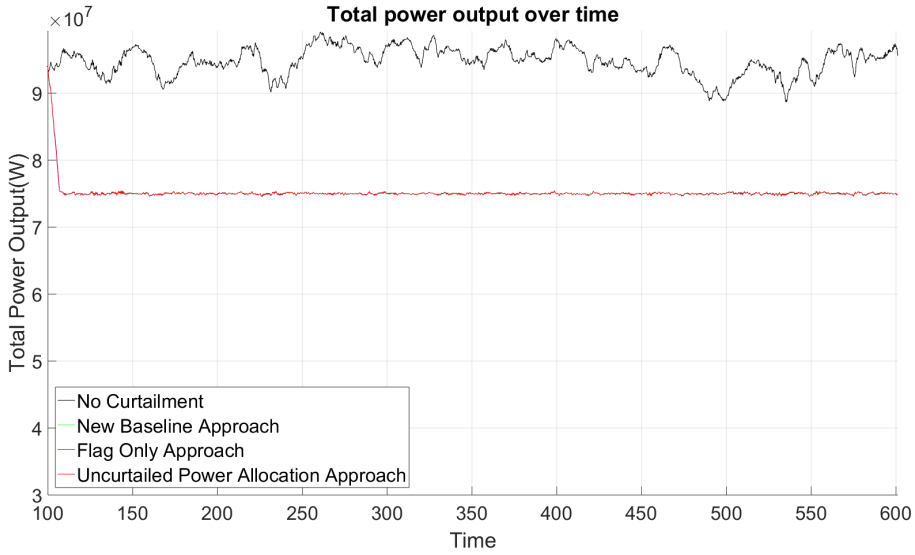


Figure 4.51: Power output from the wind farm when it is curtailed to 75MW in Model Four

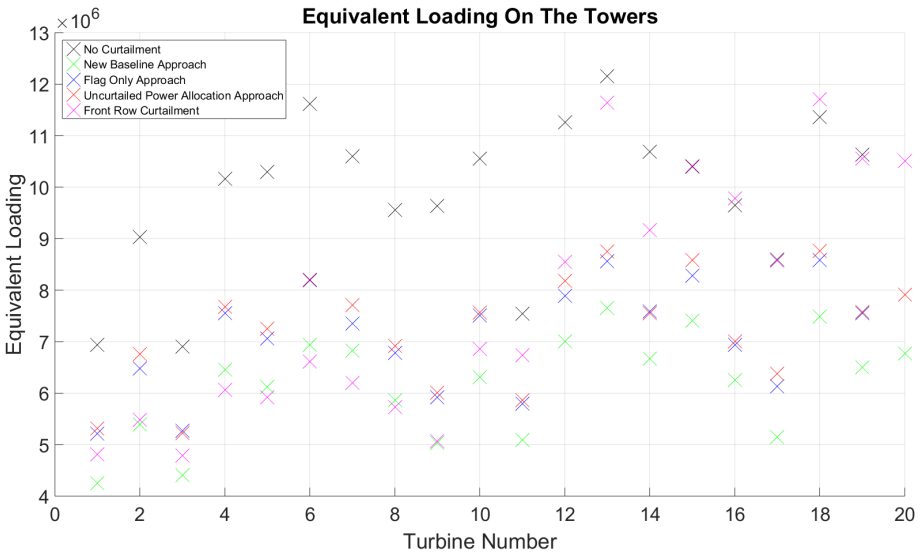


Figure 4.52: DELs for the fore-aft tower moments from the wind turbines when the wind farm is curtailed to 75MW in Model Four

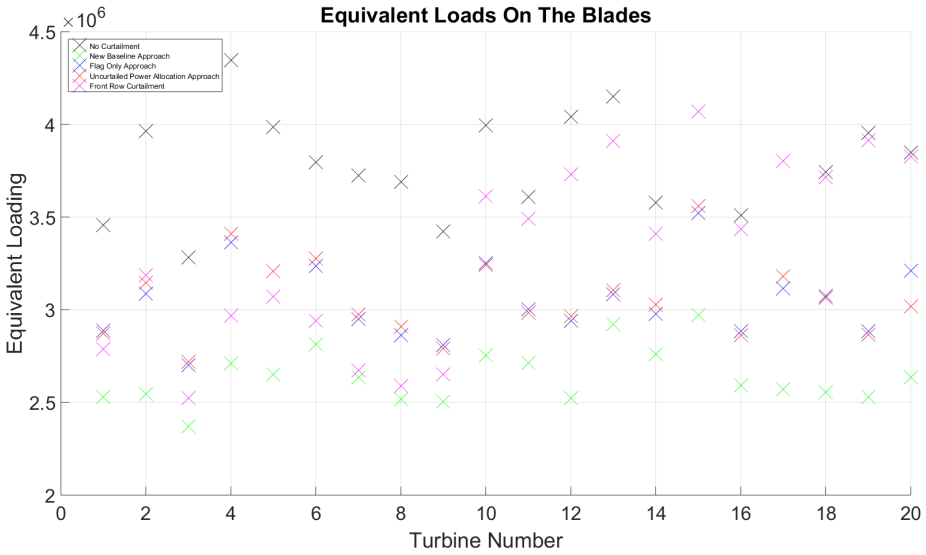


Figure 4.53: DELs for the out of plane blade bending moments from the wind turbines when the wind farm is curtailed to 75MW in Model Four.

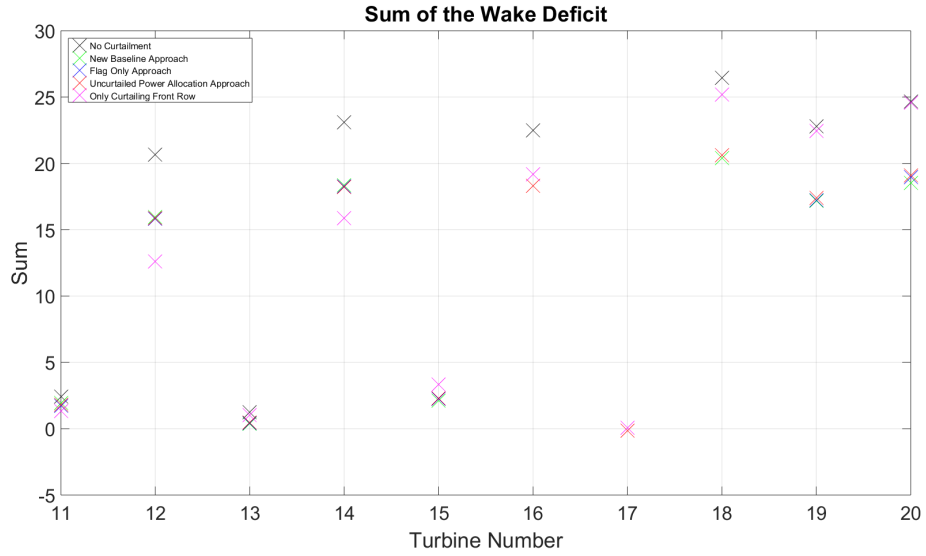


Figure 4.54: Sum of the wake deficits in the second row of wind turbines when the wind farm is curtailed to 75MW in Model Four.

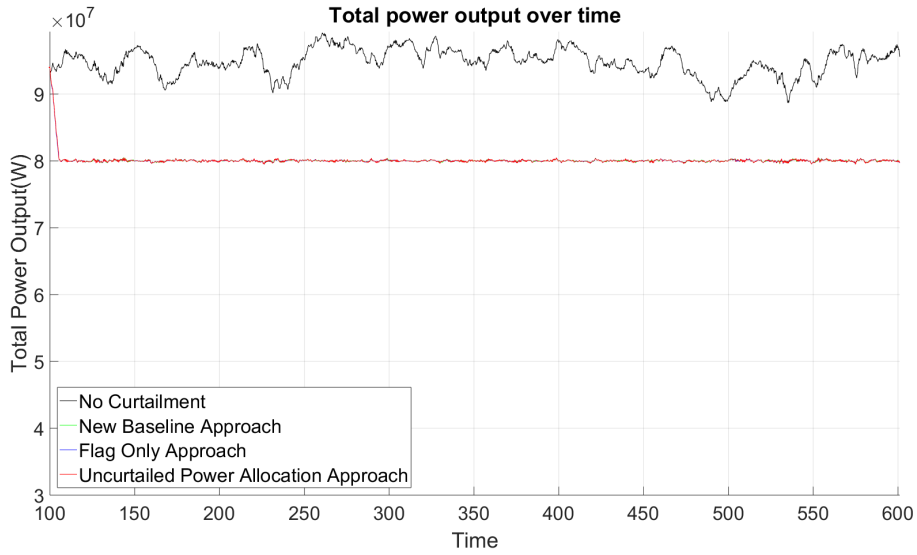


Figure 4.55: Power output from the wind farm when it is curtailed to 80MW in Model Four

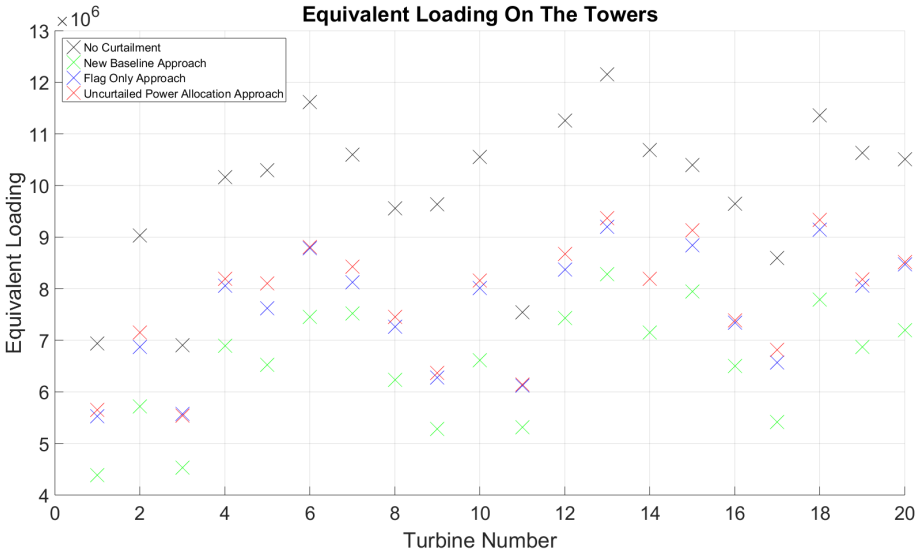


Figure 4.56: DELs for the fore-aft tower moments from the wind turbines when the wind farm is curtailed to 80MW in Model Four

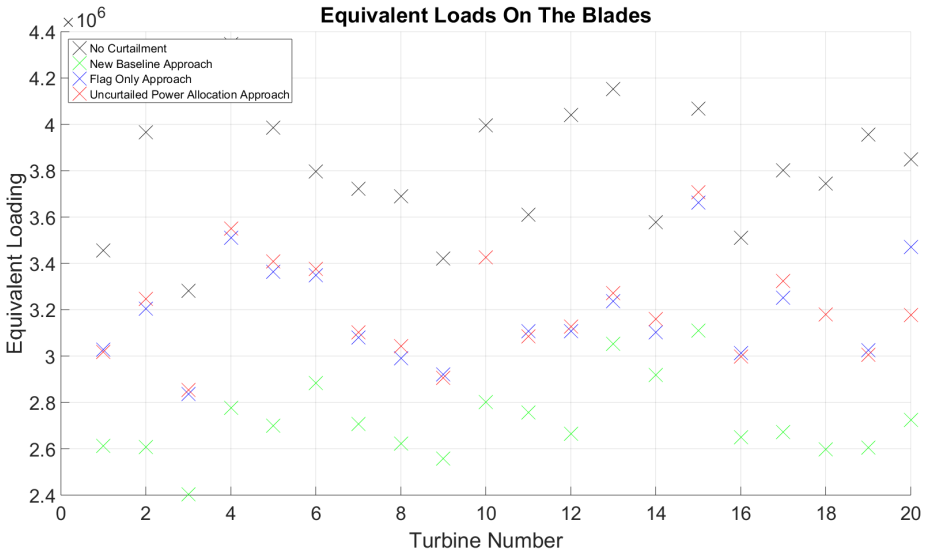


Figure 4.57: DELs for the out of plane blade bending moments from the wind turbines when the wind farm is curtailed to 80MW in Model Four.

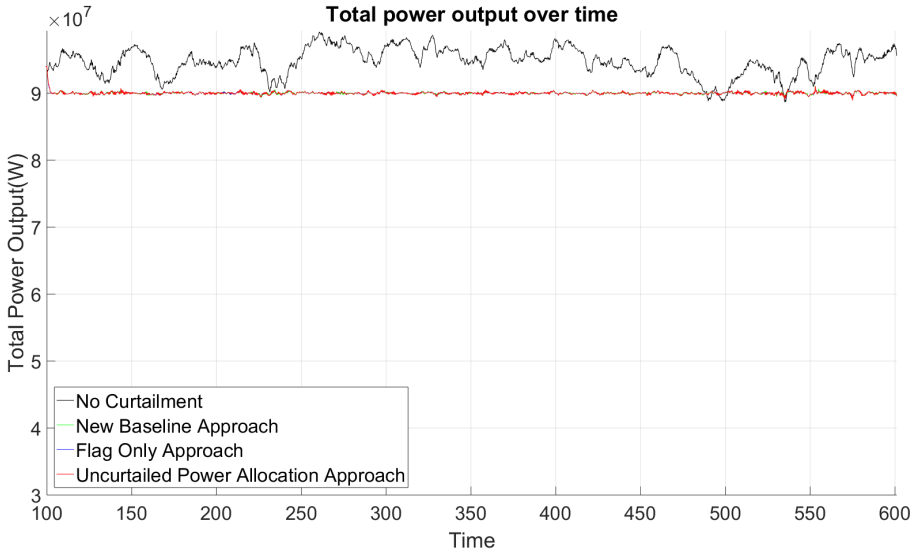


Figure 4.58: Power output from the wind farm when it is curtailed to 90MW in Model Four

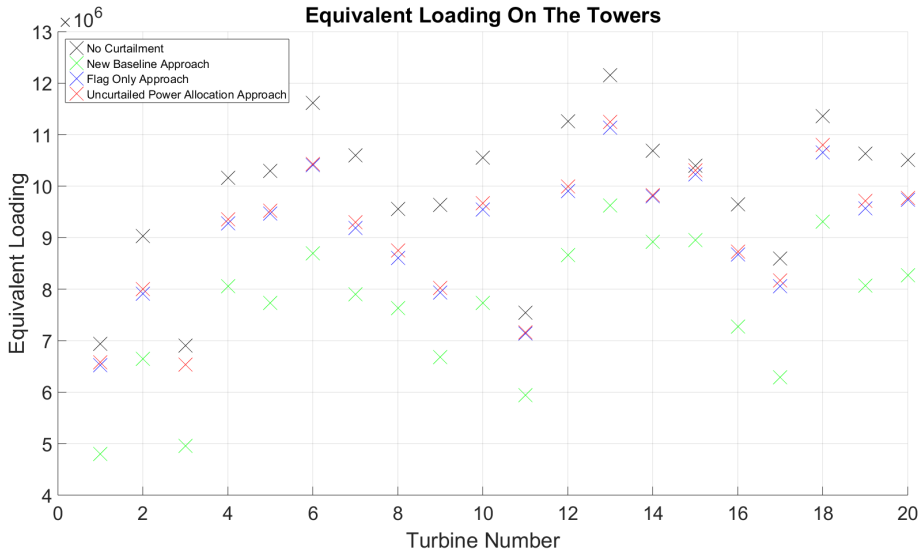


Figure 4.59: DELs for the fore-aft tower moments from the wind turbines when the wind farm is curtailed to 90MW in Model Four

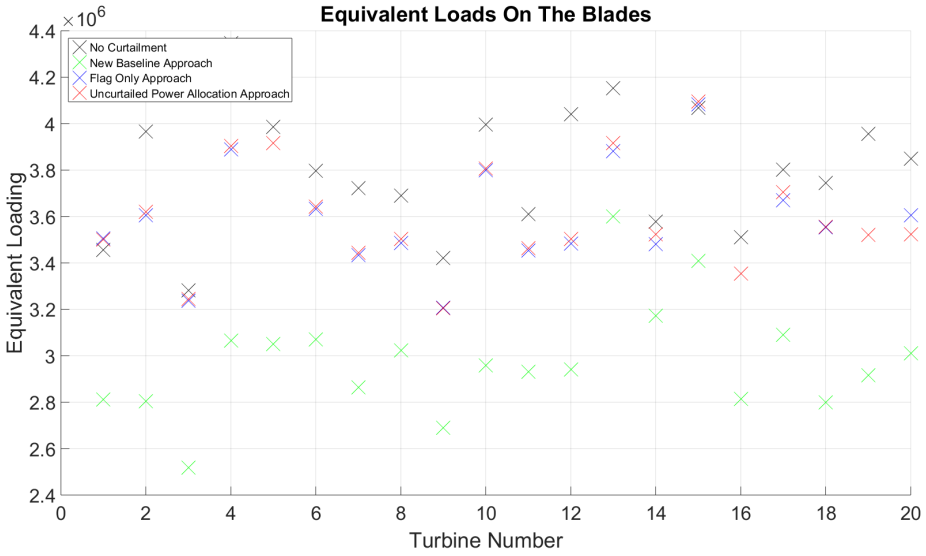


Figure 4.60: DELs for the out of plane blade bending moments from the wind turbines when the wind farm is curtailed to 90MW in Model Four.

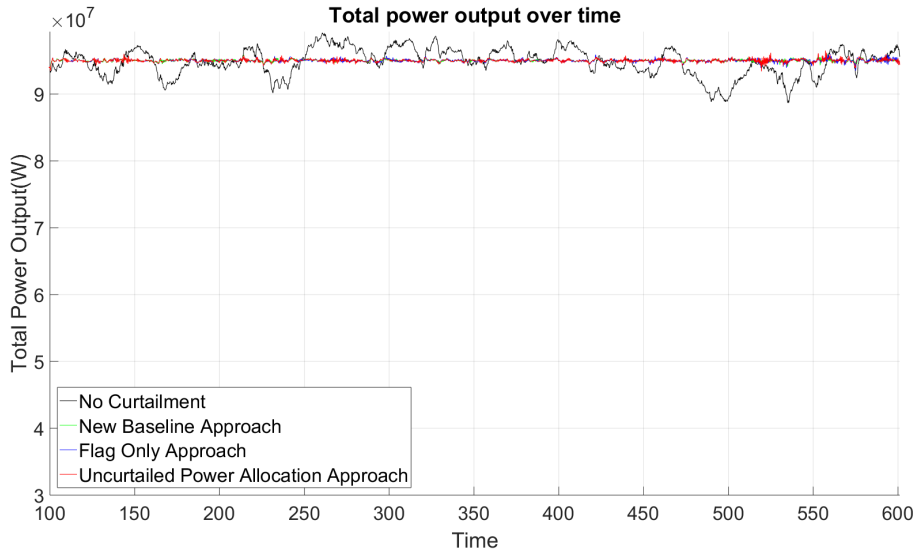


Figure 4.61: Power output from the wind farm when it is curtailed to 95MW in Model Four

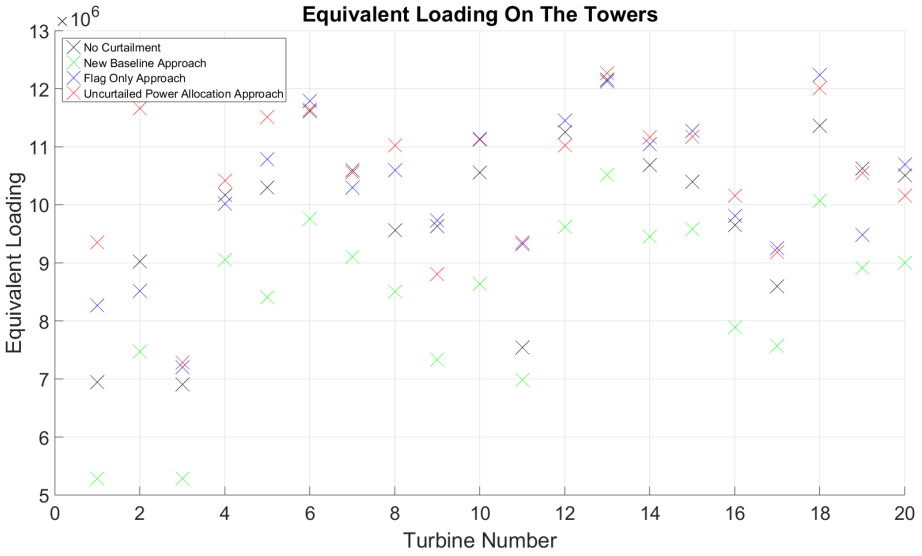


Figure 4.62: DELs for the fore-aft tower moments from the wind turbines when the wind farm is curtailed to 95MW in in Model Four

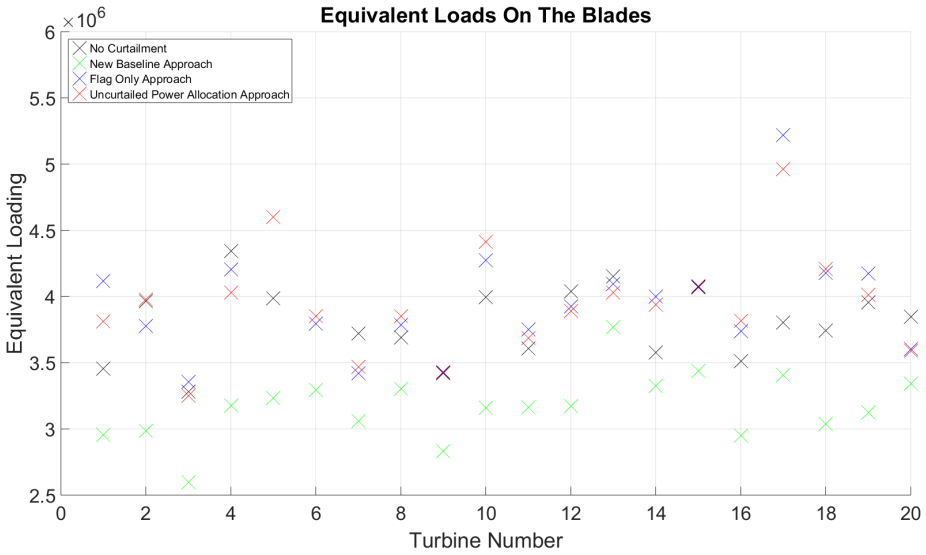


Figure 4.63: DELs for the out of plane blade bending moments from the wind turbines when the wind farm is curtailed to 95MW in Model Four.

| Allocation | 75 MW | 80 MW | 90 MW | 95MW |
|---|---|---|---|---|
| New Baseline | 37.6153 % | 33.9413 % | 23.4965% | 15.1921% |
| Flag Based | 27.8508% | 22.9300% | 8.8627% | -4.1143% |
| Uncurtailed power based | 26.5459 % | 21.3630 % | 8.0726% | -7.1959% |

Table 4.7: Change in mean damage equivalent load to the fore-aft tower moment in Model Four

| Allocation | 75 MW | 80 MW | 90 MW | 95MW |
|---|---|---|---|---|
| New Baseline | 30.2832 % | 28.1690% | 21.5243% | 16.5294% |
| Flag Based | 19.5187% | 15.8031% | 5.3717% | -6.2784% |
| Uncurtailed power based | 19.3511 % | 15.6859 % | 5.1791% | -3.9785% |

Table 4.8: Change in mean damage equivalent load to the out-of-plane bending moment in Model Four

### 4.3.3 Above Rated

#### Model Five

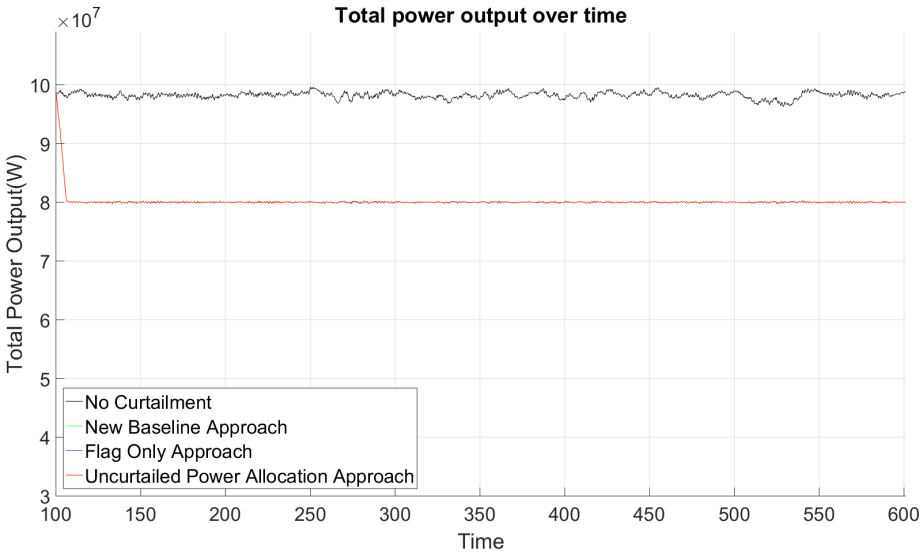


Figure 4.64: Power output from the wind farm when it is curtailed to 80MW in Model Five

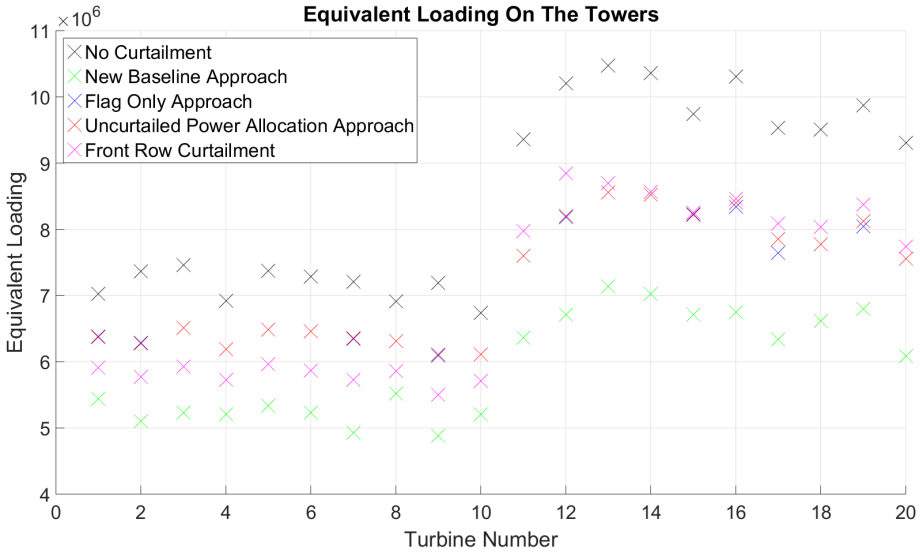


Figure 4.65: DELs for the fore-aft tower moments from the wind turbines when the wind farm is curtailed to 80MW in Model Five

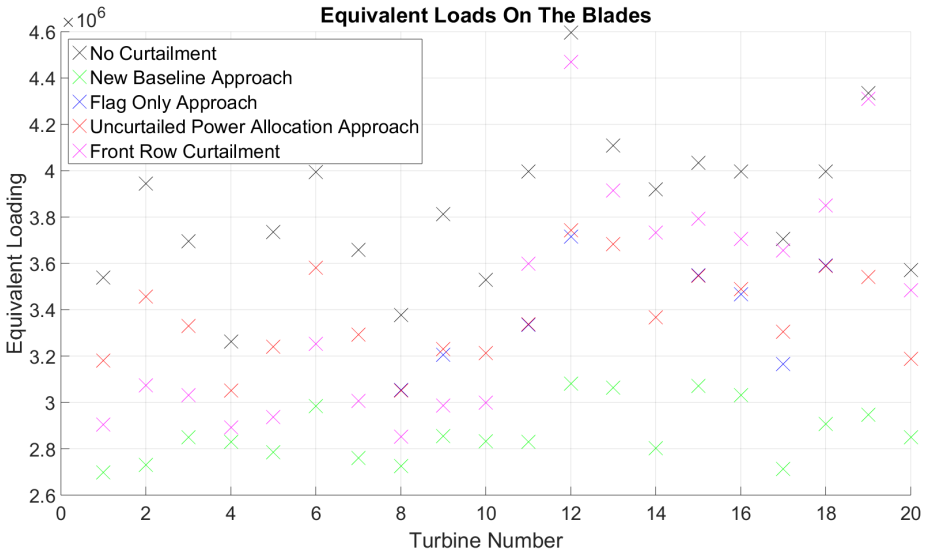


Figure 4.66: DELs for the out of plane blade bending moments from the wind turbines when the wind farm is curtailed to 80MW in Model Five.

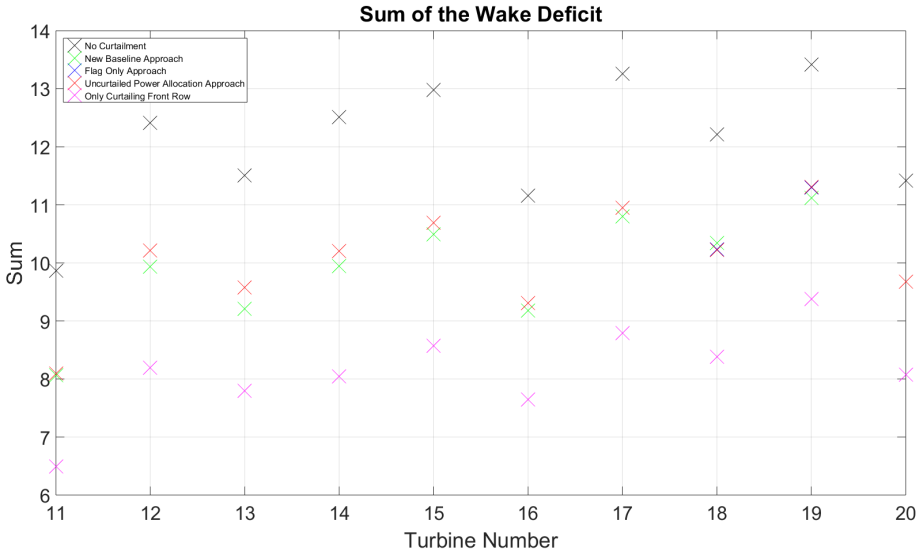


Figure 4.67: Sum of the wake deficits in the second row of wind turbines when the wind farm is curtailed to 80MW in Model Five.

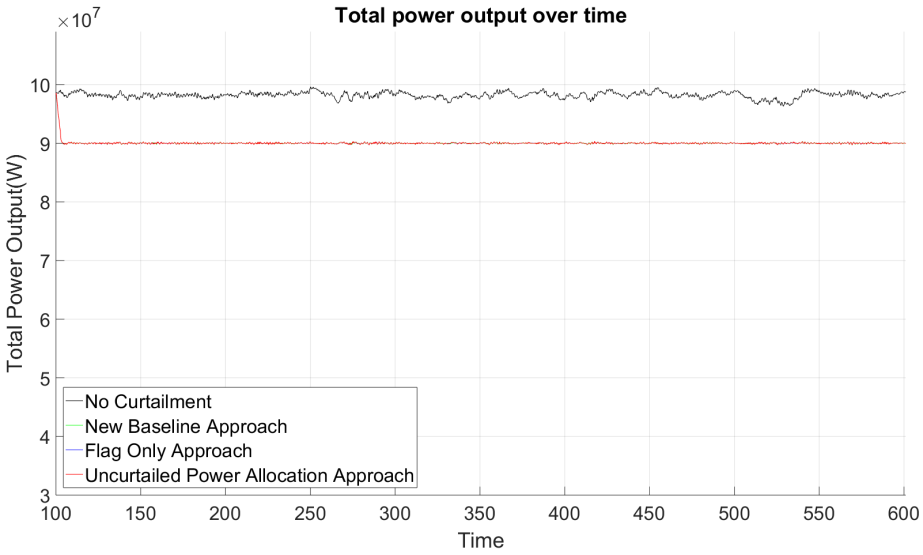


Figure 4.68: Power output from the wind farm when it is curtailed to 90MW in Model Six

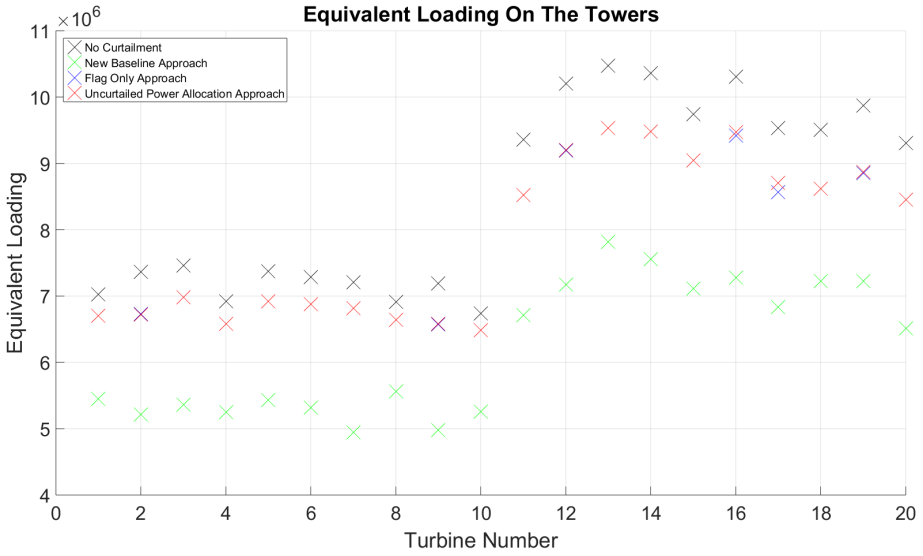


Figure 4.69: DELs for the fore-aft tower moments from the wind turbines when the wind farm is curtailed to 90MW in Model Five

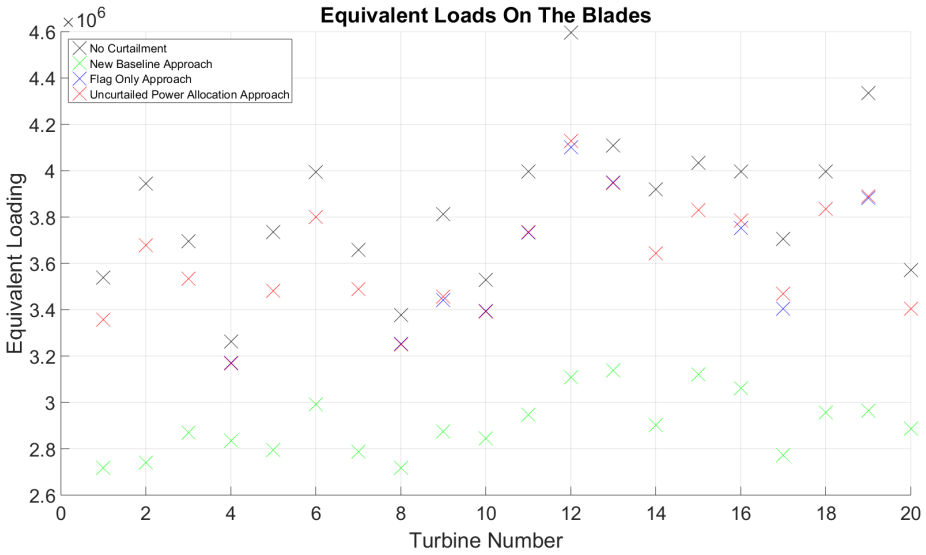


Figure 4.70: DELs for the out of plane blade bending moments from the wind turbines when the wind farm is curtailed to 90MW in Model Five.

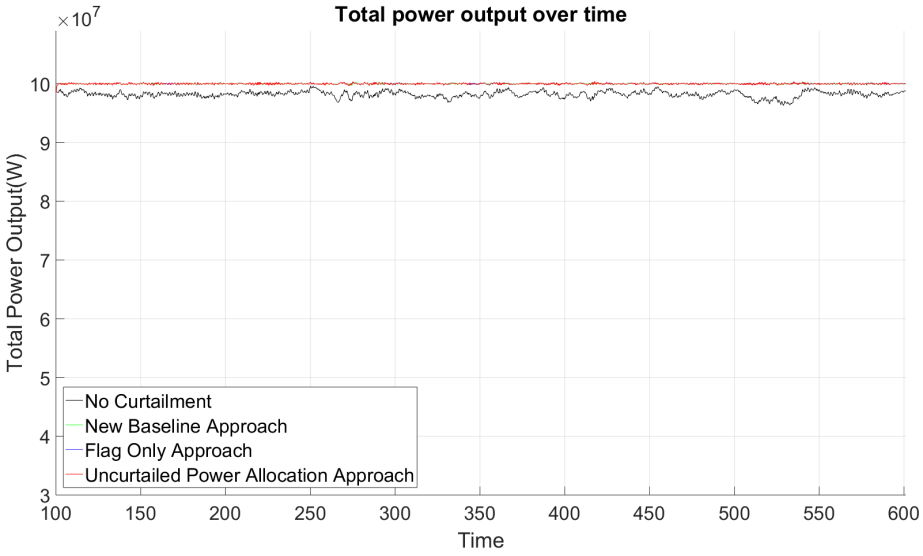


Figure 4.71: Power output from the wind farm when it is curtailed to 100MW in Model Five

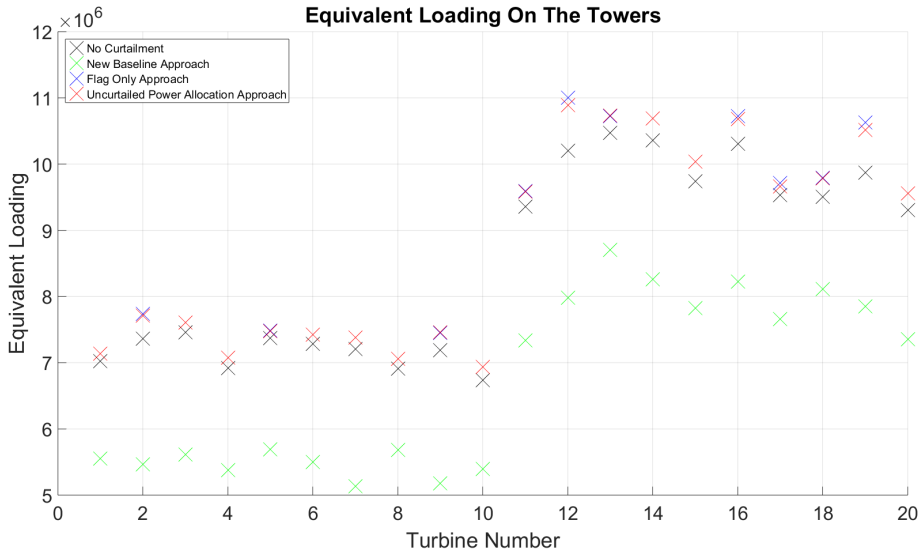


Figure 4.72: DELs for the fore-aft tower moments from the wind turbines when the wind farm is curtailed to 100MW in Model Five

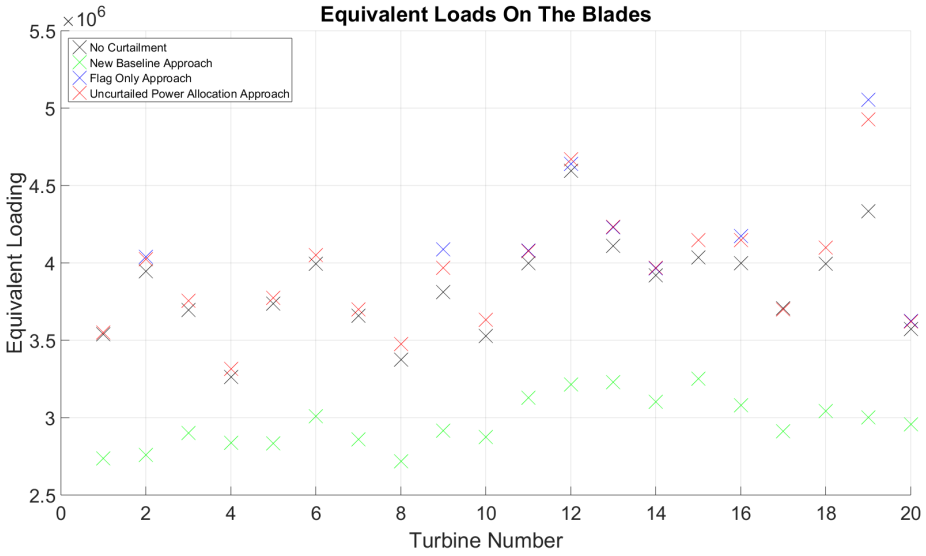


Figure 4.73: DELs for the out of plane blade bending moments from the wind turbines when the wind farm is curtailed to 100MW in Model Five.

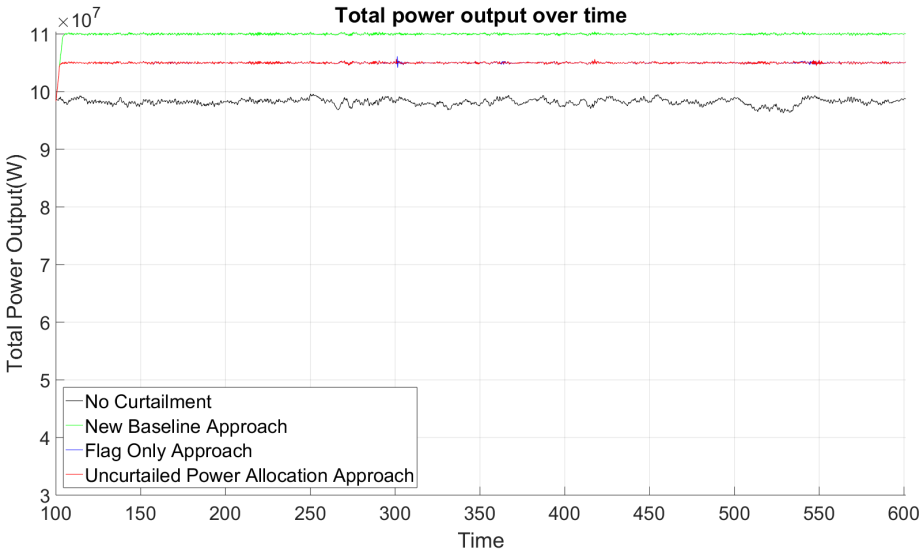


Figure 4.74: Power output from the wind farm when it is curtailed to the maximum sustainable output for each strategy in Model Five.

Figure(4.74) shows the maximum sustainable power output that each allocation strategy can maintain what can be seen is that the new baseline allocation strategy can sustain a power level more than 10% higher than the uncurtailed power output.

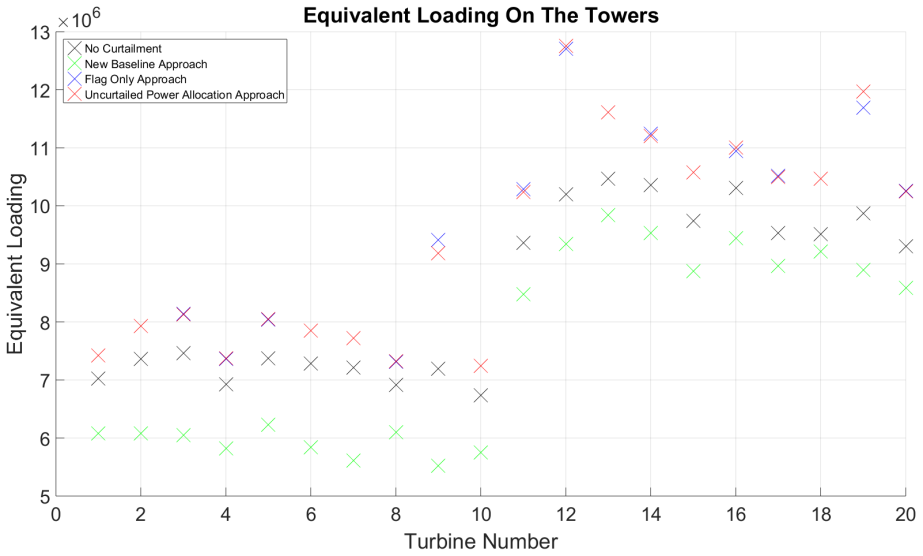


Figure 4.75: DELs for the fore-aft tower moments from the wind turbines when the wind farm is curtailed to the maximum sustainable output for each strategy in Model Five.

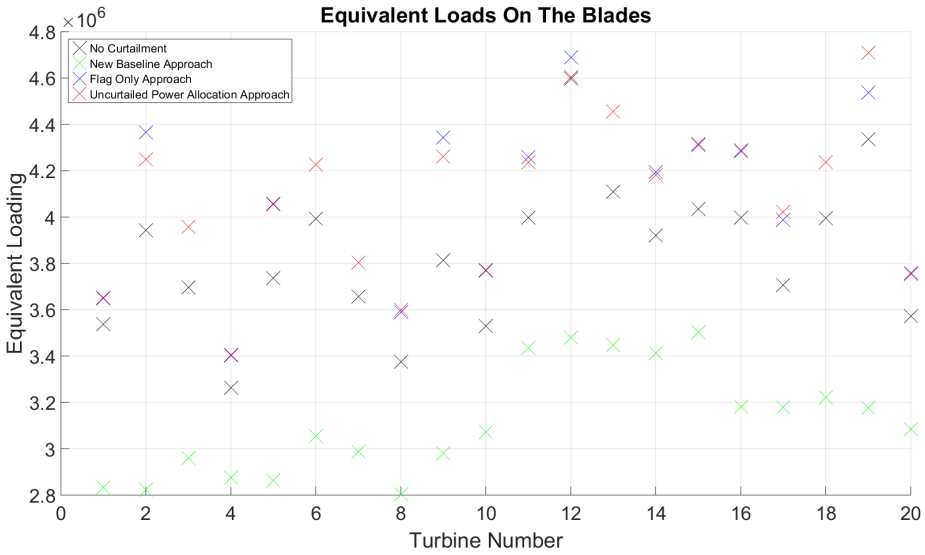


Figure 4.76: DELs for the out of plane blade bending moments from the wind turbines when the wind farm is curtailed to the maximum sustainable output for each strategy in Model Five.

Figure (4.75) and Figure (4.76) both show that the new baseline curtailment strategy has a reduction in DELs above rated even when the wind farm is outputting more than 10MWs more that its uncurtailed power output.

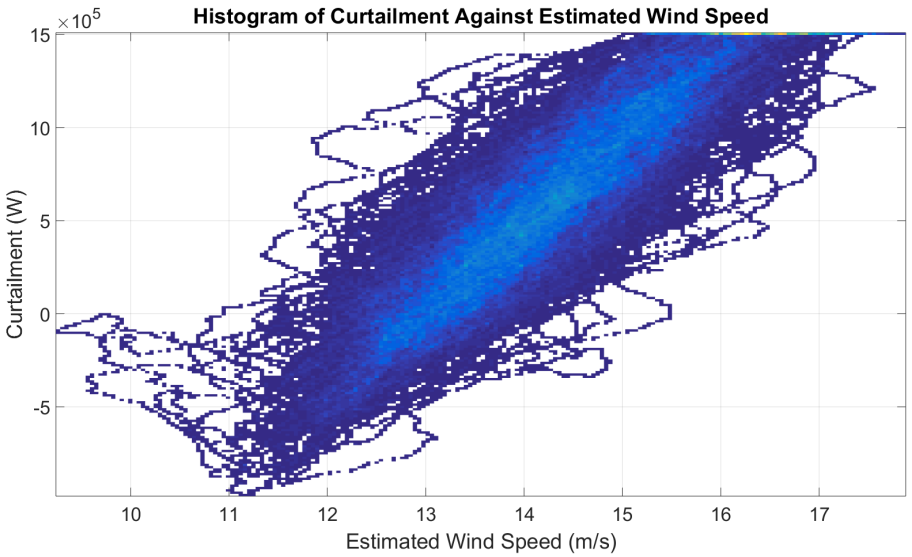


Figure 4.77: A histogram of the level of curtailment against the estimated wind speed when the New Baseline strategy is used and the wind farm is curtailed to 110MW in Model Five

| Allocation | 80 MW | 90 MW | 100 MW | 105MW | 110MW |
|---|---|---|---|---|---|
| New Baseline | 29.7953 % | 26.8519 % | 21.5929% | -% | 12.4320 % |
| Flag Based | 15.0196% | 7.4677 % | -3.1835% | -10.7347% | -% |
| Uncurtailed power based | 14.8365 % | 7.3499% | -3.0050% | -10.7237% | -% |

Table 4.9: Change in mean damage equivalent load to the fore-aft tower moment in Model Five

| Allocation | 80 MW | 90 MW | 100 MW | 105MW | 110MW |
|---|---|---|---|---|---|
| New Baseline | 25.0325 % | 24.1469 % | 22.4542% | -% | 18.5975% |
| Flag Based | 12.2991 % | 5.9682% | -2.8650% | -6.6078 % | -% |
| Uncurtailed power based | 12.0417 % | 5.7888% | -2.5444% | -6.4817% | - % |

Table 4.10: Change in mean damage equivalent load to the out-of-plane bending moment in Model Five

Table(4.9) and Table(4.10) show that even when the wind farm is outputting 10% more power than the sum baseline rated power of the wind turbines there is a significant reduction in the damage equivalent loads for both the blades and the towers in the wind farm when compared to not curtailing the wind turbines. Outputting 10% more power than the baseline rating of the individual wind turbines is significant as some countries' TSO require a 10% spinning reserve for droop control and so if the wind farm can output this level of power it would be able to output its baseline rated power with sufficient reserve.

### 4.3.4 Discussion of results

The results show that the new proposed allocation strategy for Strathfarm reduces damage equivalent loads when compared with not curtailing the wind farm, Using the present allocation using the traffic light flag status from the PACs, curtailing using the estimated uncurtailed power and also when only the front row of wind turbines is curtailed. The results have show that the proposed curtailment allocation strategy is the most successful at below, near and above rated wind fields and over a range of wind farm layouts and prevailing wind directions. In addition to this the new approach also can achieve greater flexibility of operation as it is better suited to allocating positive level of curtail to wind turbines in a way which is sustainable. However as research

progresses some additional constraints will need to be considered such as whether the turbine level power electronics will be able to be overrated in this fashion without significant fatigue and also comparing this new strategy to one which maintains the blade moments rather than the tower moments.

## 4.4 Novelty of research

The research presented here is novel as there has not been previous modeling done which uses a turbine level wind speed estimator to allocate levels of curtailment across a wind farm using a derated power curve to maintain the bending moments of components of the wind turbines.

## 4.5 future work

As the literature review has show there is a great potential in using the HVDC link in conjunction with wind farm level control to provide ancillary services This however will require the design of a power systems model to be used in Strathfarm particularly for high frequency events such as voltage ride through support.